Acta Biomaterialia xxx (xxxx) xxx

Contents lists available at ScienceDirect

Acta Biomaterialia

journal homepage: www.elsevier.com/locate/actabiomat

Review article

The influence of alloying and fabrication techniques on the mechanical properties, biodegradability and biocompatibility of zinc: A comprehensive review

J. Venezuela, M.S. Dargusch *

Queensland Centre for Advanced Materials Processing and Manufacturing (AMPAM), School of Mechanical and Mining Engineering, The University of Queensland, St Lucia, QLD 4072, Australia

ARTICLE INFO

Article history:
Received 15 October 2018
Received in revised form 14 January 2019
Accepted 16 January 2019
Available online xxxx

Keywords:
Zinc
Mechanical properties
Biocompatibility
Biodegradability

ABSTRACT

Zinc has been identified as one of the most promising biodegradable metals along with magnesium and iron. Zinc appears to address some of the core engineering problems associated with magnesium and iron when applied to biomedical implant applications; hence the increase in the amount of research investigations on the metal in the last few years. In this review, the current state-of-the-art on biodegradable Zn, including recent developments, current opportunities and future directions of research are discussed. The discussions are presented with a specific focus on reviewing the relationships that exist between mechanical properties, biodegradability, and biocompatibility of zinc with alloying and fabrication techniques. This work hopes to guide future studies on biodegradable Zn that will help in advancing this field of research.

Statement of Significance

(i) The review offers an up-to-date and comprehensive review of the influence of alloying and fabrication technique on mechanical properties, biodegradability and biocompatibility of Zn; (ii) the work cites the most relevant biodegradable Zn fabrication processes including additive manufacturing techniques; (iii) the review includes a listing of research gap and future research directions for the field of biodegradable Zn.

Contents

* Corresponding author.
E-mail address: m.dargusch@uq.edu.au (M.S. Dargusch).

https://doi.org/10.1016/j.actbio.2019.01.035
1742-7061/

1. Introduction

Metals have a long history of use as an implant material in the medical field [1–7]. The attraction of using metals is attributed to their unique combination of properties including good mechanical strength, ductility, toughness, wear resistance and formability. From a biocompatibility standpoint, the first generation of metallic materials used for implant applications was required to be inert in the physiological environment [5–7]. Some of these metals include stainless steels (316L), cobalt-chromium (CoCr) alloys, and titanium (commercially pure Ti) and Ti alloys (e.g., Ti-6Al-4V). Good corrosion resistance was necessary to ensure excellent biocompatibility by preventing the possible complications associated with the interaction of corrosion products and human cells.

Recently, biodegradable and bioabsorbable metals such as magnesium (Mg), iron (Fe) and zinc (Zn) have found increasing acceptance as an implant material [8–15]. Three words that are typically associated with these metals are ‘biodegradable’, ‘bioabsorbable’, and ‘bioresorbable’, and it may be useful to distinguish between these terms. Researchers have used these terms interchangeably, but Liu et al. [16] recently expounded on the proper use of these modifiers. A biodegradable metal is a material that degrades by a biologically-mediated process, such as enzymatic and cellular processes. The term ‘biodegradable’ is not only associated with the degradation of materials within the body but could also be used to describe those occurring in the natural, external environment. It is the most frequent modifier used for describing metals and polymers of such kind. A bioabsorbable metal is expected to decompose via similar biological pathways as a biodegradable metal, such as those encountered in the physiological environment of the body, but without the host eliciting a negative response from its degradation products. Hence, ‘bioabsorbable’ focuses more on how a host metabolizes or assimilates a material’s degradation products. A bioresorbable metal degrades in vivo, and is removed either by a cellular activity or other processes. Though very similar to bioabsorbable in meaning, the term ‘bioresorbable’ has long been associated with biological reaction, specifically relating to osteoclast-driven bone resorption processes. Liu et al. suggested that ‘resorbable’ is best used to describe implants that have the potential to allow affected tissues to grow back to its original form (e.g., bone scaffolds).

Liu et al. [16] concluded that ‘absorbable’ is the most appropriate modifier for describing implants that are expected to dissolve safely in the body. This term is adopted by standards (e.g., ASTM, ISO), is the most historically established, and the most broadly applicable to medical applications. However, since the term ‘biodegradable’ has found considerable use for describing biometals such as Mg, Fe and Zn, then in this review, we retain the use of ‘biodegradable’ and will use it interchangeably with ‘bioabsorbable’.

A bioabsorbable implant is anticipated to dissolve completely once tissue healing is accomplished. Thus, it is reasonable to assume that this should consist of elements that are safely metabolized by the body and preferably those that are essential to human functions. The biodegradable implant should also degrade at an appropriate rate so that it can extend the necessary support to the tissue for the duration that such help is warranted.

Biodegradable metals have already been considered for medical applications for many years, though it is likely that these were previously used without the advantages of biodegradability in mind. For example, a functional wrought Fe dental implant was found in a corpse dated to the first or second century AD [17]; in the 17th century, the pioneering anatomist and surgeon Hieronymus Fabricius used Fe sutures to treat soft tissue defects [11]; and, in 1878, Edward Huse used pure Mg sutures to stitch broken blood vessels [8].

Of the three candidate metals, Zn is the most recently introduced [9]. The bulk of the publications on this topic have only been available in the last five years. Research suggests that some of the issues related with Mg and Fe may be addressed by using Zn [18,19]; hence the considerable increase in scientific interest on this metal.

Literature reviews on biodegradable Zn are already available [20–23], and one of the most-cited is that by Bowen et al. [21] published in 2016. Bowen et al. reviewed the state-of-the-art in biodegradable stenting and biodegradable Zn research. However, their review of the literature on Zn covered those that were published before 2016, and a substantial number of research findings on the topic have been published since this time. Recently, Mostaed et al. [23] published a review that focused on biodegradable Zn for vascular applications. The current review builds on these works, presents updates on recent developments, and provides some framework for future scientific engagements. This work aims

Please cite this article as: J. Venezuela and M. S. Dargusch, The influence of alloying and fabrication techniques on the mechanical properties, biodegradability and biocompatibility of zinc: A comprehensive review, Acta Biomaterialia, https://doi.org/10.1016/j.actbio.2019.01.035

to present the current state of knowledge on biodegradable Zn, with a specific focus on reviewing the relationship of properties, such as mechanical properties, biodegradability, and biocompatibility, with alloying and fabrication techniques. Both traditional and advanced fabrication techniques, such as additive manufacturing (AM) or 3D printing, will be included in the discussions. Also, though an exhaustive citation of microstructures attendant to each Zn alloy is not included, discussions highlighting the microstructure-property relationship are present. This review hopes to guide future researchers on topics that will help in the advancement of the field. A mature understanding of the work done on some of the early biodegradable metals such as Mg and Fe will be beneficial, though this is beyond the scope of the current work, and will give the reader a better appreciation of the work presented herein.

2. Zinc as a potential bioabsorbable metal

2.1. Requirements of a biodegradable metal for stent and bone-fixation device

Biodegradable metals are most suitable in implants requiring temporary functions in the body. Two promising medical applications of bioabsorbable metals are in the fabrication of stents and orthopedic fixation devices. A stent is a miniature tube that is placed into a hollow bodily structure, such as a blood vessel or a urethra [24]. The primary function of the stent is to keep the hollow structure open and relieve constrictions. The stent may be delivered using different medical procedures, such as the percutaneous coronary intervention (PCI) to treat heart artery stenosis [25]. In orthopedics, an internal fixator is an implant that is used to guide the healing process of bone fractures. The implant stabilizes the fractured bone, thus preventing motion across fracture lines and allowing rapid healing of damaged structures. Orthopedic internal fixators may come in the form of plates and screws, wires (e.g., Kirschner wires), and nails (e.g., intramedullary rod) [26].

The current materials of choice for metallic stents are 316L stainless steel, nickel-titanium alloy (NiTi or Nitinol), tantalum (Ta) and the CoCr alloy [27,28]. Metallic stents may be deployed bare or drug-eluting. Drug-eluting stents (DES) are bare stents coated with a drug that is slowly released during service [29,30]. It is said that the introduction of the DES allowed the PCI to become one of the most frequently performed therapeutic interventions in medicine [30]. DES addressed the problem of in-stent restenosis (i.e., growth of tissue on the stent that results to channel blocking) associated with bare stents. Restenosis refers to the growth of tissue on the stent that results in channel blocking. Restenosis is attributed to a vascular repair process called neointimal hyperplasia. Correcting neointimal hyperplasia would require repeat revascularization [29], a procedure that adds to a patient's distress and expenses.

However, the fact that metallic stents remain permanently in the artery also creates several issues. One of the most serious is the occurrence of late stent thrombosis (i.e., blocking of the blood vessel due to a blood clot or thrombus) that requires long-term antiplatelet treatment [31]. A bioabsorbable stent has the potential to reduce or eliminate these shortcomings associated with bare and drug-eluting metallic stents. A dissolving stent ensures (i) a low stent profile regardless of tissue growth, (ii) minimal platelet accumulation and thrombus proliferation, (iii) the restoration of vasomotion, (iv) the prevention of strut-fracture induced restenosis, (v) freedom from side branch obstruction by the struts, and (vi) the possibility of repeat treatments on the same vascular site [31].

For bone fixation implants, the biocompatible metals include stainless steels (SS), cobalt alloys, titanium (Ti) and Ti alloys [32]. The use of metal-based fixation devices is related to particular issues including stress shielding, corrosion and stress-corrosion cracking (SCC), accumulation of implant metal in tissues, interference in radiological studies, and need of additional surgery for implant removal [33]. Of these issues, the need for an extra operation to remove the implant is the most distressing to a patient. With a biodegradable implant, the necessity for implant removal procedures is eliminated as the implant is expected to eventually dissolve in the body.

A biodegradable material is required to possess specific properties before it becomes viable for stent and orthopedic-fixation device fabrication. Table 1 lists some of the recognized design considerations specific to these two applications [12,18,21,34]. The first and most important attribute is that the material along with its degradation products should be innocuous and compatible in the physiological environment [9,27].

Bioabsorbable stents are designed to act as a supporting structure or scaffold to the walls of the blood vessel during the remodelling period and to slowly dissolve as the tissue heals and regenerate [21,36]. Ideally, these devices must retain mechanical properties for approximately 3–6 months before being broken down and safely processed by the body [21,37,38]. It was suggested that the mechanical properties of the candidate materials should approximate those of 316L stainless steel, a metal that has been traditionally considered as the gold standard for stents [21,39], with the advantage of permitting clinicians to possess reasonable deployment expectations when using the biodegradable stent [21].

Table 1 also indicates that the property requirements for an orthopedic fixation device are essentially similar to those required

Table 1
Specific design constraints for a biodegradable material considered for stent and bone-fixation device applications [12,18,21,34,35].

Criterion	Stent	Orthopedic internal fixation device
Biocompatibility	• Non-toxic, non-inflammatory, hypoallergenic • no harmful release or retention of particulates • promote endothelial cell attachment; discourage smooth muscle cell attachment	• non-toxic, non-inflammatory, hypoallergenic • no harmful release or retention of particulates • promote osteoblast and osteoclast attachment; avoid fibrous encapsulation
Mechanical integrity and resorption during service	• Mechanical integrity 3–6 months • Full absorption in 1–2 years	• Mechanical integrity: ○ Plates and screws < 6 mos ○ Osteotomy staples < 3 mos • Full absorption in 1–2 years
Mechanical properties	• Yield strength > 200 MPa • Tensile strength > 300 MPa • Elongation to failure > 15–18% • Elastic recoil on expansion < 4%	• Yield strength > 230 MPa • Tensile strength > 300 MPa • Elongation to failure > 15–18% • Elastic modulus approximate to that of cortical bone (10–20 GPa)
Corrosion behaviour	• Penetration rate < 20 μm year^{-1} • Hydrogen evolution < 10 μL cm^{-2} per day	• Plates and screws (0.5 mm year-1) • Hydrogen evolution < 10 μL cm^{-2} per day

Please cite this article as: J. Venezuela and M. S. Dargusch, The influence of alloying and fabrication techniques on the mechanical properties, biodegradability and biocompatibility of zinc: A comprehensive review, Acta Biomaterialia, https://doi.org/10.1016/j.actbio.2019.01.035

for a stent, except at a few points. Biodegradable metals for bone fixation need to retain their mechanical integrity longer than those used in stent applications. This is reasonable since bone fixation devices are often load-bearing, and may even encounter complex loading profiles during service. Furthermore, one particular property where orthopedic device manufacturers place a premium on is elastic modulus. The elastic modulus of potential resorbable bone scaffolds needs to be close to that of cortical bone to avoid stress-shielding [40].

2.2. The case for Zn

In the search for bioabsorbable implant material, two types of materials have found considerable acceptance in the scientific community. The first type is the polymer, with in vitro biocompatibility studies on polyglycolic acid/polylactic acid (PGA/PLA), polycaprolactone (PCL), polyhydroxybutyrate valerate (PHBV), polyorthoester (POE), and polyethyleneoxide/polybutylene terephthalate (PEO/ PBTP) being some of the first to be reported [41–43]. These studies eventually led to the development of commercial bioabsorbable implants. Examples include the Igaki-Tamai, the DESolve, and the ABSORB stents made of poly-L-lactic acid (PLLA) [44]; the Ideal BioStent consisting of salicylic acid/adipic acid (SA/AA); and the REVA stent constructed from tyrosine-derived polycarbonate [14,31]. Reports on the successful application of polymer-based bioabsorbable screws for bone grafting fixation are also available [45].

The second class of bioabsorbable materials are metals. Table 2 presents a summary of the advantages and disadvantages of the most promising biodegradable metals, Mg, Fe and Zn. These metals are considered essential micronutrient of the body, and Table 2 includes the recommended daily intake (RDI) for each metal. The RDI is suggested to be a key measure for assessing a material's biocompatibility [11].

Magnesium has a long history of successful use as an implant material, though early applications considered its biodegradability as a disadvantage [9]. Magnesium offers excellent biocompatibility as indicated by its high RDI. It has good mechanical properties, particularly having an elastic modulus that approximates that of human bone. The boom in Mg research came about with the renewed interest in the idea of degradable metals. Currently, magnesium and its alloys (e.g., Mg-Ca, Mg-Zn, Mg-Si, Mg-Sn, Mg-Zr, Mg-Al, Mg-Y, and Mg-REE) are the most widely studied and considered the most promising among the bioabsorbable metals [8,9,46,47]. In fact, in 2016 BIOTRONIK released the first commercially available, clinically proven, sirolimus-eluting bioabsorbable magnesium stent [48,49].

Corrodible iron was one of the earliest biodegradable implant materials to be tested in vivo after early reports on biodegradable polymers cast doubts on the polymers' biocompatibility [50]. Studies on bioabsorbable Fe and some Fe alloys such as Fe-Mn, Fe-W, and Fe-Mg soon followed and attracted a lot of research attention [51–53]. Fe offers excellent mechanical strength, ductility, and formability, and good biocompatibility. Recently, Lifetech Scientific created IBS [54], a sirolimus-eluting, iron-based coronary scaffold. This stent is now undergoing clinical testing in humans.

Though Mg and Fe have a head start in this field [9,12,13], the scientific community continues to look for other alternatives considering that both metals still have issues. Zinc and its alloys are promising alternatives as they seem to address some of the fundamental engineering issues associated with the use of biodegradable Mg and Fe.

In an arterial environment, the natural biocorrosion rate of pure Mg extends to the hundreds of micrometers per year, while high-purity Zn degrades at a rate of tens of micrometers per year [18]. The lower corrosion rate of Zn presents several advantages. For example, Bowen et al. [21] suggested that for stent applications, the low biocorrosion rate of Zn (i) offers greater freedom for metallurgical manipulation and consequent strengthening, (ii) better biocompatibility, and (ii) allows the engineering of lower profile stents that is crucial to limiting restenosis and thrombosis. Another advantage of Zn over Mg is that its corrosion process does not generate hydrogen gas. There are some concerns with the potential harm that this corrosion by-product poses to the body, such as the formation of gas pockets around the disintegrating implant, though this issue is still debatable [56,57].

The issues with ferrous biometals stem from its relatively low corrosion rate and the production of insoluble, albeit biocompatible, corrosion product [9,58,59]. The slow corrosion rate of iron implies that the implant stays longer than necessary in the body. Pierson et al. [60] also noted that the biocorrosion product of Fe could remain encapsulated in the neointima (or new arterial lining) in an expanded form that could interfere with arterial function. Zn has the potential to avoid these problems by having a higher corrosion rate than Fe and possessing a compact and biocompatible corrosion product similar to that of Mg [18].

Others cite that another advantage of Zn is its low melting point and low reactivity in the molten state [55]. This allows Zn to be fabricated and shaped by simple techniques such as casting and hot wrought processing.

While the full extent of some critical properties (e.g., mechanical properties, corrodibility, and biocompatibility) of biodegradable Zn is only recently being discovered, the benefits of Zn to human physiology are relatively well known. In ancient times,

Table 2
Advantages and disadvantages of magnesium, iron, and zinc-based biodegradable metals [9,11,12,15,23,55].

Biodegradable Metal	Recommended Daily intake, mg	Advantages	Disadvantages
Mg	375–700	• Excellent biocompatibility • Compact corrosion product • Good strength • Low density and elastic modulus (close to bone properties) • MRI compatible	• Excessive corrosion rate • Low strength and limited formability • Evolution of gaseous hydrogen • Premature loss of mechanical integrity • Undesirable pH increase • Susceptible to SCC
Fe	10–20	• Good biocompatibility • Excellent strength and formability • MRI compatible (austenitic phase) • No gas generated during degradation	• Corrosion rate too slow • Bulky corrosion product that accumulate and repel adjacent tissues
Zn	6.5–15	• Good biocompatibility • Corrosion rate in between Mg and Fe • No gas generated during degradation • Low melting point and low reactivity in molten state	• Poor mechanical properties • Age hardening

Please cite this article as: J. Venezuela and M. S. Dargusch, The influence of alloying and fabrication techniques on the mechanical properties, biodegradability and biocompatibility of zinc: A comprehensive review, Acta Biomaterialia, https://doi.org/10.1016/j.actbio.2019.01.035

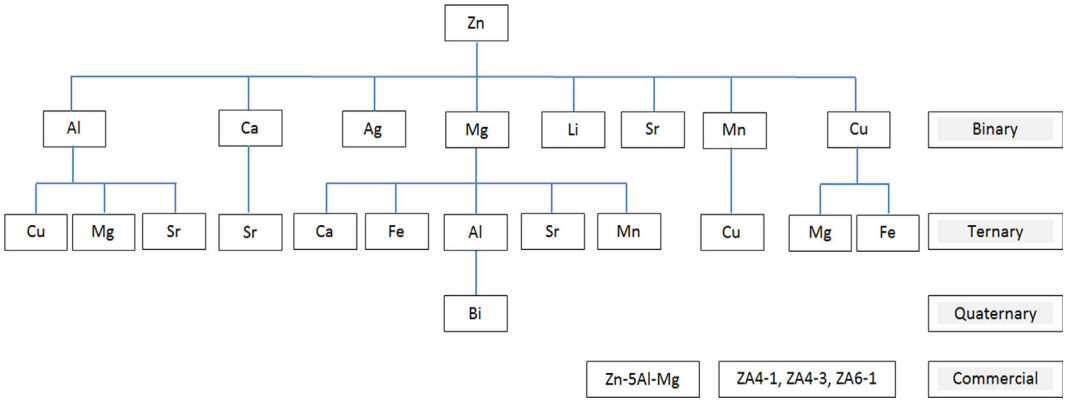

Fig. 1. Schematic showing the different Zn alloy combinations studied for biodegradable implant applications.

Egyptians (2000 BCE) and medieval Romans already used Zn in medicinal creams [61]. Zinc is counted as an essential trace element and plays catalytic, structural and regulatory roles in the human cell [61,62]. Bowen et al. [21] reviewed the many physiological functions of Zn including: (i) having a direct signalling function at different cellular levels; (ii) is necessary for the function of more than 300 enzymes involved in diverse physiological processes such as wound healing, brain development, and cell membrane stability; (iii) is vital to the structure of a number of proteins, plays a regulatory role by inhibiting and activating enzymes and proteins; (iv) is an essential component in chromatin structure; (ii) plays a role in DNA replication and repair; (v) acts as an antioxidant via the stabilisation of DNA and cell membranes; (vi) is an antiatherogenic; and (vii) improves endothelium integrity and prevents atherosclerosis.

Several studies have also observed the positive influence of the presence of Zn in different biomimetic ceramic scaffolds including hydroxyapatite, nano-hydroxyapatite, carbonated hydroxyapatite, biphasic calcium phosphate and tricalcium phosphate [63,64]. Zinc in calcium phosphate-based scaffolds was found to be completely biocompatible, induces rapid bone repair, and reduces bone resorption [63].

Zinc is not without its issues. Zn possesses relatively lower mechanical properties than Mg and Fe, which raises concerns on its ability to sustain applied loads and maintain post-corrosion structural integrity during service. Concerning toxicity, Zn is less biocompatible than Mg [65], but is very similar to Fe, as seen by comparing the RDI of each element in Table 2. Some Zn alloys [66] appear to trigger a slight cytotoxic response in healthy human cells. Zinc overdose or chronic overexposure (i.e., 100–300 mg day^{-1}) can cause nausea, vomiting, abdominal pain, diarrhea, fatigue, and severe copper deficiency [67]. An excess of Zn is considered neurotoxic, can impair immune function, and may delay bone development [9,67]. These issues need to be addressed before the adoption of Zn in biodegradable implant technology in the future.

3. Development of zinc and zinc alloys for biomedical applications

Research on biodegradable Zn and Zn alloys for biomedical application is relatively new, with a majority of the work published in the last five years.

However, some of the earliest mention of Zn as a potential biodegradable implant include those by (i) Bolz and Popp [68], who suggested, in a patent in 2001, the feasibility of bioabsorbable coronary stents made of pure Zn and some Zn-X(X= Ti, Ca) alloys; and by (ii) Wang et al. [69] in 2007.

Fig. 1 is a schematic that shows the different Zn alloys studied for biomedical applications. A wide range of composition has already been studied; namely, (i) pure Zn, (i) binary, (iii) ternary, and (iv) quaternary combinations of Zn with other elements. The following section describes the development of these Zn and Zn alloys for biomedical applications.

3.1. Pure Zn

In 2011, Vojtech et al. [19] published what appears to be the first study on biodegradable Zn (99.95%) and other Zn alloys and essentially started the formal research on the use of this metal for bioabsorbable implant applications. They observed from in vitro biodegradability tests that Zn indeed corrodes in a physiological fluid. Also, though they did not perform any biocompatibility tests, they noted that the dose of Zn ions released via corrosion is negligible compared to the maximum tolerable biological limit. They then concluded that Zn will not likely elicit a toxic response if used as an implant and is, therefore, a possible alternative to Mg-based biodegradable alloys. Subsequently, Cheng et al. [70] compared the in vitro corrosion performance of five pure metals; namely, Mg, Fe, Zn, manganese (Mn), and tungsten W, and similarly gave positive conclusions on the biocompatibility of Zn. In 2013, Bowen et al. [18] published their landmark study on the in vivo performance of pure Zn (99.99%+) using a small animal model. The study looked at the in vivo corrosion behaviour and biocompatibility of a commercial Zn wire inserted in the abdominal aorta of Sprague-Dawley rats. They observed that the Zn wire remained intact for at least four months, after which time corrosion began to accelerate. More importantly, Bowen et al. found the good in vivo biocompatibility of Zn and concluded that Zn is highly suitable for bioabsorbable cardiac stent applications. In the succeeding years, Bowen et al. [71], Drelich et al. [72,73], and Guillory et al. [74] further contributed knowledge on the in vivo performance of pure Zn.

Other notable works on pure Zn include: (i) the fabrication of ultrapure (6 N) Zn minitubes by Liu et al. [75]; (ii) the manufacture of a functional Zn (4 N) stent by Hiebl et al. [76]; (iii) studies on the feasibility of using additive manufacturing techniques to form Zn by Demir et al. [77], Yang et al. [78], and Wen et al [79,80]; (iv) a study on the in vitro degradation of Zn (99.9%) in saline solutions, plasma and whole blood by Torne et al. [81,82]; (v) studies on the influence of Zn^{+2} ions on the in vitro viability of human cells by Ma et al. [83] and Shearier et al. [84]; (vi) a study on the in silico, in vitro and antifungal activity of surface corrosion products formed during the biodegradation of Zn by Alves et al. [85]; and (vii) a long-term study on the in vivo degradation of an actual Zn

Please cite this article as: J. Venezuela and M. S. Dargusch, The influence of alloying and fabrication techniques on the mechanical properties, biodegradability and biocompatibility of zinc: A comprehensive review, Acta Biomaterialia, https://doi.org/10.1016/j.actbio.2019.01.035

stent by Yang et al. [86]. Furthermore, a lot of work on binary alloys would often characterize pure Zn as this serves as the control in the respective experiments.

3.2. Binary alloys

The primary purpose of adding alloying elements to Zn is to alter two properties: (i) mechanical properties and (ii) biocorrosion properties. The most logical approach to Zn alloying for biomedical application is to combine it with elements that are known to be biocompatible or essential to human function, such as Mg, Ca, and Cu. Magnesium is the most well-known and the most studied biodegradable metal. It is therefore not surprising that a substantial number of studies looked at the combination of Mg and Zn.

Vojtech et al. [19], in 2011, were the first to report on the use of Zn-Mg alloy for bone fixation applications. Development of binary Zn alloys continued with notable works by Zheng and co-workers [87,88] on Zn-Mg, as well as zinc-calcium (Zn-Ca), and zinc-strontium (Zn-Sr) alloys. Other reports on Zn-Mg include those by Kubasek et al. [55,89,90], Yao et al. [91],Gong et al. [92], Murni et al. [93], Shen et al. [94], Galib and Sharif [95], Mostaed et al. [96], Jablonska et al. [97], Dambatta et al. [98,99], Vida et al. [100], Jarzebska et al. [101], Jin et al. [102], Xiao et al. [103], Alves et al. [104], Wang et al. [105], and Yang et al. [78]. The range of Mg addition typically ranged from 1 to 3 wt%; though relatively high (>5%) [90] and low (<0.1 wt%) [102,103] alloy additions of Mg have also been reported.

Research on other binary combinations have also been reported, including zinc-copper (Zn-Cu) [66,106], zinc-lithium (Zn-Li) [107,108], zinc-aluminium (Zn-Al) [74,96,109], zinc-silver (Zn-Ag) [110,111], and zinc-manganese (Zn-Mn) [112,113].

3.3. Ternary alloys

Vojtech et al. [19] were also the first to report on the biocompatibility of a Zn ternary alloy; i.e., zinc-aluminium-copper (Zn-Al-Cu). Studies on other ternary combinations were similarly pursued, with most of these based on the Zn-Mg combination. Some of the reported Zn-Mg-based ternary alloys include zinc-magnesium-iron (Zn-Mg-Fe) [114], zinc-magnesium-strontium (Zn-Mg-Sr) [88,115], zinc-magnesium-calcium (Zn-Mg-Ca) [88], and zinc-magnesium-manganese (Zn-Mg-Mn) [116]. Again, using Zn-Mg as a base for the ternary alloy makes sense, since this binary combination is the most studied owing to its expected good biocompatibility. Reports on Mg additions to binary alloys of Zn-Cu [117] and Zn-Al [118] are also available.

There are also studies on ternary combinations that do not involve the Zn-Mg pair, including zinc-calcium-strontium (Zn-Ca-Sr) [88], zinc-manganese-copper (Zn-Mn-Cu) [119], zinc-copper-iron (Zn-Cu-Fe) [120], and zinc-aluminium-strontium (Zn-Al-Sr) [121].

3.4. Quaternary alloys

Currently, there are few reports on the use of Zn quaternary alloys. Only a single study may be cited; i.e., the study by Bakhsheshi-Rad et al. [122] that looked at the zinc-magnesium–aluminium-bismuth (Zn-Mg-Al-Bi) combination. The lack of studies on quaternary combinations may be due to several factors. Firstly, there is still considerable work that needs to be accomplished in the binary and ternary Zn alloys; hence, the development of these less complex alloy systems has reasonably attracted the attention of most researchers. Secondly, it is quite logical to limit the number of elemental constituents in an alloy to reduce fabrication cost and simplify manufacturing methods.

3.5. Commercial alloys

Some commercially-available Zn alloys have also been studied as a possible biodegradable implant material. Commercial alloys offer the distinct advantage of good accessibility and predictable composition. Wang et al. [123] investigated the biodegradability and biocompatibility of ZA4-1 (3.5–4.5 Al, 0.75–1.25 Cu, 0.03–0.08Mg), ZA4-3 (3.5–4.3Al, 2.5–3.2 Cu, 0.03–0.06Mg) and ZA6-1 (5.6–6.0 Al, 1.2–1.6 Cu) Zn alloys, while Kannan et al. [124] studied similar properties in Zn-5Al-4 Mg.

4. Fabrication techniques for biodegradable zinc

The choice of the fabrication process is crucial as this can influence the microstructure and the inherent properties of Zn. The following identifies and describes some of the processes adopted to create biodegradable Zn, including traditional techniques such as casting and wrought processing, and advanced processes such as powder metallurgy and additive manufacturing.

4.1. Casting

The most common method for the fabrication of the Zn alloy is via casting [19,87,89,92,95] since it allows easy customization of the alloy composition. The process involves heating the metal components above their melting temperatures (typically between 470 and 750 °C depending on alloy composition) in a protective environment (e.g., Ar, SF_6, CO_2, or vacuum), pouring the liquid metal into appropriate molds (e.g., steel or graphite), and allowing the metal to solidify. The conventional melting furnaces used are resistance and induction furnaces.

Since the purpose of most studies was to apply zinc as a biomedical implant, then the metal should be in the shape that approximates service form. For example, bone fixation devices need flat plates, while stents require thin-walled cylindrical tubes. Casting is not appropriate for generating such net shapes. However, the as-cast metal is still useful as it serves as the raw material for the ensuing forming processes that create the desired product profile.

4.2. Traditional wrought techniques

In metal processing, wrought techniques refer to processes that use an applied mechanical force to plastically deform a metal and create the desired shape [125]. The term wrought means ‘worked’, a reference to the mechanical nature of the process. Wrought processing may be done hot or cold depending on the relationship of the working temperature with the recrystallization temperature of the metal. If the metal is plastically shaped above its recrystallization temperature, then this is referred to as hot working. Otherwise, it’s cold working. The most popular wrought techniques include rolling, forging, extrusion, and drawing.

In most studies on biodegradable Zn, the primary method to create a flat profile is via hot rolling [87,108,109,119]. Hot rolling involves the passing of a heated metal stock through a pair of rolls to reduce thickness. The rolling process for Zn is often preceded by a homogenization treatment, which consists of heating the metal at 250–350 °C for 30–180 min, to attain a uniform composition in the pre-formed Zn. The thickness of the rolled product can range from a few millimeters to about 300 μm.

The elongated cylindrical profile typical of a tube may be created via extrusion [19,66,87,94,96,103,105,106,110,112] or drawing [75,107,114]. Extrusion involves pushing the metal through a die with an orifice of the desired shape. Extrusion can be direct or indirect. In direct extrusion, the die is stationary, and the billet

Please cite this article as: J. Venezuela and M. S. Dargusch, The influence of alloying and fabrication techniques on the mechanical properties, biodegradability and biocompatibility of zinc: A comprehensive review, Acta Biomaterialia, https://doi.org/10.1016/j.actbio.2019.01.035

is pushed through the die using a ram. In indirect extrusion, the die is mobile and is pushed into the billet causing the metal to flow through the die orifice. Drawing is similar to extrusion except that the metal is pulled through the die instead of being pushed. In both processes, the metal is often pre-heated at 180–300 °C for 30–180 min before shaping. Extrusion is also typically used as the preliminary forming step prior to further reduction by drawing [102,105,107]. Hollow tubes may also be fabricated via extrusion or drawing, often with the use of appropriate mandrels. Wang et al. [114] used hollow sinking and mandrel drawing to create microtubes with a diameter of 2.5 mm and thickness of 130 μm. Hollow sinking involves drawing the rolled tube through a drawing die, while mandrel drawing consists of drawing the tube through the gap between the mandrel and the die.

4.3. Advanced processing techniques

There are some published reports on the application of novel fabrication techniques to create biodegradable Zn.

Vida et al. [100] used an advanced solidification technique called directional solidification casting to create cast Zn with some interesting microstructures. The process is a modification on traditional casting and uses a water-cooled mold that was designed to promote directional solidification by controlling heat flow conditions.

Jarzebska et al. [101] produced 5 mm diameter Zn rods using cold hydrostatic extrusion, a type of extrusion where the billet is circumscribed in a pressurized fluid. The fluid pressure was maintained between 470 and 500 MPa and the strain rate was set to 4–40 s^{-1}.

Dambatta et al. [98] used equal-channel angular pressing (ECAP), which is a type of severe plastic deformation process that involves metal billet being pressed through an angled (e.g., 90°) channel. They used dies with an 8 × 8 mm channel cross section and an intersection angle of 120 °C. The strain rate was 1 mm s^{-1}. The dies were heated to 200 °C, and molybdenum disulphide lubricant was used to reduce friction loads.

Powder metallurgy (P/M) techniques have also been used to fabricate biodegradable Zn. Sotoudeh Bagha et al. [113] prepared dense Zn-Mn disks via mechanical alloying of corresponding powders, followed by uniaxial cold-pressing and sintering. The milling process was done for 20 h under an argon atmosphere, and a ball-to-powder weight ratio of 20:1. Cold pressing of the alloy powders was done at a pressure of 300 MPa, while sintering was set at 250 and 450 °C for 1 h.

The fabrication of porous Zn is also attractive as this material may be useful for some biomedical applications, particularly in the manufacture of bioresorbable, tissue-engineered bone scaffolds. Capek et al. [126] used spark plasma sintering to create porous Zn. Spark plasma sintering is a technique that uses a pulsed direct current (DC) applied to a powder compact to induce densification. The team used low compacting pressures (5 MPa) to accommodate greater pore volume in the powder compact. An average porosity of about 20% was measured in the final product. Hou et al. [127] used hot press sintering (HPS) of salt (NaCl) templates followed by pressure infiltration casting to create porous biodegradable Zn-scaffolds. The produced scaffolds were hierarchical, open porous structure consisting of central and interconnected pores, and with porosity volume of up to 75%. Yang et al. [128] used spark plasma sintering to create a novel biodegradable metal-matrix composite (MMC) with Zn as the matrix and hydroxyapatite (HA) as the reinforcement. Pure Zn powders and HA powders were mixed in a planetary ball mill under an argon atmosphere for 1 h at 300 rpm. The mixed powders were then sintered at 380 °C and a pressure of 40 MPa for 6 min. The sintered Zn-Ha composites had densities higher than 90% and a microstructure consisting of HA particulates residing at the Zn boundaries.

Surface modification techniques have also been proposed to improve the properties of biodegradable Zn further. Shomali et al. [129] investigated the corrosion properties and biocompatibility of a poly(L-lactic acid) (PLLA)-coated Zn. The coating was applied by a simple dip coating method, and coating thickness was controlled by adjusting withdrawal speed and PLLA concentration. Jablonska et al. [97] confirmed the reduction of the corrosion rate of Zn after a surface pre-treatment that involved immersion of the metal in simulated body fluid (SBF) for a prolonged period.

Recently, additive manufacturing (AM) has been attracting a lot of attention and is considered a viable option for manufacturing metallic biomaterials [130]. This technique is especially useful for creating net-shape or near-net-shape components, rapid prototyping, and for constructing one-off, customized implants that can address specific patient needs. For 3-D printing metallic biomaterials, two of the most popular techniques are the powder bed fusion (e.g., selective laser sintering (SLS) and selective laser melting (SLM)) and direct energy deposition [131,132].

The prospects for the use of AM techniques in fabricating biodegradable Zn [77,79,80,133,134] and Zn alloys (e.g., Zn-Mg) [78] appears promising. Selective laser melting (SLM), which is a type of AM process that produces metal parts by the fusion of powders using high power lasers, has been identified as a viable technique. Montani et al. [133] studied the processability of biodegradable Fe and Zn by SLM. They produced Zn parts with a relatively poor density of 88%, which they attributed to unstable laser energy caused by the attenuation of the beam by evaporated metal particles in the forming chamber. Further attempts to improve part densities were later performed in several studies. Demir et al. [77] adopted an open-air chamber instead of a closed one and, after optimizing several process conditions, reported on achieving 99% part densities. Likewise, Wen et al. [79,80] optimized the SLM processing parameters and created part densities of about 99.9%. They also noted how part porosity resulted from either (i) lack of fusion due to inadequate laser energy or (ii) via gas entrapment caused by excessive metal evaporation. Yang et al. [78] used a stockfeed of Zn and Mg powders to successfully fabricate biodegradable and biocompatible Zn-Mg alloys using SLM. Finally, Grasso et al. [134] studied the feasibility of using the plume characteristics of Zn for in-process monitoring to improve the quality of the SLM product. They proposed an automated rule that allows the extraction of pertinent information from captured video images that will be useful for monitoring purposes.

Reports on the application of different fabrication techniques to create actual Zn stents are also available and will be discussed in Section 6.6.1

5. Mechanical properties of biodegradable zinc

Zinc is not renowned for its good mechanical properties. Zinc has a lower yield and tensile strength compared to Mg or Fe. As mentioned earlier, one of the issues raised against zinc, particularly when used for cardiovascular stent applications, is its poor strength. Materials for stents are required to have a tensile strength of about 300 MPa, while pure Zn has a tensile strength of about 28–120 MPa [21].

Cast pure Zn is not technologically useful since this exhibits poor ductility (2–2.5%) at room temperature [135,136]. Zn assumes the hexagonal close-packed (HCP) structure, which inherently imparts poor ductility and toughness to the cast structure [137]. On the other hand, wrought pure Zn exhibits excellent ductility with an elongation to failure of 60–80% (tested parallel to rolling

Please cite this article as: J. Venezuela and M. S. Dargusch, The influence of alloying and fabrication techniques on the mechanical properties, biodegradability and biocompatibility of zinc: A comprehensive review, Acta Biomaterialia, https://doi.org/10.1016/j.actbio.2019.01.035

direction) [136]. This high level of ductility in wrought Zn will be crucial when manufacturing stents. Stents are typically small hollow tubes with typical diameters of about 2.5–3.0 mm [138] and strut thickness of 70–175 μm [138,139]. Stent fabrication, therefore, requires that the metal is ductile enough to be drawn and shaped to these specifications.

Various research have looked into ways to improve the mechanical properties of biodegradable Zn. The most common approach involves alloying Zn with different elements such as Mg, Cu, and Li [21,23]. The influence of fabrication techniques on the mechanical properties of Zn is also recognized by different studies [87,92,94]. A natural consequence of strengthening a metal is the reduction in ductility. This is where the excellent ductility of wrought Zn becomes useful as it allows the possibility of strengthening without significant impairment of ductility and formability.

In this chapter, results of key studies done to improve the mechanical properties of Zn are discussed. In particular, it focuses on the influence of two primary factors; i.e., alloying and fabrication method. A final section presents some critical evaluation of this topic.

Table 3 presents a catalogue of the reported mechanical properties of different biodegradable Zn and Zn alloys. This can give a quick overview of the amount of work done to improve the properties of this material.

The most commonly reported mechanical properties are (i) tensile properties, including yield strength, tensile strength, elastic modulus, and ductility derived from the standard tensile test (ASTM-E8 [140]); (ii) hardness, based on the Vickers hardness test (ASTM E384-17 [141]); and (iii) compressive properties, such as compressive yield strength and compressive elastic modulus, obtained from the mechanical compression test (ASTM-E9 [142]). Most of the tensile test specimens are often round or dog-bone-shaped and machined from plates or billets. Furthermore, tensile tests on Zn wires [102,107] and even microtubes [114] have also been reported, though these tests are not common. One challenge with tensile testing of wires is in gripping the specimen. Wires have a thin profile and are easily damaged during gripping. Tensile failures at the gripped section would often invalidate the results of a test.

As mentioned previously and seen in Table 1, the desired properties for a candidate biodegradable metal is dictated by the target medical application. Hence, future developmental work on Zn should use these set of properties as its starting framework [143,144]. It may also be suitable to use an Ashby-style materials selection chart as suggested by Bowen et al. [145], as this allows one to visualize two mechanical requirements simultaneously in a single chart. Ashby charts will also be used in the current work when appropriate.

5.1. Influence of alloying elements

Alloying refers to the process of adding impurities to enhance the properties of a metal. Alloying alters the properties of the host metal by inducing a change in the microstructure and triggering an attendant strengthening mechanism. For example, impurities that are dissolved in a single-phase microstructure cause solid solution strengthening; while alloying elements that create a second phase precipitate cause precipitation hardening [137]. For biodegradable Zn, the mechanical properties of the alloy may be influenced by (i) the type, (ii) the number, and (ii) the amount or concentration of alloying elements, as seen in Table 3.

Fig. 2 shows an Ashby chart that compares the reported mechanical properties (i.e., ductility or elongation to fracture, e_f vs. ultimate tensile strength, *UTS*) of different Zn compositions including (i) pure, (ii) binary, (iii) ternary, and (iv) quaternary alloys. The lines represent the target *UTS* (300 MPa) and e_f (18%) appropriate for some biomedical applications. This chart can help us understand the influence of alloying elements on the properties of Zn.

At first glance, what stands out is that most of the work focused on creating binary Zn alloys. Minimizing the number of alloying elements is a logical approach since each addition of an alloying element also increases expense and adds another layer of complexity during fabrication. Another observation is that very few Zn alloys, mainly extruded Zn-Mg binary alloys [94,101,102] and some ternary alloys (i.e., Zn-Mg-Sr [115] and Zn-Mg-Mn [116], have met the mechanical property standards set for cardiovascular applications. The majority of the alloys did not meet both strength and ductility requirement; while a fair amount of alloys have exceeded the ductility requirements but did not achieve the necessary strength. Even some of the commercial Zn alloys were lacking strength but possesses outstanding ductility, as indicated in Table 3. This shows the relative difficulty of producing Zn alloys that meet the standard mechanical properties.

Another important conclusion taken from these observations is that, from the point of view of enhancing mechanical properties, there's no strong justification for creating ternary and quaternary alloys. The right combination of binary alloy composition and processing may be enough to achieve the desired mechanical property levels. Again, this conclusion is made from the point of view of mechanical properties only. Considerable improvements in other properties (e.g., biocorrosion) may result from ternary or quaternary alloy combinations that will justify such practice.

Some general conclusions can be made from the tabulated mechanical property values shown in Table 3. Firstly, the addition of a new element, regardless of the type, increases the strength and decreases the ductility of Zn. This implies that, as long as the fabrication route is identical, a binary Zn alloy (i.e., Zn-X) would be stronger but less ductile than pure Zn regardless of the type of element added. The same is true when a ternary alloy derivative (e.g., Zn-Mg-X) is compared to their base binary alloy (i.e., Zn-Mg). Secondly, increasing the amount of alloying element similarly enhances the strength and reduces the ductility of Zn. However, there are exceptions such as those reported by Tang et al.[106], where both strength and ductility of Zn-Cu alloy increased with increasing Cu content, or that of Sun et al. [112], where the strength decreased while ductility increased in Zn-Mn alloys with increasing Mn content. These will be examined further in the succeeding discussions.

Fig. 3(a) and (b) show the tensile strength and ductility as a function of alloying element composition (%) for various binary Zn alloys (i.e., Mg, Ca, Sr, Cu, Ag, Al, and Mn), respectively. This comparison is made between alloys formed via one type of manufacturing technique (i.e., extrusion including the variant hot isostatic extrusion) only to eliminate the influence of fabrication method.

Fig. 3 gives a clear indication of the influence of the type of alloying element on the mechanical properties of Zn. For example, at 1% composition, the strength and ductility of the Zn alloy varied depending on the alloying element (i.e., Mg, Sr, Ca, Al, Cu). Magnesium, which is also the most common alloy addition to biodegradable Zn, had the highest impact on enhancing the mechanical strength of the Zn alloy. Copper, Ag and Sr additions also yielded alloys that are relatively strong. However, only the Zn-Mg alloys were able to meet the tensile strength of at least 300 MPa necessary for implant applications. In contrast, very few of the Zn-Mg alloys met the required ductility of 18%; while a number of the other binary alloys displayed outstanding ductility including Zn-Mn, Zn-Cu, Zn-Ag, and Zn-Al. Considering both tensile property requirements, most of the alloys did not meet the set standard values except for the Zn-1.2Mg by Shen et al. [94], the Zn-0.8Mg by Jin et al. [102], and the Zn-1Mg reported by Jarzebska et al. [101]. This

Please cite this article as: J. Venezuela and M. S. Dargusch, The influence of alloying and fabrication techniques on the mechanical properties, biodegradability and biocompatibility of zinc: A comprehensive review, Acta Biomaterialia, https://doi.org/10.1016/j.actbio.2019.01.035

Table 3
Reported mechanical properties and in vitro biodegradability of Zn and Zn alloys.

Composition	Fabrication Method	Yield strength, MPa	Tensile strength, MPa	Ductility, %	In vitro corrosion			Refs.
					Physiological test solution	Polarisation test CR, μm/yr (corrosion current density, μA/cm^2)	Immersion test CR, μm/yr (immersion time, days)	
Pure								
Zn (99.95%)	Extrusion	–	24	0.3	SBF	(*9.7*)	62 (*14*)	[19]
3 N Zn	Casting	–	20	0.3	SBF	–	64 (*14*)	[89]
4 N Zn	Casting	–	–	–	Hank's BSS	325 (*5.5*)	–	[70]
4 N Zn	Casting	10	18	0.3	Hank's BSS	–	–	[87]
	Hot-rolling	28	45	5.6		134 (*9.1*)	77 (*56*)	
	Extrusion	32	61	3.5		–	–	
4 N Zn	Casting	–	26	0	–	–	–	[92]
	Extrusion	130	180	54		–	–	
6 N Zn plate	(likely wrought)	–	35	9.4	Hank's BSS	–	11 (10) 13 (*30*)	[75]
6 N Zn tube	Extrusion + Drawing	–	44	7.6		–	28 (10) 37 (*30*)	
Zn	Casting	32	31	2.7	–	–	–	[95]
4 N Zn	Casting	23	30	3.3	Hank's BSS	50 (*3.5*)	84 (*30*) 49 (*90*)	[116]
3 N Zn	Commercial rods (likely wrought)	–	–	–	PBS Ringer's Whole blood plasma	25 (test done after 3-day immersion) 162 27 37	– – – –	[81]
Zn (99.995%)	Extrusion	51	111	60.0	Hank's BSS	131 (*9.0*)	74 (*14*)	[96]
4 N Zn	Extrusion	52	96	7.6	–	–	–	[55]
4 N Zn	Extrusion	45	89	5.5	Hank's BSS	27 (*1.8*)	–	[123]
Zn (ASTM B6-13, 99.990%)	Hot-rolled	109	140	37.0	–	–	–	[109]
4 N Zn	Hot rolling	–	–	–	SBF	160 (*11.0*)	–	[108]
4 N Zn	Extrusion + Drawing	86	116	50.0	–	–	–	[107]
Zn (99.995%)	Extrusion	55	111	64.0	Hank's BSS	(*8.9*)	77 (*14*)	[110]
4 N Zn	Extrusion	60	117	14.0	–	–	–	[112]
Zn (99.995%)	Extrusion	45	61	3.8	c-SBF	–	22 (*20*)	[106]
Zn (99.99%)	Commercial rods (likely wrought)	–	–	–	r-SBF	90 90 180	60 (1) 30 (7) 30 (*14*)	[146]
Zn (99.98%), 68% porosity	Pressure infiltration casting	5*	–	–	c-SBF	–	174+ (*60*)	[127]
75% porosity		2*	–	–			110+(*60*)	
3 N Zn	Extruded	146*	–	–	SBF	410 (*14*)	–	[126]
	Spark Plasma Sinter (Coarse powder)	43*	–	–		610	–	
	SPS (Fine powder)	31*	–	–		750	–	
Zn (99.7%)	Powder Metallurgy (PM)		33*	16*	Hank's BSS	2710 (*138*)		[113]
Zn (98.7%)	SLM	122	138	8.1	–	–	–	[80 79]
3 N Zn	SLM	43	61	1.7	SBF	–	180 (28)	[78]
Binary								
Zn-Mg								
Zn-1 Mg	Extrusion	90	155	1.8	SBF	(*1.2*)	70 (*14*)	[19]
Zn-1.5 Mg	Extrusion	–	150	0.5		(*8.8*)	63	
Zn-3 Mg	Extrusion	–	32	0.2		(7.4)	70	
Zn-1 Mg	Casting	–	153	1.5	SBF	–	53 (*14*)	[89]
Zn-1.5 Mg	Casting	–	147	0.4		–	58	
Zn-3 Mg	Casting	–	28	0.2		–	52	

(*continued on next page*)

Table 3 (*continued*)

Composition	Fabrication Method	Yield strength, MPa	Tensile strength, MPa	Ductility, %	In vitro corrosion			Refs.
					Physiological test solution	Polarisation test CR, μm/yr (corrosion current density, μA/cm^2)	Immersion test CR, μm/yr (immersion time, days)	
Zn-1 Mg	Casting	88**	–	–	3.5 wt% NaCl	(*19.1*)	–	[91]
Zn-2 Mg	Casting	143**	–	–		(*49.0*)	–	
Zn-3 Mg	Casting	165**	–	–		(*8.8*)	–	
Zn-5 Mg	Casting	250**	–	–		(*21.4*)	–	
Zn-1 Mg	Casting	92	138	0.5	SBF (Kokubo)	–	280 (7)	[92]
Zn-1 Mg	Extrusion	182	255	11.5		–	120	
Zn-1 Mg	Casting	128	185	1.8	Hank's BSS	–	–	[87]
Zn-1 Mg	Hot-rolling	181	253	11.8		76.9 (*10.8*)	83 (*56*)	
Zn-1 Mg	Extrusion	205	266	8.4		–	–	
Zn-0.5 Mg	Casting	67	134	4.8	–	–	–	[95]
Zn-1 Mg	Casting	74	143	3.3		–	–	
Zn-2 Mg	Casting	96	154	2.2		–	–	
Zn-5 Mg	Casting	101	–	–		–	–	
Zn-7 Mg	Casting	106	–	–		–	–	
Zn-0.15 Mg	Extrusion	114	250	22.0	Hank's BSS	162 (*11.0*)	79 (*14*)	[96]
Zn-0.5 Mg	Extrusion	159	297	13.0		162 (*11.0*)	81	
Zn-1 Mg	Extrusion	180	340	6.0		166 (*11.3*)	83	
Zn-3 Mg	Extrusion	291	399	1.0		125 (*8.6*)	76	
Zn-0.8 Mg	Extrusion	203	301	14.7	Ion extract from DMEM and MEM	–	69 (1)	[55]
Zn-1.2 Mg	Casting	117	130	1.4	Hank's BSS	120 (*7.7*)	80 (*30*) 70 (*90*)	[94]
Zn-1.2 Mg	Extrusion	220	363	21.3		190 (*12.4*)	110 (*30*) 90 (*90*)	
Zn-3 Mg	Casting	65	84	1.3		–	–	[98]
	Homogenized	36	46	2.1	SBF (Kokubo)	300 (*3.4*)	250 (*21*)	
	1-ECAP	137	153	4.6		240 (*2.7*)	180	
	2-ECAP	205	220	6.3		280 (*3.2*)	190	
Zn-1 Mg	Cast	–	120	0.4	–	–	–	[101]
Zn-1 Mg	Hydrostatic Extrusion	316	435	35.0		–	–	
Zn-1.6 Mg	Extrusion	232	367	4.2		–	–	
Zn-0.05 Mg	Indirect Extrusion	160	225	26.0	SBF	728	150 (*14*)	[103]
Zn-0.002 Mg	Ext + Drawing	34	63	17.0	–	–	–	[102]
Zn-0.05 Mg	Ext + Drawing	93	202	28.0		–	–	
Zn-0.08 Mg	Ext + Drawing	221	339	40.0		–	–	
Zn-0.02 Mg	Extrusion	136	167	27.0	–	–	–	[105]
	Ext + Drawing	388	455	5.4		–	–	
Zn-1 Mg	SLM	74	126	3.6	SBF	–	140 (*28*)	[78]
Zn-2 Mg	SLM	117	162	4.1		–	130	
Zn-3 Mg	SLM	152	222	7.2		–	100	
Zn-4 Mg	SLM	132	166	3.1		–	110	
Zn-Ca								
Zn-1Ca	Cast	119	165	2.1	Hank's BSS	–	–	[87]
Zn-1Ca	Hot-rolling	196	242	12.6		160 (*10.8*)	88 (*56*)	
Zn-1Ca	Extrusion	200	241	7.7		–	–	
Zn-Sr								
Zn-1Sr	Cast	120	171	2.0	Hank's BSS	–	–	[87]

Table 3 (*continued*)

Composition	Fabrication Method	Yield strength, MPa	Tensile strength, MPa	Ductility, %	In vitro corrosion			Refs.
					Physiological test solution	Polarisation test CR, μm/yr (corrosion current density, μA/cm^2)	Immersion test CR, μm/yr (immersion time, days)	
Zn-1Sr	Hot-rolling	179	218	19.7		174 (*11.8*)	95 (*56*)	
Zn-1Sr	Extrusion	216	264	10.6		–	–	
Zn-Cu								
Zn-4Cu	Extrusion	250	270	51.0	Hank's BSS	(*4.1*)	9.1 (*20*)	[66]
Zn-1Cu	Extrusion	149	186	21.0	c-SBF	–	33 (*20*)	[106]
Zn-2Cu	Extrusion	200	240	46.8		–	27	
Zn-3Cu	Extrusion	214	257	47.2		–	30	
Zn-4Cu	Extrusion	227	270	50.6		–	25.5	
Zn-3Cu	Extrusion	214	257	47.2	Hank's BSS	6 (*0.4*)	11 (*20*)	[117]
Zn-3Cu	Extrusion	247	288	45.9	SBF	85 (*5.8*)	45 (*20*)	[120]
Zn-3Cu, 68% porosity	PIC	11*	–	–	c-SBF	–	975+ (*60*)	[127]
75% porosity		6*	–	–			780+(*60*)	
Zn-Li								
Zn-0.1Li	Ext + Drawing	238	274	17.0	–	–	–	[107]
Zn-2Li	Hot-rolling	241	367	14.0	SBF	60 (*4.0*)	–	[108]
Zn-4Li	Hot-rolling	428	446	13.8		50 (*3.8*)	–	
Zn-6Li	Hot-rolling	478	569	2.4		–	–	
Zn-Ag								
Zn-2.5Ag	Extrusion	147	203	34.0	Hank's BSS	(*9.2*)	79 (*14*)	[110]
Zn-5Ag	Extrusion	207	252	36.0		(*9.7*)	81	
Zn-7Ag	Extrusion	236	287	32.0		(*9.9*)	84	
Zn-Al								
Zn-0.5Al	Extrusion	119	203	33.0	Hank's BSS	140 (*9.6*)	79 (*14*)	[96]
Zn-1Al	Extrusion	134	223	24.0		141 (*9.7*)	78	
Zn-1Al	Hot-rolling	197	238	24.0	–	–	–	[109]
Zn-3Al	Hot-rolling	202	223	31.0		–	–	
Zn-5Al	Hot-rolling	240	308	16.0		–	–	
Zn-0.5Al	Cast	–	79	1.5	SBF (Kokubo)	(*20.4*)	250 (10) 150 (*30*)	[118]
Zn-Mn								
Zn-0.2Mn	Extrusion	132	220	48.0	–	–	–	[112]
Zn-0.4Mn	Extrusion	118	200	54.0		–	–	
Zn-0.6Mn	Extrusion	118	182	71.0		–	–	
Zn-4Mn	Powder Metallurgy	–	290.8*	14.9*	Hank's BSS	720 (*48*)	–	[113]
Zn-24Mn	PM	–	132.4*	6.7*		20 (2.1)	–	
Ternary								
Zn-Mg-Ca								
Zn-1 Mg-1Ca	Casting	80	131	1.0	Hank's BSS	170	90 (*56*)	[88]
	Hot rolling	135	194	8.5				
	Extrusion	205	257	5.3				113
Zn-Mg-Sr								
Zn-1 Mg-0.1Sr	Casting	109	133	1.4	Hank's BSS	7.9 (*0.12*)	–	[115]
Zn-1 Mg-0.5Sr	Casting	129	144	1.1		7.8 (*0.11*)	–	
Zn-1 Mg-0.1Sr	Hot rolling	197	300	22.5		10.2 (*0.15*)	–	
Zn-1 Mg-1Sr	Casting	86	138	1.2	Hank's BSS	177	94 (*56*)	[88]

(*continued on next page*)

Table 3 (*continued*)

Composition	Fabrication Method	Yield strength, MPa	Tensile strength, MPa	Ductility, %	In vitro corrosion			Refs.
					Physiological test solution	Polarisation test CR, μm/yr (corrosion current density, μA/cm^2)	Immersion test CR, μm/yr (immersion time, days)	
	Hot rolling	137	198	9.7				
	Extrusion	201	253	7.4				
Zn-Mg-Fe								
Zn-5 Mg-1Fe	Hollow Sinking	151–186	180–218	5–21	SBF	–	–	[114]
Zn-5 Mg-1Fe	Mandrel Drawing	176–187	223–231	22–26		–	62 (*48*)	
Zn-5 Mg-1Fe	Hot -rolled	–	–	–		–	40 (*48*)	
Zn-Mg-Mn								
Zn-1 Mg-0.1Mn	Casting	114	131	1.1	Hank's BSS	260 (17.2)	120 (*30*) 50 (*90*)	[116]
Zn-1.5 Mg-0.1Mn	Casting	114	121	0.8		140 (9.3)	90 (*30*) 59 (*90*)	
Zn-1 Mg-0.1Mn	Hot rolling	195	299	26.1		250 (16.8)	112 (*30*) 64 (*90*)	
Zn-Ca-Sr								
Zn-1Ca-1Sr	Casting	85	141	1.1	Hank's BSS	188	109 (*56*)	[88]
	Hot rolling	140	200	8.8				
	Extrusion	212	260	6.7				
Zn-Cu-Mg								
Zn-3Cu-0.1 Mg	Extrusion	346	365	4.8	Hank's BSS	18 (*1.2*)	22 (*20*)	[117]
Zn-3Cu-0.5 Mg	Extrusion	403	416	1.9		24 (*1.6*)	30	
Zn-3Cu-1 Mg	Extrusion	427	441	0.9		180 (*12.4*)	43	
Zn-Al-Mg								
Zn-0.5Al-0.1 Mg	Cast	–	87	1.6	SBF (Kokubo)	(*17.3*)	200 (10) 130 (*30*)	[118]
Zn-0.5Al-0.3 Mg	Cast	–	93	1.7		(*11.2*)	180 (10) 110 (*30*)	
Zn-0.5Al-0.5 Mg	Cast	–	102	2.1		(*9.5*)	120 (10) 80 (*30*)	
Zn-Al-Cu								
Zn-4Al-1Cu	Extrusion	171	210	1.0	SBF	(*5.2*)	70 (*14*)	[19]
Zn-Cu-Fe								
Zn-3Cu-0.5Fe	Extrusion	231	284	32.7	SBF	105 (*7.1*)	64 (*20*)	[120]
Zn-3Cu-1Fe	Extrusion	221	272	19.6		130 (*8.8*)	69	
Zn-Mn-Cu								
Zn-0.75Mn-0.40Cu	Casting	113	120	0.4	–	–	–	[119]
Zn-0.35Mn-0.41Cu	Casting	77	84	0.3		–	–	
Zn-0.75Mn-0.40Cu	Hot rolling	196	277	15.3	SBF	62 (*4.1*)	50 (*14*)	
Zn-0.35Mn-0.41Cu	Hot rolling	198	292	29.6		98 (*6.5*)	65	
Quaternary								
Zn-Mg-Al-Bi								
Zn-0.5Al-0.5Mg-0.1Bi	Casting	–	102	2.4	SBF (Kokubo)	(*12.1*)	174 (7)	[122]
Zn-0.5Al-0.5Mg-0.3Bi	Casting	–	108	2.7		(*16.4*)	203	
Zn-0.5Al-0.5Mg-0.5Bi	Casting	–	98	2.0		(*22.7*)	283	
Commercial								
ZA4-1 (3.5–4.5Al, 0.75–1.25 Cu, 0.03–0.08Mg)	Extrusion	78	187	170	Hank's BSS	47 (*3.0*)	–	[123]
ZA4-3 (3.5–4.3Al, 2.5–3.2Cu, 0.03–0.06Mg)	Extrusion	110	201	126		374 (*7.2*)	–	

Table 3 (*continued*)

Composition	Fabrication Method	Yield strength, MPa	Tensile strength, MPa	Ductility, %	In vitro corrosion			Refs.
					Physiological test solution	Polarisation test CR, µm/yr (corrosion current density, µA/cm^2)	Immersion test CR, µm/yr (immersion time, days)	
ZA6-1 (5.6–6.0Al, 1.2–1.6 Cu)	Extrusion	130	228	111		86 (5.3)	–	
Zn-5Al-4Mg	Wrought	–	89.9***	–	SBF	320 (*17.7*)	350 (7)	[124]
Composite (MMC)								
Zn-1HA	Spark plasma sintering	68*	158*	90*	Hank's BSS	327 (*21*)	2.6 (*50*)	[128]
Zn-5HA		40*	108*	80*		630 (*39*)	10	
Zn-10HA		44*	72*	30*		856 (*51*)	425	

*Properties obtained from compression test; **Vickers Microhardnes; ***Rockwell Hardness B, +corrosion rate is reported in µg/day.

result indicates that the optimum Mg content appears to be about 1 to 1.5 wt% and that a proper fabrication technique could yield the desired mechanical properties. Copper (Cu) and silver (Ag) additions also produced alloys that are relatively strong and ductile and could be promising alloys in the future.

Fig. 3 also show the effect of the amount of alloying element on the mechanical properties of Zn. Except for a few cases, such as in the Zn-Mn alloy, the strength increases while ductility decreases in the Zn alloy with increasing alloying element concentration. The case of Zn-Mg is interesting as some reported tensile strength to be proportional with Mg content [55,95,96], while others reported the opposite [19,89].

The dependence of mechanical properties on the type and amount of alloying elements may be traced to how these factors influence the inherent microstructures of these alloys. Alloying elements may affect the strength of the host metal through different mechanisms depending on the type of microstructure created by alloy addition. For example, for a solid solution, strengthening is via the mechanism of solid solution strengthening; while for a multi-phase alloy, enhancement is achieved by second phase strengthening.

In solid solution strengthening, the degree of hardening depends on the size, and therefore the type, of alloying elements [137]. A considerable size difference between host and the impurity atom (either substitutional or interstitial impurity atom) induces higher lattice distortion and often leads to greater strengthening. For second phase strengthening, the degree of strengthening depends on the (i) characteristic, (ii) relative amount, (iii) shape and (iv) distribution of the precipitate [137]. These parameters will again depend on the type and amount of alloying elements, as well as in the kind of fabrication technique.

In most of the cited biodegradable Zn binary alloys, the microstructure consists of multiphase systems. This means that the mechanical properties of these alloys would depend primarily on the characteristics of the second phase or precipitate. Levy et al. [22] gave a good summary of the microstructures reported in different biodegradable Zn alloys; hence, an exhaustive list is not anymore included in the current work. A thorough discussion of the influence of multiphase microstructures on the mechanical properties of Zn alloys may not be any more necessary. However, two cases will be cited herein to highlight the microstructure-property relationship in Zn alloys. The first case is that of the Zn-Mg alloy, which is the most studied Zn alloy and whose behaviour is representative of the other binary alloys. The second one is the Zn-Mn alloy, which exhibited an abnormal trend concerning the relationship between mechanical properties and alloy concentration.

Fig. 4 shows the phase diagram of the Zn-Mg alloy [102]. Most of the reported biodegradable Zn-Mg alloys have Mg contents of less than 10%. The phase diagram indicates that in this composition range, a Zn-Mg solid solution (α-Zn) occurs at Mg wt% < 0.008% and a multiphase system consisting of α-Zn and Mg_2Zn_{11} at Mg wt% > 0.008%. However, note that such applies to a temperature of about 200 °C, and the solubility limit of 0.008% is expected to decrease at lower temperatures. This implies that all of the reported biodegradable Zn-Mg alloys are primarily multi-phase comprising of α-Zn and Mg_2Zn_{11}. The intermetallic Mg_2Zn_{11} is believed to be very hard but brittle; hence, the mechanical properties of the Zn-Mg alloys are largely influenced by the relative amount of this intermetallic. The amount of Mg_2Zn_{11} is expected to increase with increasing Mg content. It is then reasonable to also expect an increase in strength and a decrease in ductility with increasing amounts of Mg in the Zn alloy, consistent with published results [19,87,92,96,102]. It needs to be mentioned that the size and distribution of the Mg_2Zn_{11} are equally important, but these features are dependent on the fabrication method. The

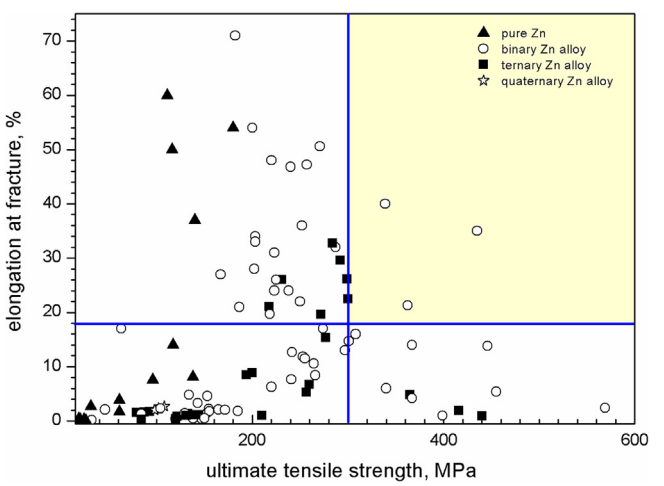

Fig. 2. Plot of elongation at fracture (%) vs UTS as a function of the number of alloying elements in Zn. Plotted values were obtained from appropriate references listed in Table 3. Superimposed lines represent the nominal standard values required for materials used for cardiovascular and orthopedic medical applications. The coloured region represents the space of acceptable properties.

influence of fabrication technique on microstructure will be discussed in the succeeding section.

For the Zn-Mn alloy, Sun et al. [112] reported that the alloy's mechanical strength decreased and ductility increased with increasing alloy content (i.e., 0.2, 0.4, and 0.6 wt% Mn), contrary to what was typically seen in other biodegradable Zn alloys. They noted that increased Mn additions significantly refined the Zn grains and also increased the presence of the intermetallic, $MnZn_{13}$. Both of these microstructural changes should have improved the strength of the alloy. However, they also noted a decrease in the number of tensile twins with increasing Mn content. They then concluded that this decrease in twin defect played a significant role in reducing strength and created the observed anomalous mechanical behaviour of the metal. This proves that while hard precipitates are expected to enhance strength, a combination of other microstructural features can still influence the mechanical properties of the alloy.

Alloying appears to be similarly effective in improving the mechanical strength of porous Zn constructs. For example, Hou et al. [127] noted that adding Cu improved the compressive strength of porous Zn, even at 68% and 75% porosity volumes.

5.2. Influence of fabrication technique

An important concept in the field of materials science is the interrelationship between processing, microstructure, and properties. Different fabrication techniques create different microstructures with varying properties. Therefore, the idea of controlling material property by adopting different fabrication techniques is reasonable and has already been implemented in different metallic systems.

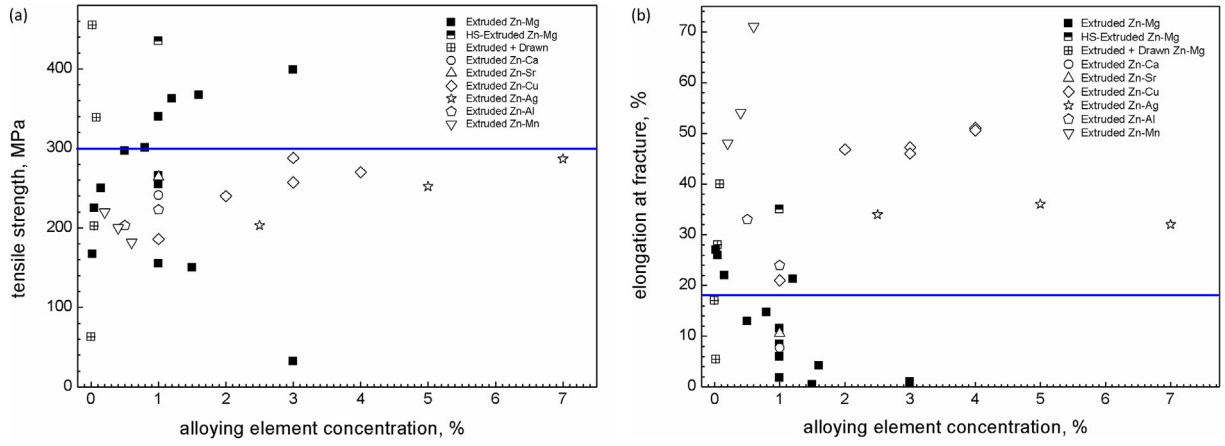

Fig. 3. The plot of (a) tensile strength and (b) elongation at fracture (%) versus alloying element concentration (%) for different binary Zn alloys formed via extrusion. Plotted values were obtained from appropriate references listed in Table 3.

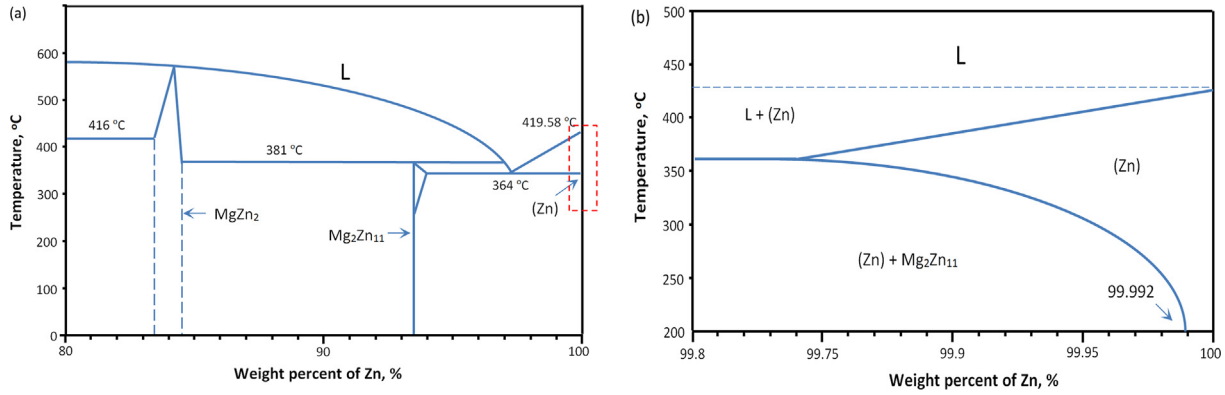

Fig. 4. The Zn-Mg phase diagram at (a) 80–100 wt% Zn and magnified at (b) 99.8–100 wt% Zn (Adopted from Jin et al. [102]).

Please cite this article as: J. Venezuela and M. S. Dargusch, The influence of alloying and fabrication techniques on the mechanical properties, biodegradability and biocompatibility of zinc: A comprehensive review, Acta Biomaterialia, https://doi.org/10.1016/j.actbio.2019.01.035

Fig. 5a and b show a plot of tensile strength vs. alloying element concentration and elongation to fracture (%) vs. alloying element concentration, respectively, of different Zn-Mg alloys as a function of various fabrication techniques. The reported methods include the traditional metal forming processes such as casting, extrusion, drawing, and hot rolling, as well as some of the advanced techniques such as cold hydrostatic extrusion, ECAP, and SLM. Other binary alloys of Zn are deliberately excluded from the plot. This allows a direct comparison between techniques by removing the influence of the type of alloying elements.

Fig. 5 clearly indicates that the products of the wrought techniques (i.e., extrusion, drawing, rolling) exhibit a better combination of mechanical properties (i.e., higher strength and better ductility) than cast products. This may be seen by comparing the strength and ductility of the Zn-Mg alloy at specific compositions (e.g., 1%). The extruded Zn and Zn alloys possessed the highest strength, followed by the rolled products, then the as-cast ones [88]. The benefits of a combined extrusion and drawing process, as well as the advanced wrought processing, are also evident. For example, the combined extrusion and drawing process [102] and the cold hydrostatic extrusion [101] yielded products with the best combination of properties among the Zn-Mg alloys; i.e., relatively high strength and high ductility. ECAP [98], another advanced wrought process, was also seen to improve both strength and ductility of the cast Zn-3Mg. In terms of ductility, wrought products generally exhibited the highest ductility; while their cast counterparts possessed the lowest ductility. Jin et al. [102] reported that a combination of extrusion and drawing, coupled with microalloying, is especially effective in significantly enhancing both the strength and ductility of the Zn alloy. In contrast, Wang et al. [105] noted that the strength increased but ductility decreased after drawing (cumulative reduction in area of 97%) of an extruded Zn-0.02Mg alloy. It is also noteworthy to mention that only the extrusion and the extrusion + drawing process yielded Zn products that have sufficient strength and ductility to meet the nominal mechanical property standards.

Fig. 5 yields some important considerations. It gives clear evidence on the influence of processing technique on the resulting mechanical properties of Zn and Zn alloys, and the evident advantages of using wrought Zn products in future implants. This is consistent with the well-known superiority of wrought Zn products over their as-cast counterparts [135,136]. The mechanical weakness of the cast Zn-Mg alloy may be linked to several factors: (i) the HCP crystal structure that makes Zn inherently poor in ductility, (ii) the presence of relatively coarse-grained microstructure (e.g., columnar, dendritic grain structures) caused by the slow cooling of the metal, (iii) casting defects such as porosity, voids, inclusions, even micro- and macrosegregation, and (iv) the presence of brittle, second phase precipitates (e.g., Mg_2Zn_{11}). It appears that Zn has a propensity to form brittle intermetallics not only when alloyed with Mg, but also with other elements such as Ca, Sr, Al, Cu, Li, and Ag [22]. The presence of intermetallic precipitates is of critical importance as it can strongly influence the mechanical properties strength of the host metal in two ways. Intermetallic precipitates can either cause weakening, when these are coarse and distributed non-uniformly; or strengthening when these are fine and distributed uniformly in the host metal.

On the other hand, Dambatta et al. [99] showed that homogenization of cast Zn could be beneficial. This additional heat treatment improves ductility by relieving stresses, reducing defects, and improving compositional uniformity in the as-cast structure. Homogenization also increases the elongation at fracture but lowers the alloy's strength due to larger grain sizes [96,99]. Vida et al. [100] fabricated cast Zn-Mg (Zn-0.3%Mg and Zn-0.5%Mg) alloys via a directional solidification process. They observed different microstructures, such as columnar, columnar/dendritic, and equiaxed, formed along the length of the cast alloy due to the different rates of cooling present during the solidification step. While they did not report on the mechanical properties of the cast Zn product, it would be logical to conclude that these different combinations of microstructures would possess a range of mechanical properties.

Though lower strength and elongation properties are intrinsic to as-cast Zn alloys [19], the mechanical properties of Zn-Mg alloys are improved by employing thermal wrought processes such as hot extrusion [55,87,92,94,96] or hot rolling [87]. Wrought processing is known to alter the microstructure of the feed metal effectively. The occurrence of recovery and recrystallization during hot working determines the final microstructure and the attendant good mechanical properties of the Zn alloy. Hot working especially improves the elongation properties [55,87,92,94] by redistributing the brittle phase particles [65], dynamically recrystallizing the Zn grains [55,96], refining grain sizes [92,94,96] and reducing the volume fraction of the eutectic mixture [94]. The combination of hot extrusion followed by cold drawing is also expected to improve the strength of Zn [137,147]. Cold working will increase the dislocation density in the hot-worked microstructure and strengthening via the strain hardening mechanism [147].

Powder metallurgy (P/M) appears to be a viable process for forming Zn. The powder process can be used for fabricating (i) fully

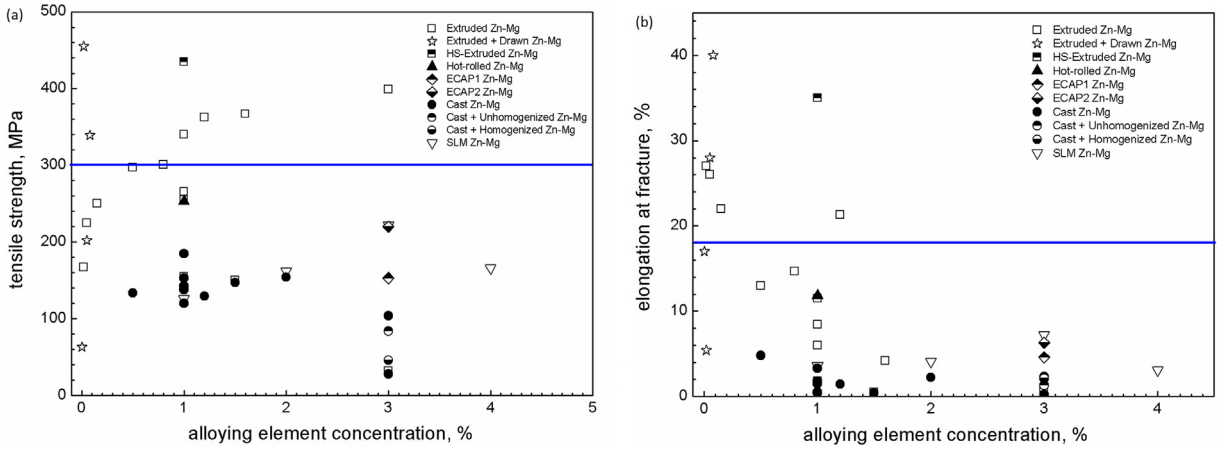

Fig. 5. The plot of (a) tensile strength and (b) elongation at fracture (%) versus alloying element concentration (%) of biodegradable Zn-Mg alloys formed via different fabrication techniques. Plotted values were obtained from appropriate references listed in Table 3.

Please cite this article as: J. Venezuela and M. S. Dargusch, The influence of alloying and fabrication techniques on the mechanical properties, biodegradability and biocompatibility of zinc: A comprehensive review, Acta Biomaterialia, https://doi.org/10.1016/j.actbio.2019.01.035

dense components [113], (ii) components with tunable porosities [126], and even (iii) metal-matrix composites (MMC) [128]. Porous Zn can also be created using NaCl as a space holder [127]. However, when adopting these techniques, the user needs to recognize the adverse influence of porosities on the mechanical properties of its products. Additionally, Capek et al. [126] observed that sintered Zn made of coarse powder exhibited better compressive properties than those made of fine powder due to a lower volume of porosity. Hou et al. [127] noted that increasing porosity content lowers the compressive strength of both Zn and Zn-3Cu, as seen in Table 3. This is consistent with other reports that describe the negative influence of porosity on the mechanical properties of 3D printed Zn [79,80]. The fact that compressive tests are more appropriate for testing porous Zn is a good indication of the adverse effects of porosity on the tensile properties of a material. This behaviour limits the applicability of porous Zn to those applications where compressive properties are more important, such as in some orthopedic applications (e.g., dental medicine) [148].

Yang et al. [128] was one of the first to report on the mechanical properties of a biodegradable Zn-hydroxyapatite (Zn-*x*HA, x = 1.5–10 wt%) MMC. This combination would be particularly useful for orthopedic applications since hydroxyapatite is a known bioactive ceramic [149]. They observed that increasing amounts of HA had no influence on compressive yield strength and microhardness, but significantly reduced the ultimate compressive strength of the composite. Though no explanation was offered for the observed weakening, it is possible that this could be attributed to poor interface adhesion between the two materials.

It will be interesting how the mechanical properties of additive-manufactured biodegradable Zn evolve in the future. 3-D printed metal products often experience much higher cooling rates during solidification compared to the cast metal. This means that the 3-D printed product will have a finer microstructure and is expected to be stronger than a cast product. Indeed, Wen et al. [79] created 3-D printed pure Zn with generally better mechanical properties than its cast and even some of its extruded counterparts, as seen in Table 3. Likewise, Yang et al. [78] reported that the SLM-manufactured Zn-3Mg alloy exhibited better mechanical properties (i.e., YS, UTS and % ductility of 152 MPa, 222 MPa, and 7.2%, respectively) than the cast alloy. However, this set of mechanical properties is still inadequate to meet the nominal standards. One particular issue with 3-D printed metals is the presence of porosities, which adversely affect both the strength and ductility of the product [79,133]. This and other issues will have to be addressed in future research to improve the feasibility of 3-D printed Zn parts in implant applications.

5.3. Critical evaluation

What is evident from the above-cited works is the certainty of manipulating the mechanical properties of Zn to the desired level via several approaches, specifically by altering the chemical composition or by adopting the appropriate fabrication technique.

The collated literature suggest that the Zn-Mg alloy coupled with an appropriate wrought processing technique (i.e., extrusion, hydrostatic extrusion, drawing) offers the best combination of mechanical strength, ductility, and formability. The recommended alloy composition range would be less than 1.5% Mg. Beyond this composition, the alloys gain strength but significantly loses ductility due to the increase in the hard but brittle phase, Mg_2Zn_{11}. Some of the microalloyed Zn-Mg alloys appeared to be equally promising, such as the extruded and drawn Zn-0.08Mg [102] and Zn-0.02Mg [105]. It is also worthwhile to consider pursuing future studies on cold hydrostatic extrusion as initial results indicate its capability to produce products with desirable mechanical properties.

Though there are still some perceived challenges with regards to fabricating Zn with properties that meet the nominal standard, it is likely that future research will be successful in finding the correct alloy composition and fabrication technique that will yield the desired product. However, it would also be beneficial if future endeavours are geared toward addressing several important issues with regard to understanding the mechanical behaviour of Zn.

Firstly, it is essential to identify the mechanical properties that are most relevant to a corresponding medical application. For example, many studies report on the alloys' tensile strength together with hardness data. For most metals, hardness is proportional to tensile strength. This means that the hardness results are redundant when tensile values are already cited, and the resources used in doing this test could have been used for a more relevant one. Also, related to the issue of identifying application-specific properties, it was observed that most studies intending to use Zn for stent applications did not measure the radial strength of Zn. For stents, radial strength is reasonably crucial to measure as this parameter directly relates to the mechanical behaviour of hollow tubes. It is clear that by establishing a hierarchy of critical parameters for specific applications (e.g., for stents, important properties may include tensile strength, ductility, fatigue, collapse pressure, and tube radial strength) then results of studies become more relevant and project resources are more efficiently utilized.

Secondly, the accurate figure of merit for these identified properties needs to be ascertained. For example, for cardiovascular stent applications, candidate metallic materials are required to possess a minimum tensile strength of 300 MPa and a minimum ductility of 18%. It appears that these values were adopted from specifications imposed on stainless steel (SS) stents. However, most of the commercially-available, bioabsorbable polymeric stents have mechanical property values that are significantly lower than the mentioned standard. For example, Abbott's Absorb BVS and Amaranth's Fortitude Aptitude stents are both made of poly-L-lactic acid (PLLA), which has a tensile strength of about 60–70 MPa and a % elongation at break of about 2–6% [139]. Even some of the proposed bio-corrodible metal-based stents use metals with properties that barely exceed the standard. For example, Biotronik's DREAMS 2G and Envison Scientific's BIOLUTE-next uses the WE43 Mg alloy that has a tensile strength of 220–330 MPa and % elongation at break of 2–20% [139]. Furthermore, Yang et al. [86] reported that a pure Zn stent is indeed viable as it was able to hold mechanical integrity for at least 6 months in vivo. From these cases, it is clear that the current nominal standard needs to be re-evaluated. A more relevant and accurate figure of merit for a specified property would undoubtedly lead to better screening and selection of future biomaterial prospects.

Finally, the issue of age-hardening and strain-rate sensitivity in Zn alloys needs to be studied and resolved. Jin et al. [102] reported on the age hardening of the Zn-0.08Mg alloy, where the tensile strength increased from 266 to 498 MPa and ductility decreased from 29.8 to 12.7% after room-temperature aging of 9 days (tested at a strain rate of 3.30×10^{-3}). After 12 months, the tensile strength was measured at 434 MPa and ductility at 3.5%. While the increase in strength is attractive, the significant drop in ductility is objectionable. This instability in mechanical properties with aging time is alarming and can severely limit the applicability of the biodegradable Zn alloy. Jin et al. also noted that the mechanical properties of the microalloyed Zn were strain-rate sensitive. For example, by increasing the strain rate from $1.67 \times 10^{-4}\ s^{-1}$ to $1.67 \times 10^{-2}\ s^{-1}$, the tensile strength of Zn-0.8Mg increased from 227 MPa to 614 MPa and ductility decreased from 92.3% to 2.3%. The strain-rate sensitivity of Zn alloys is important to assess as this will define not only the applicability of the alloy but also the proper fabrication technique for shaping the metal. It is also possible that these two phenomena occur just for some of the Zn alloys.

Please cite this article as: J. Venezuela and M. S. Dargusch, The influence of alloying and fabrication techniques on the mechanical properties, biodegradability and biocompatibility of zinc: A comprehensive review, Acta Biomaterialia, https://doi.org/10.1016/j.actbio.2019.01.035

However, it is clear that the occurrence of these phenomena needs to be ascertained and its impact on service performance be assessed before a candidate Zn alloy is endorsed for commercial use.

6. Biodegradation and biocompatibility of zinc

Biodegradation or biocorrosion refers to the decomposition of a material by the action of living organisms such as bacteria and microbes, or by other biological means such as being inside the human body. While the definition of biodegradation is reasonably straightforward, biocompatibility is a broad and complex term. Several definitions have already been proposed, yet no single definition encompasses what biocompatibility implies. Biocompatibility can describe the property of a material to exist harmoniously with living tissues without causing serious harm or deleterious changes to the living host. On the other hand, some proposed that biocompatibility should also include the ability of the material to perform its desired therapeutic function without eliciting any undesirable side effect to its host [150]. Williams [150] suggested that the key to understanding biocompatibility is to determine which chemical, biochemical, physiological, physical or other mechanisms become operative at the physiological conditions associated with the contact between the biomaterial and the tissues of the body, and then assess the consequences of such interactions.

In this section, the biodegradation and biocompatibility of Zn and Zn alloys will be discussed. The section starts with a description of the different techniques to assess biodegradability and biocompatibility, followed by a discussion of the corrosion mechanism for Zn in a physiological environment. The succeeding chapters will cover in vitro corrosion behaviour, in vitro biocompatibility, and in vivo performance of biodegradable Zn.

6.1. Assessment of biocorrosion and biocompatibility

Both biodegradability and biocompatibility are of primary importance when assessing the properties of a candidate implant material. Both properties may be evaluated in vitro or in vivo. The term in vitro literally means 'in glass'. An in vitro test, therefore, means that the test is conducted away from the usual biological surrounding. When assessing a candidate implant material, this means that the test is conducted outside of the human body. The term in vivo means 'within the living'. Hence, an in vivo test implies that the test is done within its natural biological setting; and in an implant's case, within an animal or the human body.

In vitro biocorrosion testing involves several techniques, with two of the most common being (i) electrochemical polarisation tests and (ii) immersion test. It needs to be mentioned that each method possesses salient features and applicability, hence the need for prudence when using and interpreting results from a particular technique. A review by Kirkland et al. [151] of the different techniques to assess the corrosion of biodegradable Mg reveals the shortcomings of users to understand the applicability each corrosion test, as well as a lack of control of experimental variables that profoundly impact results and its interpretation.

Potentiodynamic polarisation experiments involve the classic three-electrode apparatus consisting of a working electrode (the tested metal), a reference electrode (e.g., standard calomel electrode) and a counter electrode (e.g., platinum). Typically, the test electrolyte is a fluid that mimics the physiological environment, such as the balanced salt solutions (BSS) like Ringer's (RBSS) and Hanks', phosphate-buffered saline (PBS) solution, and simulated body fluid (SBF) [103]. In some degradation tests, actual human plasma and whole blood were used [81]. A potential is applied to the working electrode, and the output current is monitored. The scan is performed over a certain potential range and at a set scan rate (e.g., 0.1667 mV/s). The test generates a plot of current versus potential (IV curve), which is analyzed to yield important parameters such as the corrosion potential (E_{corr}) and corrosion current density (i_{corr}). The corrosion rate (CR) in mm yr^{-1} may be determined according to ASTM G59-97 [152]:

$$CR = 3.27 \times 10^3 \frac{i_{corr} EW}{\rho} \quad (1)$$

where i_{corr} ($\mu A\ cm^{-2}$) is the corrosion current density, EW ($g\ eq^{-1}$) is the equivalent weight, and ρ ($g\ cm^{-3}$) is the density of the metal.

Another popular electrochemical test is the electrochemical impedance spectroscopy (EIS) [153]. The EIS uses alternating current (AC) polarisation versus direct current (DC) polarisation in the traditional potentiodynamic test. Impedance, capacitance, and resistance values are typically obtained from the test; and such information can elucidate on the active corrosion mechanisms when the metal is exposed to a specific environment. However, EIS analysis often requires a mature and deep understanding of the corrosion process to acquire accurate interpretations of test results. Finally, EIS may also be used to estimate the rate of corrosion by using the polarisation resistance, R_p, and the Stern-Geary relationship to get i_{corr} [152]:

$$i_{corr} = \frac{\beta_a \beta_c}{2.303 R_p (\beta_a + \beta_c)} \quad (2)$$

where β_a and β_c are the anodic and cathodic Tafel slopes. This value of i_{corr} may then be used to measure the corrosion rate, CR, according to Eq. (1).

The immersion test, as the name implies, involves dipping or immersing the test material in the corrosive environment, typically in the physiological fluid, for a specified period. A common standard adopted for the immersion test is ASTM G31-72 [154]. The reported immersion tests are typically done in static flow conditions, with the test solution regularly replaced with a fresh one after a certain immersion period. Regular replacement of the test solution is important as the Zn corrosion process is found to increase the pH of the bath [19], which in turn affects the rate of corrosion of the tested metal. After the specified immersion interval has elapsed, the specimen is taken out of the solution, cleaned of corrosion products (following an appropriate standard, e.g., ASTM G1-03 [155]), and weighed. The corrosion rate, CR ($mm\ yr^{-1}$), may be evaluated using the equation [154]:

$$CR = K \frac{W}{At\rho} \quad (3)$$

where K is a constant, W (g) is the mass loss of the specimen, A (cm^2) is the surface area, t (h) is the time of exposure, and ρ ($g\ cm^{-3}$) is the density.

Another way of estimating in vitro corrosion rate is by measuring the amount of released metal ions in the cultivation medium of a biocompatibility test. Kubasek et al. [55] proposed this approached where they measured the amount of Zn ions present in the DMEM (Dulbecco's modified Eagle's medium) and MEM (minimum essential medium) extracts using ICP-MS (inductively coupled plasma mass spectrometry).

When assessing biocompatibility, a good starting point is to understand that there are a number of possible responses that a living host elicits when it comes into contact with a biomaterial. Williams [150] gave an exhaustive list of these responses, which includes (i) generalised cytotoxic effects; (ii) protein adsorption and desorption characteristics; (iii) fibroblast behaviour and fibrosis; (iv) specific cell responses such as osteoclasts and osteoblasts for bone; (v) platelet adhesion, activation, aggregation; (vi)

Please cite this article as: J. Venezuela and M. S. Dargusch, The influence of alloying and fabrication techniques on the mechanical properties, biodegradability and biocompatibility of zinc: A comprehensive review, Acta Biomaterialia, https://doi.org/10.1016/j.actbio.2019.01.035

immune cell responses; (vii) acute and delayed hypersensitivity; (viii) genotoxicity, and (ix) tumor formation. Therefore, biocompatibility tests are similarly numerous and are used to qualitatively and quantitatively assess these responses of the tissue to the new material [156].

Some of the in vitro biocompatibility tests reported for biodegradable Zn include testing for (i) cell viability or cytotoxicity [66,70,78,93,94,103,106,117,118,123], (ii) cell proliferation [55,87,157] (iii) cell adherence [92,157], (iv) hemolysis and hemocompatibility [70,75,87,94,116,123], (v) dynamic blood clotting and platelet adhesion [70,94,116,123], (vi) enzymatic and hydrolytic degradation [76], (vii) inflammatory response [93], (viii) gene expression profiles and genotoxicity [55,157], (ix) systemic toxicity [103], and (x) antibacterial effect [66,106,118]. These tests are often done in compliance with an established standard; e.g., ISO 10993-5 [158] is adopted to test in vitro cytotoxicity, ISO 10993-11 [159] for testing systemic toxicity, and ASTM F-756-17 for assessing hemocompatibility [160].

In vivo biodegradation and in vivo compatibility tests involve the implantation of the biomaterial in a living host. For Zn, the reported host animals include Sprague-Dawley rats [18,72,74,102,107,109], C57BL/6 mice [87] and rabbits [86,103]. Implant location often depended on the intended application. For example, for cardiovascular stent application, the Zn metal was implanted in the abdominal aorta [18,74,102,108]; while for orthopedic application, Zn was inserted in the bone [87,103]. A novel, low-cost method for implanting wires was proposed by Pierson et al. [60], and this was adopted in several studies [18,74,102,108]. This involves puncturing the arterial wall with the implant, directing a portion of the implant within the lumen, and eventually redirecting the implant to puncture the wall a second time to exteriorize the wire from the lumen. This allows a portion of the wire to be exposed to flowing blood and simulating the service condition of a stent. After some time, the implant is removed and the explanted material is then assessed.

The corrosion rate of the implant may be measured by determining weight loss, as determined by equation (2). However, Bowen et al. [161] suggested that this conventional method is not appropriate for determining the corrosion rate of a specimen with a high aspect ratio, such as a wire. They proposed that the corrosion rate may be assessed by measuring the reduction in cross-sectional area (CSA) over time of exposure. The corrosion penetration rate, P', is then calculated using the equation [161]:

$$P' = \frac{\sqrt{\frac{A_o}{\pi}} - \sqrt{\frac{A_t}{\pi}}}{t} \quad (4)$$

where A_o, is the nominal CSA, A_t is the instantaneous CSA at implantation time, t.

Li et al. [87] proposed another technique for measuring in vivo corrosion rate by using micro-CT imaging to measure changes in implant volume. Corrosion rate, CR, is then estimated using the equation:

$$CR = \frac{V_0 - V_t}{At} \quad (5)$$

where V_o, is the volume of the implant at week 0, V_t is the volume of the implant at the designated implantation time interval, t, and A is the initial implant surface area.

In vivo biocompatibility is determined by assessing the overall health of the tissue mass surrounding the implant via histological analysis. Cell proliferation, cell morphology, osseointegration, antibacterial properties, and inflammatory response of the affected tissues may be checked. Systemic toxicity, which refers to toxic effects in a site distant from the implant location, may also be determined. For example, viscera histology is conducted to check if the internal organs (e.g., heart, liver, and kidney) of the host carry signs of the adverse side effects of degradation products, such as infarctions, pathological changes, or corrosion product accumulation [86,103].

6.2. Corrosion mechanism of Zn in a physiological environment

The environmental conditions that metals encounter inside the body are relatively unique. It is therefore not surprising that the corrosion behaviour of an implanted metal is different compared to typical ambient or even saline corrosion performance. The characteristics of this environment, from the corrosion-inducing aspect, include [162]: (i) the presence of different salts in the blood, (ii) a slightly elevated temperature of 37 °C, (iii) an inherently neutral pH that can change from acidic to basic depending on tissue response to the implant, and (iv) a controlled amount of oxygen that depends on which part of the body (e.g., bone vs. soft tissues) the implant is attached.

Table 3 includes a list of the reported in vitro corrosion rate of pure Zn in different physiological fluids. Though the scatter in the reported corrosion rate of pure Zn may be high, what is clear is that pure Zn definitely corrodes in a physiological environment, as was observed in in vivo experiments [18].

Zheng et al. [9] proposed a generalized reaction to describe the degradation of metals in the nearly neutral environment present inside the human body. When applied to Zn, the oxidation and cathodic reaction are as follows:

$$Zn \rightarrow Zn^{+2} + 2e^- \quad (6)$$

$$2H_2O + O_2 + 4e^- \rightarrow OH^- \quad (7)$$

while the product formation reaction involves:

$$Zn^{+2} + 2OH^- \rightarrow Zn(OH)_2 \quad (8)$$

$$Zn^{+2} + 2OH^- \rightarrow ZnO + H_2O \quad (9)$$

It is believed that zincite (ZnO) is the more dominant corrosion product than zinc hydroxide ($Zn(OH)_2$) as it is the more thermodynamically stable oxide in physiological conditions. On the other hand, $Zn(OH)_2$ can redissolve due to chloride attack:

$$Zn(OH)_2 + 2Cl^- \rightarrow Zn^{+2} + 2OH^- + 2Cl^- \quad (10)$$

and the released Zn ions can react with phosphate ions to form insoluble Zn phosphate (or hopeite):

$$Zn^{+2} + 2HPO4^{-2} + 2OH^- + 2H_2O \rightarrow Zn_3(PO_4)_2 \cdot 4(H_2O) \quad (11)$$

This sequence of reactions highlights one of the advantages of Zn over Mg; i.e., the absence of gas (e.g., hydrogen) generation during biodegradation.

The above reactions show that, aside from Zn, different elements reside in the corrosion product including P, H, O, and Cl [18,19,55,92,94,99,123]. The presence of Ca and C has also been reported in the product layer, as zinc (calcium) phosphates, smithsonite or zinc carbonate ($ZnCO_3$), or bicarbonates [18,19,97,107,116,117,146]. A majority of these ions originate from the physiological environment. Complex hydroxides, carbonates, and phosphates of Zn were also observed, including hydrozincite ($Zn_5(CO_3)_2(OH)_6$), simonkolleite ($Zn_5(OH)_8Cl_2{\cdot}H_2O$), skorpionite ($Ca_3Zn_2(PO_4)_2CO_3(OH)$) $CaZn_2(PO_4)_2{\cdot}2H_2O$, $Zn_5(OH)_8Cl_2{\cdot}H_2O$, $KZnPO_4{\cdot}0.8H_2O$, and even girvasite ($H_2NaCa_2Mg_3(PO_4)_3(CO_3)(OH)_2{\cdot}4H_2O$) [82,104,107,126,163]. The presence of these compounds can vary along the thickness of the corrosion film. For example, different studies reported that the Zn-based corrosion products (e.g., ZnO, $Zn(OH)_2$, $Zn_3(PO4)_2$) are found close to the sub-

strate, while the Ca-based products (e.g., $Ca_3(PO_4)_2$, $CaHPO_4{\cdot}2H_2O$) are located on the top surface of the corrosion layer [18,19,146].

More importantly, these corrosion compounds can alter the characteristics of the product layer and consequently affect the corrosion characteristic of the underlying Zn substrate. For example, an insoluble, passive film like $ZnHPO_4$ or Zn-based carbonates (e.g., $Zn_5(CO_3)_2(OH)_6$) could protect the underlying Zn metal and delay degradation [23]. Similarly, hydrozincite and simonkolleite can form a protective layer and prevent further deterioration of biodegradable Zn [104,164]. Improvements in the degradation resistance of some Zn-Mg alloys was reported to be due to Mg-containing corrosion products that acts as a corrosion barrier [96]. In contrast, zincite enhances degradation by forming a galvanic couple with Zn [165].

Alloying elements can alter the corrosion mechanism and, consequently, the resulting corrosion product of Zn. This will be discussed in detail in the succeeding section. Furthermore, the location of the implant can influence the type of predominant corrosion layer formed on Zn. In silico tests conducted by Alves et al. [85] showed that simonkolleite [$Zn_5Cl_2(OH)_8$] predominates when Zn is implanted in the bone-muscle interface and zincite (ZnO) when implanted inside the bone. This is important as the nature of the corrosion layer could also determine the biocompatibility of the Zn implant [85].

Recently, Yang et al. [86] proposed a detailed mechanism for the degradation of a Zn stent inside a living host. Previous works have already proposed corrosion mechanisms derived from in vivo tests of Zn [18] and Zn alloys [107], and Bowen et al. [18] were the earliest to report on this subject. However, the implants used in these tests have geometries (e.g., wires or metal strips) that are fundamentally different from the typical stent. Yang et al. were the first to suggest a corrosion mechanism derived from an in vivo test where the implanted Zn has the net shape of an actual stent. Therefore, it can be stated that the conditions present during their tests are the closest to an actual cardiovascular service condition.

Yang et al. noted that Zn corrosion undergoes several stages that are coincident with artery remodelling and other biological changes occurring in the physiological environment surrounding the implant. Fig. 6 shows the evolution of the implant-tissue interaction over a period of 12 months. Fig. 7 gives a detailed schematic of the development of the degradation mechanisms, the location of the concomitant corrosion products, and the duration of the temporal tissue/implant response sequence of inflammation, granulation tissue development, and tissue remodelling.

In the first few weeks, the Zn implant is exposed to the continuously flowing blood in the artery. Under this condition, ZnO/$Zn(OH)_2$ is initially formed at the surface (Fig. 7a). Over time, this corrosion oxide eventually transforms to the more stable $Zn_3(PO_4)2{\cdot}4(H_2O)$ (Fig. 7b). Due to dynamic blood flow, mass transfer reactions are enhanced, and degradation products are removed faster thereby exposing fresh metal surface. This results in uniform or general corrosion of Zn at a relatively high rate.

Between one to three months, neointima forms on the implant by a process called endothelialization. This lining prevents direct contact between the metal and blood. Corrosion reactions are now dependent on (i) the diffusion of water, oxygen, and physiological ions through the pores of the neointima, and on (ii) the pH, which is altered from near neutral to acidic conditions due to tissue inflammation. Consequently, the degradation behaviour of the implant is altered and is significantly reduced. During this period, the Zn phosphate layer dissolves and recedes (Fig. 7c) due to a decrease in pH associated with tissue inflammation. More importantly, during the breakdown of the protective Zn phosphate film, cracks appear in the film and become sites of localized corrosion. This means that the corrosion mechanism shifts from general to localized corrosion, creating pits on the implant surface. Bowen et al. [18] had earlier reported on a similar transition in the corrosion mechanism at these exposure periods for Zn wires implanted in rats.

At 6–12 months, arterial cells continue to thicken and cover the implant. During this period, localized corrosion still dominates as the primary degradation mode. Aggressive ions (e.g., Cl^-) are able to penetrate and continuously react with Zn to form a porous, inner corrosion layer. ZnO is generated and forms a cover on top of the remaining Zn skeleton, and by this time, the Zn phosphate layer has been completely dissolved (Fig. 7d). At 6 months, though inflammation has been significantly reduced, pH in the inner layer is kept relatively high due to the slow diffusion environment. This increased pH level leads to the concentration and oversaturation of Ca ions, which is abundant in body fluids, and phosphate ions. This phenomenon induces the precipitation of calcium phosphate phases in the inner layer on top of the ZnO film (Fig. 7d). It is important to mention that the precipitation of calcium phosphate has been reported in biodegradable (e.g., Fe, Mg) and permanent metal implants (e.g., Ti, CoCr), and in both orthopedic and cardiovascular implants [9,18]. The presence of Zn ions in the region can also induce the substitution of Zn in the calcium phosphate phase. The formation of the precipitate often signals an advanced

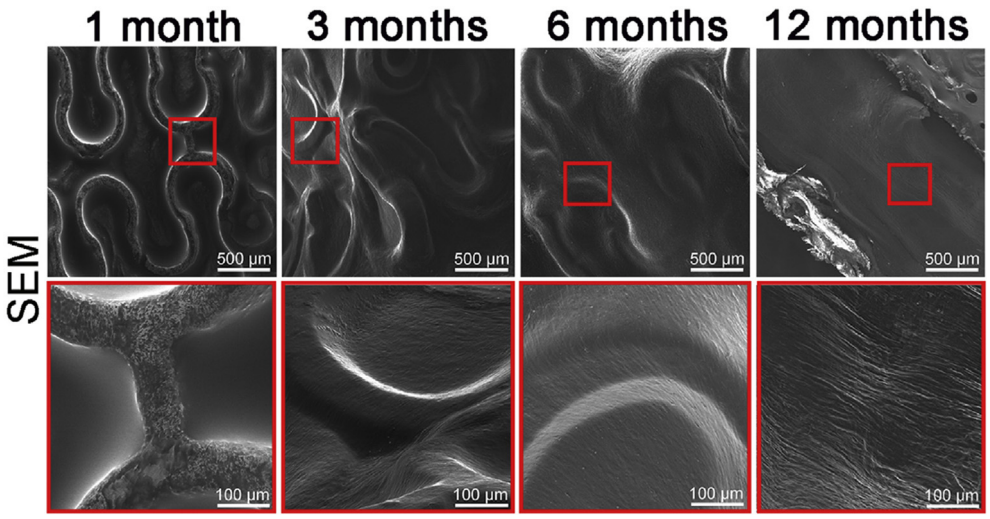

Fig. 6. Evolution of neointima growth on the zinc stent over a period of 12 months. Reprinted from [86], with permission from Elsevier.

Please cite this article as: J. Venezuela and M. S. Dargusch, The influence of alloying and fabrication techniques on the mechanical properties, biodegradability and biocompatibility of zinc: A comprehensive review, Acta Biomaterialia, https://doi.org/10.1016/j.actbio.2019.01.035

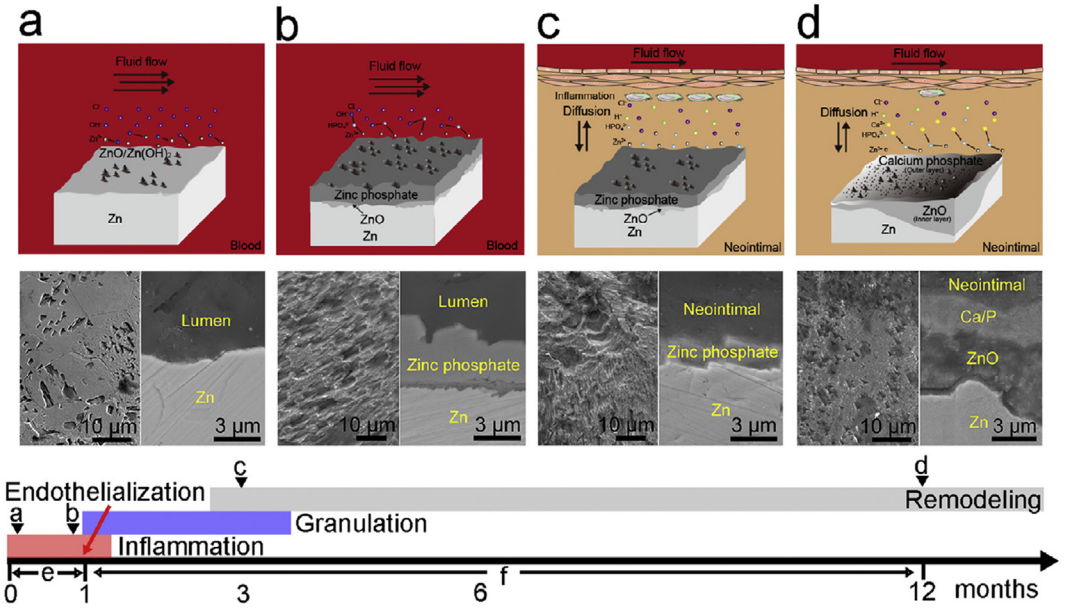

Fig. 7. Schematic showing the evolution of the in vivo degradation mechanism of Zn. (a) and (b) describes degradation during the period of endothelialisation in the first 3 months, while (c) and (d) refers to corrosion reactions occurring during granulation and remodelling between 3 and 12 months after implantation. Reprinted from [86], with permission from Elsevier.

state of degradation coincident with a maturation of the tissue healing process. It is also interesting that the amount of calcium phosphate formed in the corrosion layer depends on the type of implant material. For Mg-based stents, calcium phosphate can entirely replace the strut section, while for Zn, the calcium phosphate is only a few microns thick [86]. The presence of this dense, compact corrosion layer on Zn was similarly noted by Bowen et al. [18]. Such behaviour is attributed to Zn's two-fold ability to form soluble calcium phosphate and inhibit the phosphate layer's further growth [166].

6.3. In vitro biodegradability of Zn alloys

Table 3 includes some of the measured corrosion rates for biodegradable Zn and Zn alloys obtained from two types of in vitro test; i.e., polarisation and immersion test. In some of the studies that employed polarisation tests, corrosion rate was reported in terms of corrosion current density, and these values are also included in the table.

While comparing in vitro biocorrosion rate results with in vivo results is certainly inadvisable, comparing in vitro degradation rates reported by different studies and obtained from different experimental conditions is similarly debatable. Indeed, it is rare even to find a conformity between the corrosion rates obtained from polarisation and immersion tests done in a single study. A quick scan of Table 3 reveals that the reported in vitro tests, primarily polarisation and immersion, were done under varying test conditions such as different physiological solutions and immersion times. These test parameters, along with others such as scan rate, gas exchange in the electrolyte, ratio of specimen surface area to electrolyte volume, pH buffering techniques, and flow conditions, can influence the corrosion behaviour of the tested specimen [151,167]. Indeed, Bowen et al. [21], in their review, avoided the direct comparison of in vitro corrosion rates gathered from disparate methods declaring that doing so would be fallacious. They further advised that in vitro tests can easily produce misleading results, hence the need for great caution when adopting a methodology and interpreting results. Clearly, this is a direct consequence of the absence of an appropriate test standard for assessing the in vitro corrosion behaviour of biodegradable metals. Though efforts have been made to address this problem [168], still no such standard test exists. Hence, in the ensuing discussions, comparison of corrosion results between different studies will be avoided when possible, and conclusions would only be derived from the results of analogous works.

It would also be useful to cite a study that investigated the influence of applied stress on the biodegradability and in vitro performance of Zn in a physiological environment. Torne et al. [82] studied the susceptibility of Zn to stress corrosion cracking (SCC) in SBF and whole blood. SCC refers to the phenomenon of sudden or early failure of materials subjected to a corrosive environment [169]. SCC is critical to consider especially for implants that will be subjected to high physiological loads (e.g., bone plates, screws), and Mg is known to be susceptible to SCC [170]. Torne et al. reported that Zn remained ductile and demonstrated limited susceptibility to SCC in the physiological fluids. There was no significant reduction in UTS, though some reduction in time to failure was noted (~25% compared to reference) when Zn was in m-SBF. The SCC performance of Zn in whole blood was even better than in SBF. Torne et al. suggested that the low SCC susceptibility of Zn is due to the formation of an organic surface film that protects the corroding surface from crack formation and growth.

6.3.1. Influence of alloying

The reported values of in vitro degradation rate, as shown in Table 3, indicates that the corrosion behaviour of a Zn alloy is dependent on (i) the type and (ii) quantity (i.e., alloy concentration) of alloying element. The influence of these factors will be covered in the following discussions.

Unlike the influence of alloying elements on the mechanical properties of metals (i.e., alloying elements generally increase the strength and reduce ductility of the host metal), there is no definitive trend with regard to the influence of the type of alloying elements on corrosion behaviour. It is interesting that even reports on an individual element can be contradictory. For example, Kubasek et al. [55] noted a decrease in corrosion rate after Mg addition to cast Zn. This is favourable for maintaining post-operative load bearing capacity. Yang et al. [78] observed similar improvements

in corrosion resistance with Mg addition in 3D-printed (via SLM) Zn. However, Mostaed et al. [96] and Vojtech et al. [19] noted an increase in corrosion rate with Mg addition in extruded Zn; while Li et al. [87] and Alves et al. [104] reported the same in hot-rolled and cast Zn, respectively. Reports on Mg addition in ternary Zn alloys appear to follow the same conflicting trend. Tang et al. [117] observed that the addition of Mg enhanced the corrosion rate of extruded Zn-Cu, while Bakhsheshi-Rad et al. [122] noted the opposite when Mg was added to cast Zn-Al. In these cases, it is likely that the type of fabrication technique may have influenced the reported results.

For binary Zn alloys, additions of Ca [87], Sr [87], Cu [106], Ag [110], and Al [96] were all reported to enhance the degradation rate of wrought Zn. In contrast, Li [108] was observed to reduce the corrosion rate of hot-rolled Zn.

For ternary Zn alloys, Yue et al. [120] reported that the addition of Fe enhanced the corrosion rate of biodegradable Zn-3Cu; while for quaternary Zn alloys, Bakhsheshi-Rad et al. [122] noted that Bi increased the corrosion rate of the ternary alloy Zn-0.5Al-0.5Mg.

Concerning the influence of alloying element concentration on the degradation rate of Zn alloys, it appears that reports vary and often the trend is dictated by the type of element added. For binary Zn-Mg, the observed trends are somewhat conflicting. Mostaed et al. [96] noted that the corrosion rate of the extruded Zn-*x*Mg ($x = 0.15, 0.5, 1, 3$) alloy increased as Mg content increased to 1%, then decreased as Mg content increased to 3%. Interestingly, Vojtech et al. [19] also observed an increasing corrosion rate with increasing Mg content for extruded Zn-*x*Mg ($x = 1, 1.5$) when the corrosion rate was derived from potentiodynamic polarisation experiments (i.e., from corrosion current density); but the complete opposite was observed from the results of the immersion tests. In contrast, Yang et al. [78] only noticed a continuous reduction in degradation rate with an increasing amount of Mg in 3-D printed (SLM) Zn-*x*Mg ($x = 1, 2, 3, 4$), while Kubasek et al. [89] reported comparable corrosion rates in cast Zn-*x*Mg ($x = 1, 1.5, 3$) with different Mg content.

In some Zn-Mg-based ternary alloys, increasing Mg content reduced the corrosion rate of cast Zn-0.1Mn-*x*Mg ($x = 1, 1.5$) [116] and of cast Zn-0.5Al-*x*Mg ($x = 0.1, 0.3, 0.5$)[122]; but enhanced the degradation rate of extruded Zn-3Cu-*x*Mg ($x = 0.1, 0.5, 1$) [117].

For other binary Zn alloys, increasing Cu content improved the corrosion resistance of extruded Zn-*x*Cu ($x = 1, 2, 3, 4$) alloy [106]. Increasing Ag content enhanced the degradation rate of extruded Zn-*x*Ag ($x = 2.5, 5, 7$) alloy [110], while increasing Al content had negligible effect on the corrosion rate of extruded Zn-*x*Al ($x = 0.5, 1$) [96].

For some ternary Zn alloys, it was reported that increasing Sr and Mn amounts led to a reduction in the corrosion rate of cast Zn-1Mg-*x*Sr ($x = 0.1–0.5$) [115] and hot-rolled Zn-0.40Cu-*x*Mn ($x = 0.75, 0.35$) [119], respectively. Increasing Sr content also reduced the degradation rate of Zn–4Al–*x*Sr ($x = 0.03, 0.06, 0.1, 0.15$) [121]. In contrast, increasing Fe enhanced the degradation rate of extruded Zn-3Cu-*x*Fe ($x = 0.5, 1$) [120].

Increasing Bi concentration increased the corrosion rate of the cast quaternary alloy Zn-0.5Al-0.5Mg-*x*Bi ($x = 0.1, 0.3, 0.5$) [122]. Wang et al. [123] confirmed a significant enhancement in degradation rate after an increase in Cu amounts in some commercial Zn alloys (i.e., ZA4-1 versus ZA4-3). These alloys are quaternary Zn alloys consisting of Zn, Al, Cu, and Mg. Kannan et al. [124] found that Al temporarily improved the passivation behaviour of a commercial biodegradable Zn-5Al-4Mg alloy. After extended periods of immersion in SBF (i.e., >3 days), the alloy showed higher corrosion rate than pure Zn.

Alloying can generally alter the corrosion behaviour of a metal via several ways. However, while conclusions from studies on the mechanical behaviour of Zn alloys are fairly unanimous, the influence of alloy addition on the corrosion behaviour of Zn is arguably more complicated and is difficult to predict. This is likely due to the greater impact that microstructure and surface conditions hold on corrosion behaviour compared to chemical composition. Furthermore, the corrosion regime, i.e., either localized or uniform, has a significant impact on the corrosion products and resulting corrosion layer, and can consequently affect the degradation behaviour of the metal [171].

One way by which an alloying element changes the corrosion resistance is by causing a change in the inherent standard potential of the host metal, as indicated by shifts in the open cell corrosion potential to different values. This was cited for the increase in corrosion rate in Zn after addition of Ca [87], Sr [87], or Al [96].

Another mode is by inducing a change in the microstructure (e.g., from single to multi-phase system, change in grain size) [169,172,173]. For biodegradable Zn, a majority of the reported changes (i.e., increase or decrease in corrosion resistance) in its degradation behaviour after alloying were traced to alterations to its metallurgical structure. For example, the addition of an alloying element to pure Zn frequently creates a multiphase system consisting of an intermetallic (e.g., $MgZn_2$, Mg_2Zn_{11}, $LiZn_4$, $CuZn_5$) in a matrix of Zn-rich solid solution [22]. Ternary combinations can even add to the existing number of precipitates; e.g., in Zn-3Cu-*x*Mg ($x = 0.1, 0.5, 1$), precipitates of $CuZn_5$ and Mg_2Zn_{11} are dispersed in the Zn-rich matrix [117]. The difference in the composition of these phases creates localized micro-galvanic couples that consequently enhance the corrosion rate of the alloy, as was reported for Zn-*x*Cu with $CuZn_5$ phase [106], Zn-*x*Ag with $AgZn_3$ precipitates [110], ternary Zn-Cu-Fe with $FeZn_{13}$, ternary Zn-Cu-Fe with $FeZn_{13}$ [120], and Zn–Al–Mg–*x*Bi with the secondary phase, a-Mg_3Bi_2 [122]. Increasing alloy content could often lead to an increase in the relative amount of these second phases or induce the precipitation of another type of precipitate resulting to further alterations in the microstructural corrosion dynamics. Another case was cited by Yang et al. [78] where Mg-induced grain refinement improved the corrosion resistance of 3D-printed Zn-Mg alloy.

The role of Mg_2Zn_{11} in causing galvanic corrosion is still debatable, as indicated by the conflicting reports on the corrosion behaviour of Zn-Mg alloys. Mostaed et al. [96] suggested that galvanic corrosion due to Mg_2Zn_{11} enhanced the corrosion rates in Zn-*x*Mg alloys. In contrast, Vojtech et al. [19] stated that the formation of galvanic micro-cells between Zn and Mg_2Zn_{11} is highly unlikely since the two phases possess similar standard potentials. It is clear that further research is needed to finally ascertain the relevant corrosion mechanism in the Zn-Mg alloys.

Some elements can improve corrosion resistance by (i) forming a less conductive and passive oxide on the Zn surface (e.g., MgO, Mg hydroxyl carbonate) or (ii) by modifying the characteristic of the Zn corrosion product (e.g., Mg makes simonkolleite less soluble thus inhibiting anodic reaction) [91,164,174]. For example, For example, Mostaed et al. [96] suggested that the uniform and homogenously dispersed Mg_2Zn_{11} in Zn-3Mg induced good corrosion resistance due to the formation of a uniform protective layer of Mg-containing corrosion products. Yang et al. [78] noted similar improvements in corrosion resistance in 3D-printed Zn-Mg alloys due to Mg-induced simonkolleite corrosion films. Zhao et al. [108] reported that the good corrosion resistance after addition of Li was due to the formation of a thick passive corrosion layer.

6.3.2. Influence of fabrication technique

Compared to its influence on mechanical properties, the impact of fabrication route on the biodegradability of Zn and Zn alloys is less predictable. Assuming that there is no change in the chemical composition, the extent of influence of the fabrication route on the corrosion behaviour of a metal will ultimately depend on the type

Please cite this article as: J. Venezuela and M. S. Dargusch, The influence of alloying and fabrication techniques on the mechanical properties, biodegradability and biocompatibility of zinc: A comprehensive review, Acta Biomaterialia, https://doi.org/10.1016/j.actbio.2019.01.035

of microstructure created during processing. For example, a fine-grained, homogenous microstructure is expected to have a lower corrosion rate compared to its coarse-grained counterpart; or a multi-phase metal is often likely to corrode faster than its single-phase counterpart as the second phase can promote galvanic corrosion.

Casting is considered to create a natural, unstrained structure; hence the cast metal can be a good reference for measuring the inherent corrosion rates of metals. On the other hand, wrought processes strain the metal structure, the extent of which depends on the processing parameters (e.g., amount of working, working temperature, etc.), and consequently alters the corrosion behaviour.

In cast Zn alloys, Dambatta et al. [99] noted that homogenization improved the corrosion resistance of Zn-3Mg. Homogenization (i) dissolved the prevailing dendritic microstructure and created a uniform dispersion of precipitates, and (ii) reduced casting defects thus improving microstructure homogeneity in the alloy. They observed that the corrosion attack on the homogenized alloy was generally uniform and that the homogenized microstructure aided the formation of a compact corrosion film that protected the underlying metal from further degradation.

Wrought processing had different effects on the corrosion behaviour of Zn alloys.

Some noted enhancement of biodegradation rate after wrought processing. Shen et al. [94] reported that extrusion increased the corrosion rate in cast Zn-1.2Mg, while Liu et al. [115] noted an increase in corrosion rate after hot-rolling of cast Zn-1Mg-0.1Sr. Wang et al. [114] also observed an increase in corrosion rate after mandrel drawing of hot-rolled Zn-5Mg-1Fe. This increase in degradation is often related to the presence of a second phase (intermetallic) that creates galvanic micro-cells, such as Mg_2Zn_{11} [94], $MgZn_2$, and $SrZn_{13}$ [115]. The galvanic effect can be especially enhanced if fabrication caused uneven distribution of precipitates thereby creating regions where there is a low ratio of anode area to cathode area, such as when coarse or dendritic, anodic precipitates are present [96].

In contrast, other studies reported an improvement in corrosion resistance after wrought processing. Gong et al. [92] noted a significant reduction of corrosion rates in cast Zn-1Mg after extrusion. Dambatta et al. [99] observed similar improvements in corrosion resistance in homogenized, cast Zn-3Mg after ECAP, while Liu et al. [116] noticed only a slight decrease in corrosion rate after hot-rolling of cast Zn-1Mg-0.1Mn. Mostaed et al. [96] noted large and deep corrosion pits in as-cast compared to fairly uniform corrosion in extruded Zn-Mg alloys. This enhancement in corrosion resistance is traced to improvements in microstructure such as (i) general homogenization of chemical distribution [92], (ii) grain refinement [92,98], (iii) breakdown of large precipitates [92], and (iv) uniform distribution of intermetallic phase [96,98].

The biodegradability of porous Zn is also of interest, especially if the metal is considered for tissue-engineered bone scaffold applications [175]. Hou et al. [127] observed an increase in the biodegradability of porous Zn with an increasing specific area of porosities. This is reasonable since corrosion attack is expected to initiate at any exposed surfaces on the metal [169] (i.e., in the case of porous Zn, this refers not only to the external surface but also to the surfaces of the interconnected pores).

It is also useful to understand the possible influence of a reinforcing phase on the corrodibility of a Zn-based composite. Yang et al. [128] noted that as the amount of hydroxyapatite increased (i.e., from 1, 5, to 10 wt%) the degradation rate of the composite increased. For example, the corrosion rate of Zn-10HA was about 5 times higher than that of pure Zn. Corrosion pits were found distributed in the Zn matrix and particle boundaries. They proposed that the reduction in corrosion resistance was due to the pores and voids at the interface of Zn and HA agglomerates. These defects promoted the penetration of the physiological fluid allowed corrosion to occur. The presence of these defects is consistent with the observed reduction in the strength of the composite with increasing HA amount. Furthermore, the addition of HA altered the compositional nature of the degradation products, as there was an observed increase in O, P and Ca amounts in the corrosion layer.

6.4. In vitro biocompatibility of Zn alloys

Table 4 gives a summary of published reports on in vitro biocompatibility tests done on different biodegradable Zn and Zn alloys.

Cytotoxicity tests, which assess the ability of a substance to destroy living cells, and hemocompatibility tests, which evaluates the interaction between a substance and blood, are the most commonly employed tests to assess Zn biocompatibility. Antibacterial tests are popular mainly for cases when Zn is alloyed with known antibacterial elements such as Cu and Ag. Other tests to determine genotoxicity, mutagenicity, cell functionality, and inflammatory response have also been conducted on biodegradable Zn.

For cell viability or cell cytotoxicity tests on Zn, human (e.g., aortic, osteoblast, osteosarcoma, fibroblast, endothelial) and murine (e.g., fibroblast, osteoblast) cells were employed. The proper choice of cell lines used in the test is deemed crucial as results can give an accurate idea of the applicability of the tested implant [176]. For example, Cheng et al. [70] suggested that the cytocompatibility of Zn with human endothelial cells (ECV304) implies suitability of the metal in cardiovascular-related applications. The commonly used cytotoxicity tests are the (i) extract test (e.g., MTT assay test), which assess the toxicity of soluble substances from the implant, and the (ii) direct test, which assesses the viability of cells grown in contact with the implant [177]. These tests were conducted at exposure times that range from 1 to 7 days.

In hemocompatibility tests, human blood is exposed to the implant and can yield valuable information such as hemolysis rate, which is the rate of destruction of red blood cells, platelet morphology, platelet adherence, and dynamic blood clotting.

Different in vitro studies have already concluded on the good biocompatibility of pure Zn. However, while studies are unanimous in confirming the excellent hemocompatibility of Zn, there are conflicting reports on the cytocompatibility of the biodegradable metal.

Early on, Cheng et al. [70] noted that pure Zn exhibited no cytotoxicity to human endothelial cells but reduced the viability of murine fibroblast cells. Liu et al. [75], Hiebl et al. [76], Li et al. [88], and Kannan et al. [124] reported no cytotoxicity in pure Zn even at 100% extract concentration. In contrast, Yang et al.[78], Kubasek et al. [55], Xiao et al. [103], Murni et al. [93], Tang et al. [106] and Wang et al. [123] reported cytotoxicity for Zn at 100% extract concentration, though no cytotoxic effects of Zn were observed in diluted extracts ($\leq$50%). It is logical to assume that the differences in these results may be due to slight differences in test methodologies, as results of the MTT assay can be influenced by factors such as the type of cell line, exposure time, extract concentration, and extraction medium [55,177].

On the other hand, the number of studies reporting the in vitro cytotoxicity of Zn is compelling. Some of these studies observing cytotoxicity in pure Zn or in other Zn alloys [66,106] have suggested that the high concentration of extract (i.e., 100%) used in the test was not suitable for biodegradable metals. Previously, Wang et al. [178] have similarly concluded while studying the in vitro cytotoxicity of biodegradable Mg. Hence, they proposed a re-evaluation of the current standard for assessing cytotoxicity (i.e., ISO 10993) and suggested a minimum of 6 to 10 times extract

Please cite this article as: J. Venezuela and M. S. Dargusch, The influence of alloying and fabrication techniques on the mechanical properties, biodegradability and biocompatibility of zinc: A comprehensive review, Acta Biomaterialia, https://doi.org/10.1016/j.actbio.2019.01.035

Table 4
Summary of reported in vitro biocompatibility of biodegradable Zn and Zn alloys. The fabrication technique is indicated as follows: W – commercial wrought product, C – casting, E – hot extrusion, SLM – selective laser melting, HR – hot rolling, PM – powder metallurgy.

Specimen (Fabrication)	In vitro Biocompatibility Tests					Other Important Conclusions	Refs.
	Cell viability			Hemocompatibility	Other Tests (antibacterial, genotoxicty, etc)		
	Cell line	Exposure time, d	Results				
Pure Zn							
4 N Zn (W)	i. Murine fibroblast cells (L929) ii. Human endothelial cells (ECV304)	1, 2, 4	Exhibits no cytotoxicity to ECV304 cells but significantly reduces the cell viability of L929 cells	Hemolysis and platelet adhesion tests showed excellent blood compatibility		Results indicates Zn may be suitable for vascular-related applications	[70]
6 N Zn (W)	i. Human endothelial cells (ECV304) ii. Murine vascular smooth muscle cells (VSMC)	3	Exhibits no cytotoxicity to both type of cells at 100% extract concentration	Hemolysis tests showed excellent blood compatibility and no destructive effect on erythrocyte			[75]
4 N Zn	i. Murine fibroblast cells (3T3)	2	Cell viability characteristics including cellular phenotype, cell activity, cell proliferation and cell membrane integrity showed no cytotoxic effects on cells				[76]
Zn/Zn^{+2}	i. Human endothelial cells (HAEC) ii. Human aortic smooth muscle cells (AoSMC) iii. Human dermal fibroblasts (hDF)	2	i. Cytotoxicity tests show that LD_{50} values of 3.5 ppm (50 μM) for hDF, 4.5 ppm (70 μM) for AoSMC, and 17.5 ppm (265 μM) for HAEC ii. All cell types were able to attach and proliferate on Zn surface			i. HAEC showed highest tolerance for Zn which indicates suitability to cardiovascular applications ii. Cell attachment, spreading, and migration was sensitive to Zn^{+2} concentration, particularly in the hDF and AoSMC	[84]
Zn^{+2}	Human aorta smooth muscle cell (HASMC)	1	i. Low concentrations of Zn^{+2} (<80 μM) is beneficial to HASMC viability, adhesion, spreading, proliferation, and migration ii. Above 80 μM, cell health markers are significantly reduced		Gene expression profiling showed that the adversely affected genes were related to angiogenesis, inflammation, cell adhesion, vessel tone, and platelet aggregation	Cellular behaviour and corresponding biocompatibility is tightly related to Zn^{+2} concentrations	[83]
Zn (SLM)	Human osteosarcoma cells (MG63)	1, 3, 5	Zn was cytotoxic at 100% extract (1 and 3 days), non-cytotoxic at 100% at 5 days and 50% dilution at all exposure times			Cell viability is influenced by the concentration of the extract and exposure time	[78]
Zn					Antifungal tests showed that C. albicans colonized on Zn corrosion products	Simonkolleite corrosion layer was more effective in inhibiting C. albicans than zincite	[85]

(*continued on next page*)

Table 4 (*continued*)

Specimen (Fabrication)	In vitro Biocompatibility Tests					Other Important Conclusions	Refs.
	Cell viability			Hemocompatibility	Other Tests (antibacterial, genotoxicty, etc)		
	Cell line	Exposure time, d	Results				
Binary							
Zn-0.05 Mg (E)	Murine fibroblast cells (L-929)	1, 3, 5	i. Both Zn and Zn-0.05 Mg were cytotoxic at 100% extract; non cytotoxic at 50% and 10% dilution ii. Very little difference in the biocompatibility of Zn and Zn-0.05 Mg		Both Zn and Zn-0.05 Mg alloy possess strong antibacterial activity against E. coli and S. aureus	i. Cell viability is influenced by the concentration of the extract ii. Cell viability improved with increasing exposure time	[103]
Zn-0.8Mg (E)	i. Human osteosarcoma cells (U-2 OS) ii. Murine fibroblast cells (L929)	1	i. Alloy induced cytotoxic effects to both cell lines in 100% and 75% extracts ii. At 50% dilution, the alloy was non-cytotoxic to U2-OS, but cytotoxic to L929		Alloy is non-genotoxic (comet assay) and non-mutagenic (Ames test)	The highest safe Zn^{+2} concentration is 120 μM for U-2 OS and 80 μM for L929 cell line	[55]
Zn-1 Mg (C)	Murine fibroblast cells (L-929)	1, 3	The alloy did not adversely affect cell viability and can support cell attachment and growth				[92]
Zn-1.2Mg (C,E)	i. Human osteosarcoma cells (HOS) ii. Human osteosarcoma cells (MG63)	3	i. HOS had cytotoxic reaction at 100, 75 and 50% dilutions, while MG63 cells had no cytotoxic response to the alloy ii. Both cells had better viability in diluted extracts	Hemolysis rate test, platelet adhesion tests, and dynamic blood clotting tests showed no signs of thrombogenicity and indicated excellent hemocompatibility of alloys		i. Cell viability depended on the type of cell and the concentration of extract ii. Cells had better viability in as-cast than extruded alloy iii. As-cast alloy had lower hemolysis rate than extruded one	[94]
Zn-1.5Mg (E)	i. Murine fibroblast cells (L929) ii. Human osteosarcoma cells (U-2 OS)	1	Pretreatment by incubation improved cytocompatibility of the alloy, with osteoblast-like cell growth observed directly on the metal surface				[97]
Zn-*x*Mg (*x* = 1, 2, 3, 4) (SLM)	Human osteosarcoma cells (MG63)	1, 3, 5	Cells exhibited good viability in all the specimens in 100% extract, and better viability in 50% extracts of Zn-xMg			i. Cell viability is influenced by the concentration of the extract ii. Cell viability increased with increasing exposure time iii. Increasing Mg increases biocompatibility of Zn, with Zn-3Mg exhibiting best biocompatibility	[78]
Zn-3Mg (C)	Human osteoblast cells (NHOst)	3	i. Zn and Zn–3 Mg showed significant toxicity after 1 day ii. Cell viability of both specimens improved at 3 and 7 days		Cell functionality and inflammatory response tests showed that the alloy has acceptable toxicity	i. Addition of Mg enhanced biocompatibility ii. Zn was genotoxic and caused DNA fragmentation, while Zn-3 Mg was non-genotoxic	[93]

Table 4 (*continued*)

Specimen (Fabrication)	In vitro Biocompatibility Tests					Other Important Conclusions	Refs.
	Cell viability			Hemocompatibility	Other Tests (antibacterial, genotoxicty, etc)		
	Cell line	Exposure time, d	Results				
Zn-1Mg Zn-1Ca Zn-1Sr (HR)	i. Human osteosarcoma cells (MG63) ii. Human umbilical vein endothelial iii. cells (ECV304) iv. Murine vascular smooth muscle cells (VSMC)	3	i. Zn and Zn alloys exhibited no cytotoxic effect on cell lines ii. Cell viabilities was higher in the Zn-1X alloy compared to pure Zn iii. Unhealthy morphology in cells cultured on pure Zn, healthy morphology in cells cultured in binary alloys	The Zn-1X alloys exhibited good hemocompatibility, excellent in vivo anti-platelets adhesion property, and antithrombotic properties		i. Cell viability was influenced by the type of cell line ii. Ranking in terms of promotion of cell proliferation: Mg < Ca < Sr	[87]
Zn-4Cu (E)	human endothelial cell (EA.hy926)	1, 3, 5	The alloy was cytotoxic at 100% extract; non cytotoxic at 50% and 10% dilution		Alloy showed good antibacterial properties against S. aureus, while inhibiting biofilm formation	Cell viability did not significantly change with exposure time	[66]
Zn-*x*Cu (x = 1,2,3,4) (E)	human endothelial cell (EA.hy926)	1, 3, 5	Pure Zn and the Zn-xCu alloys were cytotoxic at 100% extract; non cytotoxic at 50% and 10% dilution		i. Alloys showed good antibacterial (*S. aureus*) properties, with inhibition effect enhanced by addition of Cu (best results at > 2% Cu)	i. In 100% extract, pure Zn and Zn-3Cu possessed the highest cell viabilities. ii. No difference in viability between Zn and Zn-xCu at 50% and 10%.	[106]
Zn-0.5Al (C)	Murine osteoblast precursor cells (MC3T3-E1)	2, 7	Cells showed good viability in the binary alloy		The alloy have good antibacterial activity against E. coli		[118]
Zn-4Mn Zn-24Mn (PM)	Murine fibroblast cells (L929)	1, 3, 7	i. Both Zn-Mn alloys were cytotoxic at 100% extract; non cytotoxic at 50% dilution ii. Cell viability, cell adhesion and cell morphology tests confirms Zn-24Mn has better biocompatibility than Zn-4Mn			Cell viability slightly decreased with increasing exposure time	[113]
Zn-4.0Ag (HR)	i. Murine fibroblast cells (L929) ii. Human primary osteosarcoma cell (Saos-2)	1, 2	i. Alloy was cytotoxic at 100% extract; noncytotoxic at 33%, 16.67% and 10% dilutions ii. Alloy showed comparable biocompatibility with pure Zn		Alloy exhibited good antibacterial properties against S. gordonii	Cytoxicity depended on cell lines and type of test (L929 showed better viability than Saos-2)	[111]
Ternary							
Zn-1Mg-0.1Mn Zn-1.5Mg-0.5Mn (C) Zn-1Mg-0.1Mn (HR)				Hemolysis and platelet adhesion tests showed that all specimens showed good hemocompatibility, with no signs of thrombogenicity		Hot rolled Zn-1 Mg-0.1Mn showed lower hemolysis rate than as cast specimen	[116]

(*continued on next page*)

Table 4 (*continued*)

Specimen (Fabrication)	In vitro Biocompatibility Tests					Other Important Conclusions	Refs.
	Cell viability			Hemocompatibility	Other Tests (antibacterial, genotoxicty, etc)		
	Cell line	Exposure time, d	Results				
Zn-1Mg-0.1Sr Zn-1Mg-0.5Sr (C) Zn-1Mg-0.1Sr (HR)				i. Pure Zn and the ternary alloys exhibit good hemocompatibility ii. Hemolysis rate in the ternary alloy is lower than in pure Zn		There was no difference in hemocompatiility between as-cast and hot-rolled alloy	[115]
Zn-3Cu-*x*Mg (x=0.1, 0.5, 1.0) (E)	human endothelium-derived cells (EA.hy926)	1, 3, 5	i. Zn, Zn-3Cu, and Zn-3Cu-0.1Mg are cytotoxic, while Zn-3Cu-0.5Mg and Zn-3Cu-1.0Mg are non-cytotoxic at 100% ii. All specimens are non-cytotoxic at 50% and 10%			i. Cell viability is enhanced with increasing Mg content ii. In 100% extract, in vitro cytotoxicity of Zn-3Cu-xMg is better than that of the pure Zn iii. In 50% and 10% dilution, the cytoxicity of Zn and the ternary alloys are similar	[117]
Zn-0.5Al-*x*Mg (*x* = 0.1, 0.3, 0.5) (C)	Murine osteoblast precursor cells (MC3T3-E1)	2, 7	i. Cells showed good viability in the ternary alloy extracts ii. Addition of Mg (from 0.1 to 0.5 wt%) to the binary Zn-0.5Al alloy improves cell viability		Zn-based binary and ternary alloys have good antibacterial activity against E. coli	i. Ternary Zn-Al-Mg alloys samples indicated better antibacterial property than binary Zn-0.5Al alloy against E. coli. ii. Antibacterial property iii. increased with increasing Mg content in the ternary alloy	[118]
Zn-1Mg-1Ca Zn-1Mg-1Sr Zn-1Ca-1Sr (C, HR)	Human osteosarcoma cells (MG63)	1, 3, 5	Cell viability and cell morphology tests showed excellent cell viabilities in Zn and the Zn ternary alloy extracts at all exposure times	Both as-cast and as-rolled pure Zn and ternary alloys exhibited good hemocompatibility		The ternary alloys exhibits better cytocompatibility than pure Zn with the ranking of biocompatibility as follows: Zn < Zn–1 Mg–Ca < Zn–1 Mg–1Sr < Zn–1Ca–1Sr	[88]
Quaternary							
Zn-0.5Al-0.5 Mg-*x*Bi (*x* = 0.1, 0.3. 0.5) (C)	Murine osteoblast precursor cell line (MC3T3-E1)	2, 7	i. The quaternary alloys showed no cytotoxic effects on cells ii. Cell viability decreased with increasing Bi content				[122]
Commercial							
ZA4-1 ZA4-3 ZA6-1 (W)	human umbilical vein endothelial cells (HUVECs)	1, 2, 4	i. All specimens (including pure Zn) were cytotoxic at 100% extract concentration, but were non cytotoxic at 50% dilution ii. Significantly improved biocompatibility was observed in ZA4-1 and ZA6-1 alloys compared with pure Zn	Hemolysis and platelet adhesion tests showed good hemocompatibility in both pure Zn and commercial alloys	Commercial alloys have similar/better viability than Pure Zn		[123]

Table 4 *(continued)*

Specimen (Fabrication)	In vitro Biocompatibility Tests					Other Important Conclusions	Refs.
	Cell viability			Hemocompatibility	Other Tests (antibacterial, genotoxicty, etc)		
	Cell line	Exposure time, d	Results				
Zn-5Al-4Mg (W)	human alveolar lung epithelial (A549)	4	Zn and commercial alloy showed no cytotoxic effect to cell line at 100% extract concentration				[124]
Composite							
Zn-1HA Zn-5HA Zn-10HA (P/M)	Murine osteoblast precursor cell line (MC3T3-E1)	1, 2, 4	Cells exhibited better viability in Zn-HA than pure Zn	Zn-HA showed excellent hemocompatibility.	Zn-HA showed excellent antibacterial properties against S. aureus		[128]

dilution as more appropriate when testing biodegradable metals. This argument becomes stronger in light of the fact that in vivo tests have already proven the excellent biocompatibility of Zn [18]; thus, there is a reason to doubt in vitro tests indicating its cytotoxicity. However, it is important to mention that in vivo tests involved much longer exposures times (i.e., months) than those used in in vitro tests (i.e., days). A study by Yang et al. [78] suggests that pure Zn's cytotoxic effect on cells at 100% extract concentration is only temporary and exist in the short-term. They observed that Zn (SLM) was cytotoxic to human osteosarcoma cells (MG63) at 100% extract at 1 and 3 days exposure, but was non-cytotoxic at 5 days. Yang et al.'s conclusions appear to be more consistent with what was observed from in vivo tests [18,74]. It is possible that the absence of cytotoxic influence on surrounding tissues reported from in vivo experiments could be due to the fact that these tests are often conducted under prolonged exposure times.

In vitro cytocompatibility studies on Zn^{+2} ions have also been conducted to determine the limit of tolerance of living cells. Shearier et al. [84] noted that the safe Zn^{+2} concentration level depends on the type of cell line, with some cell lines exhibiting better tolerance than others. They measured LD_{50} values of 3.5 ppm (50 μM) for human dermal fibroblasts (hDF), 4.5 ppm (70 μM) for human aortic smooth muscle cells (AoSMC), and 17.5 ppm (265 μM) for human endothelial cells (HAEC). Ma et al. [83], who studied the cytocompatibility of Zn^{+2} with human aorta smooth muscle cells (HASMC), appear to agree with the observations by Shearier et al. Ma et al. noted that Zn^{+2} induced a biphasic cellular response from HASMC. They found that at concentrations of <80 μM Zn^{+2} is beneficial to HASMC viability, adhesion, spreading, proliferation, and migration. At Zn^{+2} concentrations above 80 μM, cell markers are significantly reduced. This information is important as this defines the limit of applicability of biodegradable Zn based on the rate of corrosion and ion release.

Alves et al. [85] noted that the type of corrosion film formed at the surface influences the antifungal properties of Zn. Initially, they observed how different species of corrosion products predominate depending on implant location in the body (i.e., simonkolleite dominates when the Zn implant is attached to the bone-muscle interface, and zincite dominates when the implant is inside the bone). They then reported that the simonkolleite corrosion layer was more effective in inhibiting C. albicans than zincite.

Murni et al. [93] reported that Zn is genotoxic and caused DNA fragmentation. Xiao et al. [103] observed that Zn possess antibacterial properties against Escherichia coli (E. coli) and Staphylococcus aureus (S. aureus). Ning et al. [179] explained that the antibacterial properties of Zn originate from its ability to damage bacterial cell membranes via the generation of reactive O_2 species; while Phan et al. [180] observed Zn ions' ability to inhibit several aspects of bacterial activity such as transmembrane proton translocation, glycolysis, and acid tolerance.

6.4.1. Influence of alloying

In terms of toxicity, Zn is less biocompatible than Mg in that the upper limit of recommended daily intake is much lower than Mg [65]. Therefore, it is expected that the addition of Mg would increase the biocompatibility of Zn.

Numerous in vitro cytocompatibility [55,78,92–94,97,103] and hemocompatibility [87,94] studies have put forth enough evidences proving the good biocompatibility of different Zn-xMg alloys (x = 0.05, 0.8, 1.0, 1.2, 1.5, 2, 3, 4). Similar to reports on Zn, some Zn-Mg alloys [55,93,103] have also been reported to trigger cytotoxic responses in cells exposed to 100% extract concentrations; though this could be attributed to the perceived incompatibility of the current testing standard (i.e., ISO 10993) to biodegradable metals. Murni et al. [93] also concluded from cell functionality and inflammatory response tests that Zn-3Mg alloy

has acceptable toxicity, while Xiao et al. [103] observed the antibacterial qualities of Zn-0.05Mg against E. coli and S. aureus.

Though pure Zn is not as favourable for bone integration as pure Mg [65,181], several studies confirm that Mg additions to Zn could promote osseointegration. Li et al. [87] noted that Zn-1Mg stimulated the growth of new bone tissue. Alves et al. [104] concluded that cast and homogenized Zn-*x*Mg ($x = 1, 2$) might support osseointegration due to the formation of Ca phosphate corrosion layer containing bone-analogous skorpionite and hydroxyapatite.

Some studies suggest that Mg can also improve the genotoxicity and mutagenicity of Zn. Mutagenicity refers to the introduction of permanent and transmissible changes in the amount or structure of the cell's genetic material (e.g., DNA, RNA), while genotoxicity refers to the to the ability of substances to damage the cell's genetic material without necessarily causing mutation [182]. Indications of mutagenity could signify that a material is carcinogenic. Murni et al. [93] reported that Zn was genotoxic (comet assay) as it induced significant damage to cells after a 7-day exposure test. In contrast, Zn-3Mg was observed to be non-genotoxic. Kubasek et al. [55] similarly reported no genotoxic (comet assay) and mutagenic (Ames test) effect in Zn-0.8Mg.

Li et al. [87] observed that swapping Mg with other IIA elements such as Ca and Sr in Zn-1Mg created alloys with better biocompatibility than pure zinc. They found that Sr was the best in promoting the proliferation of human osteosarcoma cells (MG63), followed by Ca, then Mg. Li et al. [88] also observed that ternary combinations of Zn with these IIA elements were cyto- and hemocompatible. They noted that the ranking of biocompatibility; i.e., Zn < Zn–1Mg–Ca < Zn–1Mg–1Sr < Zn–1Ca–1Sr, were consistent with their earlier observation than Sr and Ca were more biocompatible than Mg when combined with Zn.

Some studies reported that the addition of micro-amounts of Mn (0.1 and 0.5%) [116] or Sr (0.1 and 0.5%) [115] in Zn-1Mg maintained the good hemocompatibility of the binary alloy, with the ternary alloys even exhibiting slightly lower hemolysis rate than pure Zn.

Copper is another biocompatible element that is essential to bodily functions. Alloying with Cu does not reduce the good biocompatibility of Zn [66,106]. However, it needs to be mentioned that though these studies conclude good biocompatibility of Zn-*x*Cu ($x = 1, 2, 3, 4$) [66,106], these also observed that 100% extracts from pure Zn and these alloys were cytotoxic and only the 50% and 10% extract dilutions were cytocompatible. Tang et al. [106] further noted that there is no difference in the viability between Zn and Zn-*x*Cu at 50% and 10%. Again, the cytotoxicity observed in the alloys was attributed to the unsuitability of the current test standard to biodegradable metals. Copper, a known antibacterial element [179], appears to impart the same antibacterial qualities to the Cu-Zn alloy [66,106]. Tang et al. [106] also observed that inhibition effects on (S. aureus) is enhanced by increasing addition of Cu, with the best results obtained at >2%Cu concentrations.

The addition of Mg to Zn-Cu appears to improve the cytocompatibility of the binary alloy. Tang et al. [117] reported that Zn, Zn-3Cu, and Zn-3Cu-0.1Mg are cytotoxic to human endothelium-derived cells (EA.hy926) at 100% extract, while Zn-3Cu-0.5Mg and Zn-3Cu-1.0Mg are non-cytotoxic at the same extract concentration. At 50% and 10% extract dilution, the cytotoxicity of Zn and the other alloys are similar. It was also noted that cell viability was promoted despite the increase in corrosion rate after Mg addition. This means that the beneficial effect of Mg on the cytocompatibility of the Zn-Cu alloy may be due to Mg having better biocompatibility than Cu. This means that though more ions are released with the enhanced corrosion rate in the Zn-Cu-Mg alloy, less of the more toxic Cu is present in the extract as it was replaced by the more benign Mg.

Manganese has also been observed to have positive influences on the biocompatibility of Zn. Sotoudeh-Bagha et al. [113] noted that Zn-4Mn and Zn-24Mn were non-cytotoxic to murine osteoblast precursor cells (MC3T3-E1) at 50% extract dilution, though both alloys are cytotoxic at 100% extract concentration. Results of cell viability, cell adhesion, and cell morphology tests further confirm that Zn-24Mn has better biocompatibility than Zn-4Mn, likely due to better corrosion resistance in Zn-24Mn.

Li et al. [111], studying the cytocompatibility of Zn-4.0Ag with murine fibroblast cells (L929) and human primary osteosarcoma cell (Saos-2), noted that the addition of silver does not alter the biocompatibility of Zn. Moreover, Ag adds antibacterial qualities to biodegradable Zn against Streptococcus gordonii (S. gordonii).

Bakhsheshi-rad et al. [118] reported that alloying with small amounts of Al (0.5%) retained the good biocompatibility of Zn and imparted antibacterial properties against E. coli. The addition of Mg to Zn-Al further improved the biocompatibility of the binary alloy.

Bakhsheshi-rad et al. [118] noted that the addition of *x*Mg (x = 0.1, 0.3, 0.5%) improves the viability of murine osteoblast precursor cells (MC3T3-E1) by reducing the dissolution rate of the Zn-0.5Al alloy. Additionally, they also observed that increasing Mg content increased the binary alloy's antibacterial properties against E. coli [118]. In another work, Bakhsheshi-rad et al. [122] found that the addition of *x*Bi ($x = 0.1, 0.3, 0.5$) to ternary Zn-0.5Al-0.5Mg alloys showed no cytotoxic effects on murine osteoblast precursor cell line (MC3T3-E1); though, cell viability decreased with increasing Bi content attributed to increased dissolution rate of the alloy in the physiological environment.

Wang et al. [123] reported that some of the wrought commercial Zn alloys have good cell viability and hemocompatibility. Though 100% extracts of commercial Zn alloy and pure Zn showed toxicity, the 50% diluted extracts were non-cytotoxic to human endothelial cells. Indeed, ZA4-1 and ZA6-1 alloys displayed better biocompatibility than pure Zn. Kannan et al. [124] observed that a commercial ternary alloy, Zn-5Al-4Mg, had no cytotoxic effect on human alveolar lung epithelial (A549) even at 100% extract concentration. These results are significant as these identify alternative and readily-accessible sources of biodegradable and biocompatible Zn alloys in the future.

Improvements in the biocompatibility of Zn after alloying addition may be traced to different factors. Ultimately, cell response in an in vitro test depends on the quality and quantity of corrosion products (e.g., ions) released during the degradation of Zn. It is known that each cell has a unique tolerance level for a specific substance, and toxicity effects are triggered when this limit is breached. Some alloying elements such as Mg [55,78] or Ca [87] are inherently more biocompatible than Zn, and, therefore, cells can tolerate much higher amounts of these elements than Zn. Consequently, adding such elements to Zn improves the overall biocompatibility by a simple principle of displacement; i.e., via the reduction in the amount of the less biocompatible components and an increase in the amount of more biocompatible counterparts in the corrosion product that consequently lowers the cytotoxic response of the cell. Other alloying elements such as Mn [113], Sr [87,115] and even Mg [78,93,118] improve biocompatibility by lowering the degradation rate of Zn and consequently reducing the total amount of ions released to the physiological environment. An alloy element's influence on degradation rate may be traced to its effect on the microstructure of the most material, as was discussed in Section 6.3.1. Interestingly, Tang et al. [117] observed that cell viability was promoted after Mg addition in Zn-3Cu despite an increase in corrosion rate. This would imply the primacy of the inherent biocompatibility of the alloying element in determining the overall biocompatibility of the alloy.

Please cite this article as: J. Venezuela and M. S. Dargusch, The influence of alloying and fabrication techniques on the mechanical properties, biodegradability and biocompatibility of zinc: A comprehensive review, Acta Biomaterialia, https://doi.org/10.1016/j.actbio.2019.01.035

Table 5
Reported in vivo biocorrosion and biocompatibility properties of biodegradable Zn and Zn alloys.

Composition	Shape of implant	Fabrication method	Type of host	Location	In vivo corrosion		In vivo biocompatibility	Refs.
					Exposure Duration, months	Corrosion rate CR, μm/yr		
Pure Zn								
4 N Zn	Wire (∅ 0.25 × 15 mm)	Commercial (likely wrought)	Sprague–Dawley rat	Abdominal aorta	1.5 3 4.5 6	12 19 41 50	Implant showed good biocompatibility and antiatherogenic properties	[18]
4 N Zn	Wire (∅ 0.25 × 10 mm)	Commercial (likely wrought)	Sprague–Dawley rat	Abdominal aorta	2.5 to 6.5	–	Implant showed good biocompatibility, no risk factor for in-stent restenosis with no discernible chronic inflammatory response, necrosis, or hyper-proliferative response	[71]
4 N Zn	Wire (∅ 0.25 × 20 mm)	Extrusion + Drawing	Sprague–Dawley rat	Abdominal aorta	2 4 6 8 10 12	20 30 19 35 16 23	Implant showed good biocompatibility; moderate inflammation with non-obstructive neointima; neointima thickness is lower in pure Zn than alloy (Zn-0.1Li)	[107]
99.995% Zn	Stent (∅ 3.0 × 10 mm); strut thickness 165 μm	Laser cutting of microtube	Rabbit	Abdominal aorta	1 3 6 12	~30 ~10 ~15 ~15	Implant stent showed excellent biocompatibility; with no severe inflammatory response, platelet aggregation, thrombosis formation, and obvious intimal hyperplasia	[86]
4 N Zn	Wire (∅ 0.25 × 20 mm)	Commercial (likely wrought)	Sprague–Dawley rat	Abdominal aorta	1 to 20	25 ± 10	Long-term biocompatibility was observed. Fibrotic encapsulation allowed for bio-integration by reducing inflammation while still promoting biodegradation	[72]
99.9% Zn coated with PLLA	Wire (∅ 0.25 × 15 and 30 mm)	Commercial (likely wrought)	Sprague–Dawley rat	Abdominal aorta	0.5 3 4.5 6	~8 ~10 ~20 ~35	1-μm thin PLLA coating delayed implant degradation by 6 months; however, PLLA reduced biocompatibility with signs of toxicity and active neointima.	[129]
Zn	Disc (∅ 7 mm × 2 mm height)	Gravity casting	Wistar rats	Subcutaneous midline of back	3.5 6	62 25	Implants showed good biocompatibility obtained from hematological profiles and histological analysis.	[188]
Binary								
Zn-1Mg Zn-1Ca Zn-1Sr	Wire (∅ 0.7 × 5 mm)	Hot-rolling	C57BL/6 mice	Femoral shaft	2 2 2	170 190 220	All alloys showed excellent biocompatibility; alloys promoted new bone formation	[87]
Zn-0.002 Mg	Wire (∅ 0.25 × 15 mm)	Extrusion + drawing	Sprague–Dawley rat	Abdominal aorta	1.5 3 4.5 6 11	29 19 27 32 51	Alloys are sufficiently biocompatible; though biocompatibility decreased with increasing Mg content due to enhanced corrosion resistance by the Mg_2Zn_{11}	[102]
Zn-0.005 Mg					1.5 3 4.5 6 11	21 19 23 30 38		
Zn-0.08 Mg					1.5 3 4.5 6 11	12 13 15 27 23		

(*continued on next page*)

Table 5 (*continued*)

Composition	Shape of implant	Fabrication method	Type of host	Location	In vivo corrosion		In vivo biocompatibility	Refs.
					Exposure Duration, months	Corrosion rate CR, μm/yr		
Zn-0.1Li	Wire (∅ 0.25 × 20 mm)	Extrusion + Drawing	Sprague–Dawley rat	Abdominal aorta	2 4 6.5 9 12	8 16 19 39 46	Implant showed good biocompatibility; moderate inflammation with non-obstructive neointima; neointima thickness is higher in Zn-Li than pure Zn	[107]
Zn-0.05 Mg	Strip (12 × 0.30 × 0.30 mm)	Hot rolling	Rabbit	Femoral shaft	6	–	Implant did not induce systemic toxicity, promoted bone tissue growth, and possessed antibacterial qualities	[103]
Zn-1Al, Zn-3Al, Zn-5Al	Strip (12 × 0.30 × 0.30 mm)	Hot rolling	Sprague–Dawley rat	Abdominal aorta	6	>20 (40% area oxidised)	Implants showed good biocompatibility; resisted fibrotic encapsulation; moderate degrees of inflammation	[74 109]
Zn-2Fe	Disc (∅ 7 mm × 2 mm height)	Gravity casting	Wistar rats	Subcutaneous midline of back	3.5 6	112 55	Implants showed good biocompatibility obtained from hematological profiles and histological analysis.	[188]
Composite								
Zn-5HA	Cylinder (∅ 2 × 5 mm		Sprague-Dawley rat	Femur condyle	1.2	Zn-5HA displayed higher corrosion rate than pure Zn	Addition of HA resulted in a better performance in osteogenesis with prolonged implantation time.	[128]

Finally, it is worth mentioning that the addition of the bioceramic hydroxyapatite (HA) can also improve the in vitro biocompatibility of Zn. Yang et al. [128] reported better cell (MC3T3-E1) viability in Zn-HA composite than in pure Zn. Furthermore, the composite exhibited excellent hemocompatibility and good antibacterial qualities against S. aureus.

6.4.2. Influence of fabrication technique

Table 4 indicates that most fabrication techniques, i.e., casting, wrought, P/M, and even additive manufacturing, are viable options for producing biocompatible Zn and Zn alloys. However, while there is a considerable number of reports on the influence of alloying elements on the biocompatibility of Zn, there are very few reports on the impact of fabrication technique on the biocompatibility of Zn. Often a study reports on the biocompatibility of Zn made via a specific fabrication process only. Due to slight differences in the details of biocompatibility tests adopted (e.g., different cell lines, exposure times, extract medium, etc.), it may be difficult to directly compare biocompatibility results as these differences influence the results of each test. Therefore, it would be best to only draw conclusions from results that originate from the same work.

Reports from four studies are presented here. Shen et al. [94], who studied the in vitro biocompatibility of Zn-1.2Mg with human osteosarcoma cells (HOS and MG63), observed that cell viability and hemocompatibility is better in as-cast than extruded alloy. This could be related to the increase in corrosion rate of Zn-1.2Mg after extrusion. Li et al. [87] reported that there was no significant difference in the hemocompatibility of as-cast and as-rolled pure Zn and some Zn ternary alloys (i.e., Zn-1Mg-1Ca, Zn-1Mg-1Sr, Zn-1Ca-1Sr). Liu et al. [116] noted that hot-rolled Zn-1Mg-0.1Mn showed better hemocompatibility than its as-cast counterpart. They did not expound on a reason for this observation. However, the corrosion rate of the hot-rolled specimen was slightly lower than the as-cast. In another work, Liu et al. [115] concluded that there was no difference in hemocompatibility between as-cast and hot-rolled Zn-1Mg-0.1Sr alloy.

Clearly, the amount of information is not yet enough to justify a definitive conclusion on the matter. However, one can draw from other relevant observations. As was observed in alloyed Zn, the biocompatibility was largely associated to (i) the composition of the released corrosion products (i.e., toxic or non-toxic) and on (ii) the corrosion rate, as this dictates the amount of material interacting with the surrounding cells and tissues. Since fabrication technique influences microstructure, and consequently the biodegradability of Zn, then it is reasonable to assume that fabrication technique will also influence, either positively or adversely depending on the interplay of corrosion product and corrosion rate on the surrounding tissues, the biocompatibility of the metal. Such an assumption is consistent with what was observed in other biodegradable metals [9,183,184].

Physicochemical properties of the surface, specifically wettability and surface roughness, can also influence the biocompatibility of an implant [185,186]. Wettability affects protein adsorption that is crucial for cell proliferation on the surface of the implant]. It is believed that moderate hydrophilicity, which is achieved at an optimal range of surface energy, can enhance cell growth and improve biocompatibility. Surface roughness influences a number of physiological phenomenon including cell spreading, cell differentiation, osseointegration as well as biofilm formation. For example, high surface roughness is essential to induce tissue and bone tissue in bone implants. These physicochemical properties are also dependent on the choice of processing technique, and future studies are needed to investigate the correlation between surface properties and biocompatibility of Zn.

Please cite this article as: J. Venezuela and M. S. Dargusch, The influence of alloying and fabrication techniques on the mechanical properties, biodegradability and biocompatibility of zinc: A comprehensive review, Acta Biomaterialia, https://doi.org/10.1016/j.actbio.2019.01.035

6.5. In vivo biocorrosion and biocompatibility of Zn alloys

There are relatively fewer reports on the in vivo performance compared to the in vitro performance of Zn and Zn alloys. This discrepancy is understandable as in vitro tests are generally expensive, time-consuming, and complex; hence the reluctance of researchers to immediately engage in these type of experiments. However, in vivo tests are indispensable and are considered the more relevant approach for evaluating the biocorrosion and biocompatibility of a candidate implant material [187].

Table 5 shows a summary of in vivo biodegradation and biocompatibility reports on several Zn and Zn alloys. The first report on the in vivo performance of Zn was by Bowen et al. [18] in 2013. They implanted commercially-available 4 N Zn wires into the abdominal aorta of Sprague-Dawley rays and observed the implants' behaviour up to a period of 6 months. They made some important observations including: (i) the in vivo corrosion rate of pure Zn ranged from 10 to 50 μm yr^{-1}, which is within the ideal rate of about 20 μm yr^{-1}, (ii) the thin, compact corrosion product of Zn similar to Mg, and (ii) the excellent biocompatibility and antiatherogenic properties of the Zn implant. They also noted that Zn, though a promising alternative to Mg in bioabsorbable stent applications, do not possess sufficient mechanical properties for this application. Though Bowen et al. were not the first to report on the biocompatibility of Zn, they were the first to confirm the in vivo biocompatibility of Zn and paved the way for future work on this metal. Further works by Bowen et al. [71] on the in vivo biocompatibility of Zn led to similar conclusions; i.e., Zn implant showed good biocompatibility while showing no risk factors for in-stent restenosis due to the absence of a discernible chronic inflammatory response, necrosis, or hyperproliferative (hyperplasia) response. Early tissue regeneration was also observed within the footprint of the implant. Zhao et al. [107] also echoed these observations. They implanted a fabricated, wrought (extruded and drawn) 4 N Zn wire in the abdominal aorta of Sprague-Dawley rats and monitored in vivo performance for 12 months. They reported that the Zn implant showed good biocompatibility, though with some moderate inflammation occurring in the non-obstructive neointima. They further noted that the neointima thickness formed on pure Zn is lower than those formed on Zn-0.1Li alloy. Drelich et al. [72] confirmed the long-term (1-year) biocompatibility of pure Zn, noting that fibrotic encapsulation allowed for bio-integration by reducing the inflammatory response of the affected tissues. In another work, Drelich et al. [73] observed the importance of the presence of the oxide film on the biodegradation of pure Zn. By using an appropriate surface engineering treatment (e.g., anodizing, electropolishing), the quality of the oxide films may be altered and consequently lead to tunable rates of biocorrosion.

Shomali et al. [129] studied the in vivo degradation of a PLLA-coated Zn wire. They noted that even a very thin coating of the biopolymer (~1 μm) is effective in delaying Zn degradation by about 6 months. However, the coating induced a toxic response from the surrounding tissue indicating a reduction in the biocompatibility of Zn after the surface treatment. Studies on polymer coatings are important in stent technologies as these have already been proven effective for drug delivery in drug-eluting stents [29,30].

Aside from pure Zn, the in vivo performances of several Zn alloys were also reported. A number of these reports involve Zn-Mg alloys. All the studies on Zn-Mg alloys were unanimous in declaring the excellent in vivo biocompatibility of this alloy. Though pure Zn is not as favourable for bone integration as pure Mg [65], Li et al. [87] noted that hot-rolled Zn-1Mg promoted the formation of new bone tissues and also displayed excellent radiopacity. Similarly, Xiao et al. [103] found that hot-rolled Zn-0.05Mg did not induce systemic toxicity, possessed antibacterial properties, and promoted bone tissue growth. Jin et al. [102] observed that increasing Mg content in wrought Zn-*x*Mg (x = 0.002, 0.00, 0.08) wires decreased the in vivo biocompatibility but increased the corrosion resistance of the alloy.

Other binary Zn alloys such as Zn-1Ca [87], Zn-1Sr [87], Zn-0.1Li [107], Zn-Al [109] and Zn-2Fe [188] were all reported to possess good in vivo biodegradability and biocompatibility. Li et al. [87] reported that Zn-1Ca and Zn-1Sr were also capable of inducing new bone growth, similar to Zn-1Mg. Zhao et al. [107] observed that Zn-0.1Li induced thicker non-obstructive neontima formation and a higher inflammatory response than pure Zn, indicating a slight reduction in biocompatibility due to Li. Bowen et al. [109] noted an interesting in vivo behaviour in Zn-Al alloys. While pure Zn was noted to degrade starting from the surface towards the core, the Zn-Al alloys were found to be degraded internally even in the early stages of corrosion (1.5 mos). Cracks were found at the core of the alloys, and these grew in size with implantation time. The implants were found to resist a fibrotic encapsulation response. Also, the moderate inflammatory response was not directly due to Al but rather caused by intergranular corrosion. Only the Zn-Al alloys were particularly susceptible to intergranular corrosion, driven by micro-anodic sites consisting of Al precipitates located at the grain boundaries. Finally, Kafri et al. [188] reported an almost two-fold increase in corrosion rate after the addition of 2 wt% Fe in Zn.

A majority of the reported in vivo studies involved implantations in the abdominal aorta, the results of which are targeted for cardiovascular stent applications. In contrast, only three studies [87,103,128] reported implantations in bone (i.e., femoral shafts) in which results are more suitable for orthopedic applications. Also, one study implanted Zn subcutaneously [188]. It is noteworthy that the corrosion rate reported for Zn implanted in the femoral shaft was significantly higher (3X) than for those implants in the abdominal aorta. Li et al. [87] reported a corrosion rate of about 170–220 μm for Zn-1X (X= Mg, Ca, Sr) implanted in the femoral shaft of a C57BL/6 mice for a 2-mos implantation time, while the range of corrosion rate for several types of Zn implants (i.e., Zn, Zn-Mg, Zn-Al) generally falls in between 10 and 50 um when implanted in abdominal aorta for a period of 1–12 mos. This observation suggests the influence of implant location on corrosion rate. However, it may be argued that this conclusion is premature since there were some differences in these studies that could account for this disparity, such as differences in specimen dimension, animal host, and alloy composition. This issue could be resolved by additional studies in the future.

The addition of HA appears to increase the in vivo degradation rate of the Zn-based MMC, consistent with the results of in vitro degradation tests [128]. HA induced localized corrosion in the composite, particularly at the Zn-HA interface, in contrast to the observed uniform corrosion mode in pure Zn. On the other hand, the Zn-HA composite exhibited excellent in vivo biocompatibility and was better than pure Zn in stimulating new bone formation.

All of the in vivo studies used a small animal model; i.e., rat, mice or rabbit. This approach is logical and prepares the groundwork for future studies in larger models. As studies on biodegradable Zn move forward, it would be interesting to see the in vivo behaviour of Zn-based implants in larger animals such as pigs or horses, and eventually in humans.

Reports on the behaviour of the in vivo corrosion rate over time are also interesting to consider as these appear contradicting. Bowen et al. [18] noted a non-linear increase in the corrosion rate of pure Zn with time. The corrosion rate was observed to accelerate after 3 mos then normalized at 6 mos. In contrast, Drelich et al. [72] noted a linear increase in cross-sectional area reduction due to corrosion. Consequently, they measured a fairly steady in vivo

Please cite this article as: J. Venezuela and M. S. Dargusch, The influence of alloying and fabrication techniques on the mechanical properties, biodegradability and biocompatibility of zinc: A comprehensive review, Acta Biomaterialia, https://doi.org/10.1016/j.actbio.2019.01.035

corrosion rate of about 25 μm yr^{-1} in pure Zn over a 20-month period despite the presence of fibrotic encapsulation. Jin et al. [102] noted that the in vivo corrosion rate of Zn-*x*Mg (x = 0.002, 0.005, 0.08) increased with time, while Zhao et al. [107] observed a fluctuating corrosion rate in pure Zn over a 12 month period and a steadily increasing corrosion rate in Zn-01Li over the same period. Kafri et al. [188] reported a drop in the corrosion rate of Zn and Zn-2Fe after comparing 3.5 and 6 mos implantation times. Yang et al. [86], who tested the in vivo corrosion performance of an actual stent, noted that the corrosion rate of the Zn stent decreased over time and became steady after 6 months. They proposed that this behaviour is primarily influenced by the physiological changes occurring in the vicinity of the degrading stent, as previously discussed in Section 6.2. The difference in the reported results may be due to slight differences in the experimental details of each study, and future work may be needed to ascertain which corrosion behaviour is accurate.

Finally, most of the in vivo tests reported for Zn used specimens with simple geometric shapes such as wires or strips. Very few studies reported on the in vivo behaviour of actual stents, and there is no report on Zn-based bone fixation devices. The succeeding sections describe the fabrication and the in vivo performance of Zn stents.

6.6. Fabrication and in vivo performance of actual Zn stents

6.6.1. Stent fabrication

There exist several options for creating metallic stents. Often, the choice of a particular fabrication route depends on the inherent property of the base metal. For ductile metals like SS or nitinol, options can range from wire weaving or braiding, laser machining, and electroforming [189]. Post-processing techniques are employed to improve cut quality and meet other property requirements. These techniques include cleaning, deburring, etching, and final polishing.

However, for metals with limited ductility like Zn the most feasible approach involves a combination of fabrication techniques. Stent fabrication starts with creating the hollow microtube. This preform may be made using a suitable wrought process (e.g., drawing or extrusion). The microtube is then processed further to create the necessary stent design. For example, Hiebl et al. [76] and Yang et al. [86] used laser cutting, while Wang et al. [114] reported on using a combination of laser etching and electrochemical polishing to create the stent. Mostaed et al. [96] further confirmed that the use of laser cutting does not induce significant changes in the microstructure and properties of the cut Zn alloy. This implies that this cutting technique is a feasible process for machining Zn preforms to stents. Fig. 8 shows some examples of fabricated vascular Zn stents reported in the literature. The in vivo performance of the laser cut stent fabricated by Yang et al. [86] will be reported in the succeeding section.

Catalano et al. [190] reported on the fabrication of flat pure Zn stents by a two-step process involving laser microcutting and chemical etching. The starting material is a flat sheet that is laser cut then chemically etched to form a flat mesh. The flat mesh is later expanded using a balloon catheter to form a 3D tubular shape. Though the planar stents was successfully fabricated, additional tests to determine in vivo and in vitro performance is still needed.

Additive manufacturing (aka 3-D printing) techniques remain a viable option for fabricating stents in the future, especially useful for creating patient-specific customized implants. Reports on 3-D printed polymer-based, bioabsorbable vascular stents already exist [191]. Recently, Wen et al. [80] reported on the successful fabrication of Zn stents using SLM, as shown in Fig. 9. They used a starting raw material of nitrogen-atomized pure Zn powder with an average diameter of 28.2 μm and an oxygen content of 0.98%. These 3D-printed stents had diameters of 5, 4, 3 and 2 mm, with strut diameters of 500, 300, 300 and 200 μm, respectively. The as-printed surface roughness of the stent was still unideal but could be improved with an appropriate finishing technique (e.g., chemical or electrochemical polishing). It would be interesting to see the in vivo performance of this 3-D printed stent.

6.6.2. In vivo performance of Zn stents

Reports on the performance of actual Zn stents are quite rare. Early reports on zinc's in vivo performance did not involve an actual stent design, but rather reasonably simple shapes such as wires [18,71,87]. Liu et al. [75] reported testing Zn mini-tubes, which is the precursor shape of the stent, but these were done in vitro.

In 2015, Hiebl et al. created a zinc stent prepared by laser cutting. The stent possessed a closed-cell design consisting of interlocked stent segments. However, the stent was tested only in vitro, using a serum-supplemented cell (3T3) culture medium.

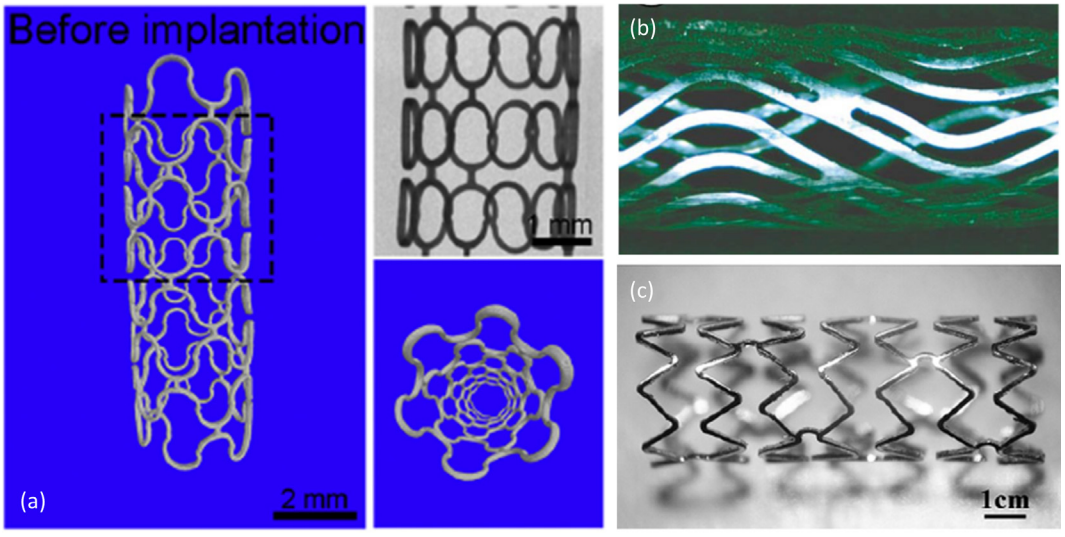

Fig. 8. Examples of fabricated vascular Zn stents using a combination of wrought processing and laser machining, as reported by (a) Yang et al. (reprinted from [86], with permission from Elsevier) (b) Hiebl et al. (reprinted from [76], with permission from IOSPress) (c) Wang et al. (reprinted from [114], with permission from Elsevier).

Please cite this article as: J. Venezuela and M. S. Dargusch, The influence of alloying and fabrication techniques on the mechanical properties, biodegradability and biocompatibility of zinc: A comprehensive review, Acta Biomaterialia, https://doi.org/10.1016/j.actbio.2019.01.035

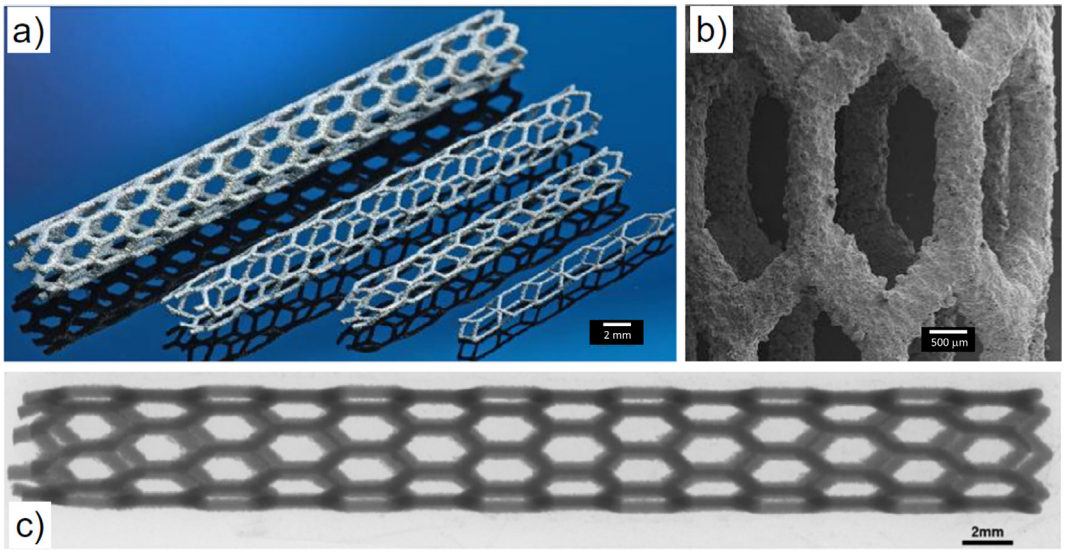

Fig. 9. The 3D-printed cardiovascular stent produced by Wen et al.: a) sample photo, b) SEM. image, and c) radiographic image. Scale bars for (a) and (b) were improved for better visibility. Reprinted from [80], with permission from Elsevier.

Tang et al. [106] reported fabricating vascular stents from Zn-Cu microtubes (3 mm outer diameter and 0.2 mm thickness) but failed to describe the performance of this stent in the report. Similarly, Wang et al. [114] cited the successful fabrication of a prototype vascular stent from Zn-5Mg-1Fe microtubes. They reported on the in vitro degradation of the microtube, as well as on the mechanical behaviour (i.e., balloon expansion capabilities) of the fabricated stent, but did not describe the in vivo performance of the stent.

In 2017, Yang et al. [86] published arguably the first report on the performance of an actual zinc stent tested in vivo. The test was a one-year study that involved inserting the stent in the abdominal aorta of a rabbit. Fig. 10 shows some of the images taken by Yang et al. of the stained section of the abdominal aorta at different implantation times. Their work resulted in a deeper understanding of zinc degradation in a physiological environment. Significant findings from this work include: (i) the retention of mechanical integrity of the zinc stent for 6 months, (ii) the degradation of about 40% (i.e., 41.75 ± 29.72%) of the stent volume after 12 months, (iii) the excellent biocompatibility of the degradation product of Zn, and (iv) the proposal of an in vivo degradation mechanism for Zn (discussed in detail in Section 6.2). They noted the significant influence of the blood vessel's healing process (e.g., the formation of neointima) on the degradation behaviour of Zn. The most important conclusion from this study is the favourable recommendation of Zn as a future biodegradable metal for stent fabrication.

Yang et al. [86] also noted that the corrosion rate of the Zn stent started high at 30 µm yr^{-1} during the first month, decreased to 10 µm yr^{-1} at the 3rd month, then steadied to about 15 µm yr^{-1} at the 6th and 12th months. This was owing to the formation of neointima that protected the implant from the typical aggressive

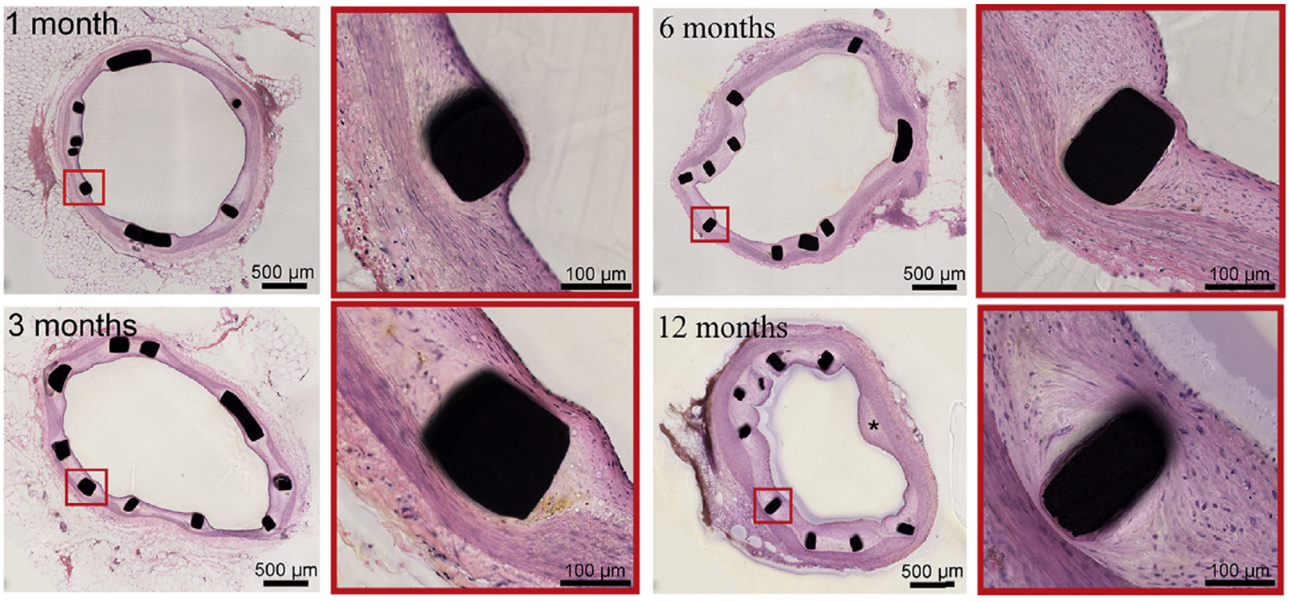

Fig. 10. Low and high magnification micrographs of the stained sections of the abdominal aorta of a rabbit after 1, 3, 6 and 12 months implantation of the pure Zn stent, as reported by Yang et al. These images show the evolution of neontima around the stent struts over time. Reprinted from [86], with permission from Elsevier.

Please cite this article as: J. Venezuela and M. S. Dargusch, The influence of alloying and fabrication techniques on the mechanical properties, biodegradability and biocompatibility of zinc: A comprehensive review, Acta Biomaterialia, https://doi.org/10.1016/j.actbio.2019.01.035

conditions present when wholly exposed to flowing blood. This is in contrast to some previous observations on Zn implants in which the formation of neointima did not adversely affect the degradation rate. For example, Guillory et al. [74] stated that the Zn implant degradation was higher in the covered areas (i.e., regions facing the arterial wall) than in the exposed sections (i.e., those in contact with flowing blood). Open contact with blood tended to passivate the metal surface and reduce the rate of degradation. Drelich et al. [72] noted a steady corrosion rate despite fibrotic encapsulation of the Zn implant. The difference in these observations may be due to the difference in implant geometry; i.e., wires vs. actual stents. Indeed, the dimension of the implanted wires was set to be similar to the typical aspect of a stent strut, with the idea that the wire would simulate the behaviour of a single strut. However, though cross-sectional areas of the wire and the strut were comparable, the shapes are different. Struts are typically quadrilateral (square or rectangular) while the implanted wires were circular. The difference in the exposed surface area could have influenced the corrosion behaviour of the implant; i.e., higher corrosion rates are favoured for shapes with higher surface area. Furthermore, the stent applied a radial force on the arterial wall during service whereas the implanted wires were non-load bearing. The influence of such stress could have been two-fold: (i) altered the degradation behaviour of the Zn implant, and (ii) changed the response of the affected arterial wall by causing localized endothelial damage.

6.7. Critical evaluation

The high number of positive reports on the biocompatibility of Zn and Zn alloys proves undoubtedly that the metal has considerable potential in the fabrication of biodegradable implants. In terms of biodegradability and biocompatibility, again it is the Zn-Mg alloys that appear to offer the most promise. Magnesium, by virtue of its excellent biocompatibility, enhances the biocompatibility of Zn. Also, the ability of the Zn-Mg alloy to promote bone growth makes it suitable for orthopedic applications. Though reports contradict on how Mg influences the biodegradability of Zn, such issues may be resolved by future studies. It is also anticipated that better control of composition and microstructures could allow finer tuning of the alloy's corrosion rate.

There is still no definite conclusion on how processing affects the biocompatibility of Zn due to the shortage of publications on the matter. At best, the influence of processing on biocompatibility may be linked with how processing affects microstructure and biodegradability. For now, wrought processing would still be the best option as it is not found to have an adverse influence on biodegradability and biocompatibility of Zn, and offers improvements on mechanical properties.

One issue that is important to address is the establishment of standards that are suitable for assessing degradability and biocompatibility of bioabsorbable metals. As was discussed previously, corrosion results from different in vitro tests are not ideal for comparison due to differences in methodologies. In other cases, some Zn and Zn alloys were observed to elicit a cytotoxic response from biological cells exposed to 100% concentration extracts [66,106]. This was attributed similarly attributed to the unsuitability of the test methodology for assessing biodegradable Zn. Clearly, a lot of ambiguity in the interpretation of these results would have been avoided if the proper test standards were in place and duly adopted.

In August 2018, the latest version of ISO-10993-1, Biological Evaluation of Medical Devices—Part 1: Evaluation and Testing within a Risk Management Process [192] was released. This standard is the most commonly used for assessing biocompatibility of medical device materials. The new standard has now placed greater emphasis on risk management process (i.e., biological safety planning and implementation process), together with characterization of the biomaterial. Particularly useful are the changes done in Table 1 of Annex A, Evaluation tests for consideration, of ISO-10993-1. This table is now normative and includes six additional test categories (physical and/or chemical information, material mediated pyrogenicity, chronic toxicity, carcinogenicity, reproductive/developmental toxicity, and degradation) [193]. Unlike in previous versions where several mandatory tests are identified, the current version has only one mandatory test requirement (i.e., chemical characterization), and other toxicological evaluations are decided on a case-by-case basis within a risk assessment framework. More importantly, it also includes information on the assessment of bioabsorbable materials.

There are other standards containing provisions for bioabsorbable metals, such as ASTM F1983-14, 'Standard Practice for Assessment of Selected Tissue Effects of Absorbable Biomaterials for Implant Applications' [194], and ISO/TR 37137, 'Cardiovascular biological evaluation of medical devices – Guidance for absorbable implants'[195]. Several standards are also under development [196,197]. This suggests that the standards development organizations (e.g., ASTM, ISO) are beginning to see the importance of biodegradable materials in future medical applications. The continued development of more standards requires the availability of experimental methods that yield results that are highly reproducible. The academe could certainly take the lead in pushing for this agenda, but the cooperation of other stakeholders (i.e., standards development body, medical field, industry) is essential for this effort to succeed [197].

Finally, a short but critical discussion on the issue of conducting in vivo or in vitro tests to assess the biocompatibility of biodegradable Zn is presented.

Biocompatibility is probably the most important property to ascertain for a candidate biomaterial. As mentioned, the term biocompatibility is broad and complex; hence proving the biocompatibility of a material requires assessing not only a single property but several properties. This also means that proving biocompatibility in materials is arduous, complicated, and expensive if not conducted with prudence. It is therefore essential for researchers to ascertain the value of performing either of the two types of biocompatibility test (i.e., in vivo or in vitro test). A lot of resources would be saved if researchers can discern when in vitro tests are worth doing or when it is better to skip in vitro testing and jump straight to in vivo experiments. To add some historical context, it is interesting to mention that Bowen's breakthrough in vivo study on Zn was conducted without the aid of substantial prior knowledge on the in vitro biocompatibility of the metal.

Both in vivo and in vitro testing have unique advantages and limitations. Since in vitro tests do not involve a living host, these tests are relatively simple, easy to implement, inexpensive to conduct, can be standardized, and amenable for large-scale screening [156,187]. Also, in vitro tests often involves only one type of cell, thus tests are easy to control, and results are easy to interpret. However, the relevance of in vitro tests results to in vivo performance is often questionable, and this is due to some limitations inherent to in vitro testing [156,177,198]. For example, a review by Sanchez et al. [199] stated that the measured in vivo corrosion rate for biodegradable Mg is about 1 to 4 times lower than the in vitro corrosion rate, which is attributed to the in vitro tests' inability to accurately mimic the complex physiological conditions found in vivo. As a consequence, comparison of in vivo and in vitro biocorrosion results, and even comparison of results of in vitro corrosion tests gleaned from disparate techniques, is ill-advised - a view which is similarly shared by other researchers [21].

In vivo tests using animal models are known to give more relevant information than in vitro tests as these provide a close approximation to human response. This implies that results can

Please cite this article as: J. Venezuela and M. S. Dargusch, The influence of alloying and fabrication techniques on the mechanical properties, biodegradability and biocompatibility of zinc: A comprehensive review, Acta Biomaterialia, https://doi.org/10.1016/j.actbio.2019.01.035

be used to predict the service behaviour of an implant. In vitro tests typically involve a single type of cell culture, while in vivo tests involve multi-cellular environments that display complex systemic interactions. Consequently, a more comprehensive response is obtained from in vivo tests [187]. However, the test is expensive, time-consuming, difficult to control, involves addressing the ethics of conducting research with animals, and sometimes results are difficult to interpret and quantify [187].

There is also an ongoing debate of the usefulness and applicability of animal tests [200]. Barnard and Kaufmann [201] suggested that animal experiments are poorly suited to address medical research needs and can even mislead researchers to wrong conclusions. They cited several historical cases to prove their argument. For example, they cited one case where a research team found that 25 compounds that were effective in reducing the damage of ischemic stroke in different animal models (e.g., rodents, cats, etc.) were completely ineffective to humans. Another is a case where scientists deduced from animal experiments that inhalation of tobacco smoke does not cause cancer.

In contrast, Botting and Morrison [202] defended the use of animal experiments. They cited the many contributions that this practice made to the advancement of medicine; from the pioneering work by Pasteur on identifying the role of microorganism in causing diseases, to subsequent studies of scientists on establishing causes and vaccines for numerous diseases (e.g., diphtheria, tetanus, rabies, tuberculosis, poliomyelitis, etc.), to the development of open heart surgeries and replacement heart valves, to kidney dialysis and kidney transplantations. They concluded that a majority of misconceptions about animal research that lead to the widespread activism against such practice could be cleared by a proper and thorough examination of the literature.

Clearly, there are numerous strong arguments for and against the practice of animal experiments, though one cannot deny that this practice has been beneficial to humans. To completely abandon in vivo animal testing may be too rash, and could lead to a regression in the rate of advancement in medicine. Interestingly, some hold the view that animal experiments, because of their irrelevance, have actually retarded progress. They argued that had animal research been outlawed earlier, researchers would have been forced to be creative and superior technologies would have resulted. A good example is the emergence of an in vitro test that used a reconstructed human skin (i.e., Corrositex) to test biocorrosivity [203]. It replaced the traditional tests where the substance is applied in on a rabbit's shaved back to determine how far it eats into the skin. This debate is indeed difficult to settle and time may tell how this will be resolved [200].

So is the way to go in vivo or in vitro? The answer is not as clear-cut. What is certain is that it will be foolish to assume that these tests are mutually exclusive. It may be better to assume that they are complementary. At this point, it is also reasonable to declare that in vitro tests should precede in vivo testing, and in vivo animal testing should precede human testing.

We believe the challenge lies in judging how best to implement each type of test.

For assessing in vitro biocompatibility, test options are numerous (e.g., cytocompatibility, hemocompatibility, mutagenicity, antibacterial test, etc.). Sometimes, the assessment of a single property can even be performed via several methods. For example, cytotoxicity can be tested using direct, indirect and extraction methods, and accuracy of results depends on the type of test adopted [177]. Thus, it is vital that users need to know which one of these are relevant, and decide how much information is necessary before in vivo tests are justified. The standard ISO-10993-1:2018 would be a good reference for researchers trying to decide which in vitro biocompatibility tests are appropriate to perform on a candidate material.

For in vivo testing, before the commencement of a test, it is essential to choose essential parameters such as the type of animal model to employ, the test duration, and the implant location. Concerning physiology, it is claimed that humans are identical to laboratory animals [202], yet the choice of animal subjects should still be determined by the scientific question at hand [203]. Anti-animal research proponents argue that animals in the laboratory do not undergo the same conditions as humans and, hence, the irrelevance of subsequent results. But animal experiments are fundamentally not designed to be so [202]. Instead, in vivo testing provides a means for studying a procedure. However, it does require meticulous interpretation of results to avoid misrepresentation of one's work.

7. Concluding remarks: research gaps and future directions

A number of foundational research studies have already established the tremendous potential of Zn as the next-generation, biodegradable metallic material. Substantial work has also been undertaken to understand the relevant properties of Zn for biomedical applications. Current literature suggests that the wrought Zn-*x*Mg alloy ($x < 1.5\%$) offers the best combination of mechanical strength, biodegradability, and biocompatibility. Improved control of processing techniques could optimize concomitant microstructures and further enhance the properties of this Zn alloy.

However, while Mg-based implants are already commercially available, rapid adoption of Zn in implant fabrication is not yet foreseeable. Compared to the amount of knowledge gained in biodegradable Mg, knowledge in Zn is still wanting. Several issues need to be addressed before the successful adoption of this metal in biomedical implant applications. The following lists some of the issues and some future research directions in this field:

i. Creation of test standards for biodegradable metals

As mentioned in an earlier discussion, one issue that needs to be addressed is the lack of test standards that are appropriate to assess the properties (e.g., biocorrosion, cytotoxicity) of biodegradable metals. This idea is not entirely new and has already been espoused by many researchers [9,178,197].

The existence of such standards will significantly contribute to the advancement of research in biodegradable Zn. One immediate benefit of having a standard is it would allow valid comparisons between results of different studies; hence research gaps will be easily identified. Subsequent studies can then be refocused on areas of concern and will result in the exponential growth of knowledge on the field of biodegradable materials.

ii. Age-hardening and strain-rate sensitivity of Zn

Jin et al. [102] have proven the age-hardening and strain rate sensitivity of certain biodegradable Zn-Mg alloys. Both phenomena bear important implications for mechanical properties, and would consequently influence the processability and applicability of the metal. Therefore, studying this behaviour should be an important consideration in future works on Zn and alloys.

iii. Biodegradable micro- and nano-porous Zn

Another possible application of biodegradable Zn is in making resorbable scaffolds for bone tissue engineering. This application requires an open cell pore structure akin to cancellous or spongy bone microstructure. Early studies by Capek et al. [126] and Hou et al. [127] on the fabrication of porous Zn implants showed promising results. These studies primarily involved using powder

Please cite this article as: J. Venezuela and M. S. Dargusch, The influence of alloying and fabrication techniques on the mechanical properties, biodegradability and biocompatibility of zinc: A comprehensive review, Acta Biomaterialia, https://doi.org/10.1016/j.actbio.2019.01.035

metallurgy. The foam replication technique [204] is another viable option for making open-cell microporous materials, and it would be interesting to see the properties of Zn fabricated via this process.

On the other hand, nano-scale alterations (e.g., hierarchical design) of metal surfaces are proven effective in enhancing cell attachment and proliferation on implants [205]. In biodegradable metals, nanoporous surfaces have been produced via dealloying or micro-arc oxidation [206].

iv. Application of advanced fabrication techniques

As highlighted in this work, the properties of biodegradable Zn are inherently dependent on the manufacturing method. While conventional forming techniques (i.e., casting, rolling, extrusion and drawing) have been thoroughly studied, it would be interesting to see how other advanced fabrication techniques can influence the properties of biodegradable Zn. The use of additive manufacturing techniques, in particular, selective laser melting (SLM), has started to gain considerable attention and offers tremendous promise [79,80,133,134]. Other fabrication methods such as electron beam melting (EBM) [207] and electroforming [208] are also viable and could offer some unique benefits.

v. Understanding the influence of surface treatment on biodegradable Zn

Surface treatment techniques can significantly alter the properties of a material. This surface treatment can be a coating or something that alters the mechanical and chemical behaviour of the material. Polymer coatings are especially popular for creating drug-eluting stents, and some studies are beginning to see how these coatings can affect biodegradable Zn. For example, Shomali et al. [129] have already reported on the in vivo performance of PLLA-coated Zn alloy. The application of biodegradable metal coating (e.g., Zn-coated Mg, Zn-coated Fe) on existing biodegradable metals is also worth considering. This combination of biodegradable metals could offer some unique properties that are not available in any of its single metal components. It will also be interesting to see how some of the advanced surface treatments, such as plasma surface engineering [209], and electrochemical polymerisation, that have been previously applied to biomaterials can alter the properties of Zn.

vi. Understanding the influence of physiological elements on Zn corrosion

Though some outstanding work has been performed to understand the corrosion mechanisms of Zn in vivo, several aspects are not yet completely understood. For example, in a recent study on biodegradable Fe-based implants after prolonged in vivo exposure [59], it was noted that O_2 concentration had a significant influence on the corrosion behaviour of the metal. Hence, due to the difference in the O_2 concentration between in vitro and in vivo tests, the measured rates of corrosion for biodegradable Fe in these two tests are significantly dissimilar. A comprehensive understanding of the influence of elements (e.g., O_2), ions (e.g., Cl^-, CO_3^-, HPO_4^-), and compounds (e.g., CO_2) present in the physiological environment on the corrosion mechanism of Zn could be the key to explaining the significant difference between in vitro and in vivo corrosion, and allow accurate prediction of the service performance of the metal.

vii. An in vitro test that accurately replicates in vivo test results

A lot of effort has been made to create an in vitro test apparatus that could precisely match the in vivo performance of implants. Such a device will be a true 'disruptive technology' in the medical field, as it will simplify and will bring down the cost of biocompatibility testing. Some examples of these apparatus include the pseudo-physiological test bench proposed by Levesque et al. [210] or the stentable in vitro artery by Antoine et al.[211]. Both were used for understanding in vitro stent performance and potentially offer tremendous help in the design and development of future endovascular devices.

Identifying and replicating the relevant microenvironment specific to the biomedical application is one of the keys in creating such an in vitro test [212], but this is certainly difficult. Indeed, some in the scientific community believe that the tremendous technological challenge in creating this test is due to the fact that an isolated and cultivated cells' behaviour is significantly different from the corresponding cell's behaviour inside of the human body [156,213]. Some even suggest that the body of knowledge necessary for creating this type of in vitro test is centuries rather than decades away [198]. Though the task appears daunting, efforts to develop this technology needs to continue since the benefits of such a device would be enormous.

In line with the development of in vitro tests for biodegradable metals is the push towards standardization of these tests.

viii. Establishing the accurate mechanical property requirements specific to a medical application

A lot of research has been performed to improve the mechanical properties of Zn in order to meet the minimum standard requirements of specific biomedical applications. However, as cited earlier, some of the recent commercially-available, absorbable stents are composed of a material with properties that appear to be 'substandard', i.e., having properties inferior to the required 300 MPa UTS and 18% elongation at fracture ductility for stent applications. If the medical community already embraces mechanically 'substandard' materials, then it means that it may be a good time to re-evaluate the adopted standards. Establishing a more accurate and relevant standard value will allow for precise screening of future biomaterials.

Acknowledgement

J. Venezuela and M. S. Dargusch acknowledge the support of the Australian Research Council through the ARC Research Hub for Advanced Manufacturing of Medical Devices (IH150100024).

Declarations of Interest

All authors have read and understood Acta Biomaterialia's policy on declaration of interests and declare that we have no financial relationship with any organisations that might have an interest in the submitted work.

References

[1] A.C. Fraker, A.W. Ruff, Metallurgical Surgical Implants: State of the Art, 29 (1977) 2–-28.
[2] I. Gotman, Characteristics of metals used in implants, J. Endourol. 11 (1997) 383–389.
[3] P. Triclot, Metal-on-metal: history, state of the art (2010), Int. Orthop. 35 (2010) 201–206.
[4] H. Hermawan, D. Ramdan, J.R.P. Djuansjah, Metals for Biomedical Applications, INTECH Open Access Publisher, 2011.
[5] M. Saini, Y. Singh, P. Arora, V. Arora, K. Jain, Implant biomaterials: a comprehensive review, World J. Clin. Cases: WJCC 3 (2015) 52–57.
[6] N.S. Manam, W.S.W. Harun, D.N.A. Shri, S.A.C. Ghani, T. Kurniawan, M.H. Ismail, M.H.I. Ibrahim, Study of corrosion in biocompatible metals for implants: a review, J. Alloys Compd. 701 (2017) 698–715.

[7] N. Sykaras, A.M. Iacopino, V.A. Marker, R.G. Triplett, R.D. Woody, Implant materials, designs, and surface topographies: their effect on osseointegration. A literature review, Int. J. Oral Maxillofac. Implants 15 (2000) 675–690.
[8] F. Witte, The history of biodegradable magnesium implants: A review, Acta Biomater. 6 (2010) 1680–1692.
[9] Y.F. Zheng, X.N. Gu, F. Witte, Biodegradable metals, Mater. Sci. Eng. R Rep. 77 (2014) 1–34.
[10] H. Hermawan, Biodegradable Metals From Concept to Applications, Springer-Verlag Berlin Heidelberg, 2012.
[11] J.M. Seitz, M. Durisin, J. Goldman, J.W. Drelich, Recent advances in biodegradable metals for medical sutures: a critical review, Adv. Healthc. Mater. 4 (2015) 1915–1936.
[12] M. Heiden, E. Walker, L. Stanciu, Magnesium, iron and zinc alloys, the trifecta of bioresorbable orthopaedic and vascular implantation – a review, J. Biotechnol. Biomater. 5 (2015) 178.
[13] H. Li, Y. Zheng, L. Qin, Progress of biodegradable metals, Proc. Nat. Sci-Mater. Int. 24 (2014) 414–422.
[14] S.H. Im, Y. Jung, S.H. Kim, Current status and future direction of biodegradable metallic and polymeric vascular scaffolds for next-generation stents, Acta Biomater. 60 (2017) 3–22.
[15] H. Hermawan, Updates on the research and development of absorbable metals for biomedical applications, Prog. Biomater. 7 (2018) 93–110.
[16] Y. Liu, Y. Zheng, B. Hayes, Degradable, absorbable or resorbable—what is the best grammatical modifier for an implant that is eventually absorbed by the body?, Sci China Mater. 60 (2017) 377–391.
[17] E. Crubzy, P. Murail, L. Girard, J.P. Bernadou, False teeth of the Roman world, Nature 391 (1998) 29.
[18] P.K. Bowen, J. Drelich, J. Goldman, Zinc exhibits ideal physiological corrosion behavior for bioabsorbable stents, Adv. Mater. 25 (2013) 2577–2582.
[19] D. Vojtech, J. Kubasek, J. Serak, P. Novak, Mechanical and corrosion properties of newly developed biodegradable Zn-based alloys for bone fixation, Acta Biomater. 7 (2011) 3515–3522.
[20] M.S. Dambatta, D. Kurniawan, S. Izman, B. Yahaya, H. Hermawan, Review on Zn-based alloys as potential biodegradable medical devices materials, Appl. Mech. Mater. 776 (2015) 277–281.
[21] P.K. Bowen, E.R. Shearier, S. Zhao, R.J. Guillory, F. Zhao, J. Goldman, J.W. Drelich, Biodegradable metals for cardiovascular stents: from clinical concerns to recent Zn-alloys, Adv. Healthc. Mater. 5 (2016) 1121–1140.
[22] G.K. Levy, J. Goldman, E. Aghion, The prospects of zinc as a structural material for biodegradable implants—a review paper, Metals 7 (2017) 402.
[23] E. Mostaed, M. Sikora-Jasinska, J.W. Drelich, M. Vedani, Zinc-based alloys for degradable vascular stent applications, Acta Biomater. 71 (2018) 1–23.
[24] C.H. Chen, A.J. Kirtane, Stents, Restenosis, and Stent Thrombossi, in: M.J. Kern, M.J. Lim, P. Sorajja (Eds.), The Interventional Cardiac Catheterization Handbook, fourth ed., Elsevier, Philadelphia, PA, 2018, pp. 179–199.
[25] S. Khera, D. Kolte, D.L. Bhatt, Chapter 16 – Percutaneous Coronary Intervention, in: W.S. Aronow, J.A. McClung (Eds.), Translational Research in Coronary Artery Disease, Academic Press, Boston, 2016, pp. 179–194.
[26] R. Lakatos, M.A. Herbenick, General Principles of Internal Fixation, in, 2015.
[27] M. Moravej, D. Mantovani, Biodegradable metals for cardiovascular stent application: interests and new opportunities, Int. J. Mol. Sci. 12 (2011) 4250–4270.
[28] T. Hanawa, Materials for metallic stents, J Artif. Organs 12 (2009) 73–79.
[29] S. Garg, P.W. Serruys, Coronary stents: current status, Am. College Cardiol. 56 (2010) 1–42.
[30] G.G. Stefanini, R.A. Byrne, S. Windecker, A. Kastrati, State of the art: coronary artery stents – past, present and future, EuroIntervention 13 (2017) 706–716.
[31] J.A. Ormiston, P.W.S. Serruys, Bioabsorbable coronary stents, Circulation: Cardiovasc. Interventions 2 (2009) 255–260.
[32] M.P. Staiger, A.M. Pietak, J. Huadmai, G. Dias, Magnesium and its alloys as orthopedic biomaterials: a review, Biomaterials 27 (2006) 1728–1734.
[33] M.S. Dhillon, S. Prabhakar, C. Prasanna, Preliminary experience with biodegradable implants for fracture fixation, Indian J. Orthop. 42 (2008) 319–322.
[34] R.J. Werkhoven, W.H. Sillekens, J.B.J.M. van Lieshout, Processing aspects of magnesium alloy stent tube, in: Magnesium Technology 2011, John Wiley & Sons, Inc., 2011, pp. 419–424.
[35] F. Barca, R. Busa, Resorbable poly-l-lactic acid mini-staples for the fixation of Akin osteotomies, J. Foot Ankle Surg. 36 (1997) 106–111.
[36] H. Hermawan, Biodegradable Metals: From Concept to Applications, Springer Berlin, Heidelberg, 2012.
[37] R. Waksman, Biodegradable stents: they do their job and disappear, J. Invasive Cardiol. 18 (2006) 70–74.
[38] Y. Onuma, J. Ormiston, P.W. Serruys, Bioresorbable scaffold technologies, Circulation 75 (2011) 509–520.
[39] R. Balcon, R. Beyar, S. Chierchia, I. De Scheerder, P.G. Hugenholtz, F. Kiemeneij, B. Meier, J. Meyer, J.P. Monassier, W. Wijns, Recommendations on stent manufacture, implantation and utilization, Eur. Heart J. 18 (1997) 1536–1547.
[40] G.O. Hofmann, F.D. Wagner, New implant designs for bioresorbable devices in orthopaedic surgery, Clin. Mater. 14 (1993) 207–215.
[41] W.J. van der Giessen, A.M. Lincoff, R.S. Schwartz, H.M. van Beusekom, P.W. Serruys, D.R. Jr Holmes, S.G. Ellis, E.J. Topol, Marked inflammatory sequelae to implantation of biodegradable and nonbiodegradable polymers in porcine coronary arteries, Circulation 94 (1996) 1690–1697.
[42] A.M. Lincoff, J.G. Furst, S.G. Ellis, R.J. Tuch, E.J. Topol, Sustained local delivery of dexamethasone by a novel intravascular eluting stent to prevent restenosis in the porcine coronary injury model, J Am. Coll. Cardiol. 29 (1997) 808–816.
[43] M. Vert, Degradable, biodegradable, and bioresorbable polymers for time-limited therapy, in: Y. Onuma, P.W.J.C. Serruys (Eds.), Bioresorbable Scaffolds: From Basic Concept to Clinical Applications, CRC Press, 2017.
[44] J.S. Bergström, D. Hayman, An overview of mechanical properties and material modeling of polylactide (PLA) for medical applications, Ann. Biomed. Eng. 44 (2016) 330–340.
[45] B. Zhao, X. Qiu, D. Wang, H. Li, X. He, Application of bioabsorbable screw fixation for anterior cervical decompression and bone grafting, Clinics 71 (2016) 320–324.
[46] D. Persaud-Sharma, A. McGoron, Biodegradable magnesium alloys: a review of material development and applications, J. Biomim. Biomater. Tissue Eng. 12 (2012) 25–39.
[47] S. Agarwal, J. Curtin, B. Duffy, S. Jaiswal, Biodegradable magnesium alloys for orthopaedic applications: a review on corrosion, biocompatibility and surface modifications, Mater. Sci. Eng. C 68 (2016) 948–963.
[48] C. Rapetto, M. Leoncini, Magmaris: a new generation metallic sirolimus-eluting fully bioresorbable scaffold: present status and future perspectives, J. Thorac. Dis. 9 (2017) S903–S913.
[49] Z. Barlas, BIOTRONIK Successfully Concludes Magmaris 2,000 Program at Two Years Since CE Mark, in, BIOTRONIK, 2018.
[50] M. Peuster, P. Wohlsein, M. Brügmann, M. Ehlerding, K. Seidler, C. Fink, H. Brauer, A. Fischer, G. Hausdorf, A novel approach to temporary stenting: degradable cardiovascular stents produced from corrodible metal-results 6–18 months after implantation into New Zealand white rabbits, Heart 86 (2001) 563–569.
[51] A. Francis, Y. Yang, S. Virtanen, A.R. Boccaccini, Iron and iron-based alloys for temporary cardiovascular applications, J. Mater. Sci.: Mater. Med. 26 (2015) 138.
[52] J. He, F.L. He, D. Li, Y.L. Liu, Y.Y. Liu, Y.J. Ye, D.C. Yin, Advances in Fe-based biodegradable metallic materials, RSC Adv. 6 (2016) 112819–112838.
[53] H. Hermawan, A. Purnama, D. Dube, J. Couet, D. Mantovani, Fe–Mn alloys for metallic biodegradable stents: degradation and cell viability studies, Acta Biomater. 6 (2010) 1852–1860.
[54] D. Zhang, W. Lin, H. Qi, IBS bioresorbable scaffold by Lifetech, in: Y. Onuma, P. W.J.C. Serruys (Eds.), Bioresorbable Scaffolds: From Basic Concept to Clinical Applications, CRC Press, 2017.
[55] J. Kubásek, D. Vojtěch, E. Jablonská, I. Pospíšilová, J. Lipov, T. Ruml, Structure, mechanical characteristics and in vitro degradation, cytotoxicity, genotoxicity and mutagenicity of novel biodegradable Zn–Mg alloys, Mater. Sci. Eng. C 58 (2016) 24–35.
[56] F. Witte, J. Fischer, J. Nellesen, H.A. Crostack, V. Kaese, A. Pisch, F. Beckmann, H. Windhagen, In vitro and in vivo corrosion measurements of magnesium alloys, Biomaterials 27 (2006) 1013–1018.
[57] S. Zhang, X. Zhang, C. Zhao, J. Li, Y. Song, C. Xie, H. Tao, Y. Zhang, Y. He, Y. Jiang, Y. Bian, Research on an Mg–Zn alloy as a degradable biomaterial, Acta Biomater. 6 (2010) 626–640.
[58] M. Peuster, C. Hesse, T. Schloo, C. Fink, P. Beerbaum, C. von Schnakenburg, Long-term biocompatibility of a corrodible peripheral iron stent in the porcine descending aorta, Biomaterials 27 (2006) 4955–4962.
[59] T. Kraus, F. Moszner, S. Fischerauer, M. Fiedler, E. Martinelli, J. Eichler, F. Witte, E. Willbold, M. Schinhammer, M. Meischel, Biodegradable Fe-based alloys for use in osteosynthesis: outcome of an in vivo study after 52 weeks, Acta Biomater. 10 (2014) 3346–3353.
[60] D. Pierson, J. Edick, A. Tauscher, E. Pokorney, P. Bowen, J. Gelbaugh, J. Stinson, H. Getty, C.H. Lee, J. Drelich, J. Goldman, A simplified in vivo approach for evaluating the bioabsorbable behavior of candidate stent materials, J. Biomed. Mater. Res. B Appl. Biomater. 100 (2012) 58–67.
[61] C.J. Frederickson, J.Y. Koh, A.I. Bush, The neurobiology of zinc in health and disease, Nat. Rev. Neurosci. 6 (2005) 449–462.
[62] B.L. Vallee, K.H. Falchuk, The biochemical basis of zinc physiology, Physiol. Rev. 73 (1993) 79–118.
[63] R. Cruz, J. Calasans-Maia, S. Sartoretto, V. Moraschini, A.M. Rossi, R.S. Louro, J. M. Granjeiro, M.D. Calasans-Maia, Does the incorporation of zinc into calcium phosphate improve bone repair? A systematic review, Ceram. Int. 44 (2018) 1240–1249.
[64] X. Luo, D. Barbieri, N. Davison, Y. Yan, J.D. de Bruijn, H. Yuan, Zinc in calcium phosphate mediates bone induction: in vitro and in vivo model, Acta Biomater. 10 (2014) 477–485.
[65] J. Kubasek, D. Vojtech, E. Jablonska, I. Pospisilova, J. Lipov, T. Ruml, Structure, mechanical characteristics and in vitro degradation, cytotoxicity, genotoxicity and mutagenicity of novel biodegradable Zn-Mg alloys, Mater. Sci. Eng. C-Mater. 58 (2016) 24–35.
[66] J. Niu, Z. Tang, H. Huang, J. Pei, H. Zhang, G. Yuan, W. Ding, Research on a Zn-Cu alloy as a biodegradable material for potential vascular stents application, Mater. Sci. Eng. C 69 (2016) 407–413.
[67] G.J. Fosmire, Zinc toxicity, Am. J. Clin. Nutr. 51 (1990) 225–227.
[68] A. Bolz, T. Popp, Implantable, bioresorbable vessel wall support, in particular coronary stent, in: USPTO (Ed.), Biotronik Mess- und Therapiegeraete GmbH and Co USA, 2001.
[69] X. Wang, H.M. Lu, X.L. Li, L. Li, Y.F. Zheng, Effects of cooling rate and composition on microstructures and properties of Zn-Mg alloys, Trans. Nonferrous Met. Soc. China 17 (2007) s122–s125.

Please cite this article as: J. Venezuela and M. S. Dargusch, The influence of alloying and fabrication techniques on the mechanical properties, biodegradability and biocompatibility of zinc: A comprehensive review, Acta Biomaterialia, https://doi.org/10.1016/j.actbio.2019.01.035

[70] J. Cheng, B. Liu, Y.H. Wu, Y.F. Zheng, Comparative in vitro study on pure metals (Fe, Mn, Mg, Zn and W) as biodegradable metals, J. Mater. Sci. Technol. 29 (2013) 619–627.
[71] P.K. Bowen, R.J. Guillory, E.R. Shearier, J.M. Seitz, J. Drelich, M. Bocks, F. Zhao, J. Goldman, Metallic zinc exhibits optimal biocompatibility for bioabsorbable endovascular stents, Mater. Sci. Eng. C Mater. Biol. Appl. 56 (2015) 467–472.
[72] A.J. Drelich, S. Zhao, R.J. Guillory, J.W. Drelich, J. Goldman, Long-term surveillance of zinc implant in murine artery: surprisingly steady biocorrosion rate, Acta Biomater. (2017).
[73] A.J. Drelich, P.K. Bowen, L. LaLonde, J. Goldman, J.W. Drelich, Importance of oxide film in endovascular biodegradable zinc stents, Surf. Innov. 4 (2016) 133–140.
[74] R.J.I.I. Guillory, P.K. Bowen, S.P. Hopkins, E.R. Shearier, E.J. Earley, A.A. Gillette, E. Aghion, M. Bocks, J.W. Drelich, J. Goldman, Corrosion characteristics dictate the long-term inflammatory profile of degradable zinc arterial implants, ACS Biomater. Sci. Eng. 2 (2016) 2355–2364.
[75] X. Liu, J. Sun, Y. Yang, Z. Pu, Y. Zheng, In vitro investigation of ultra-pure Zn and its mini-tube as potential bioabsorbable stent material, Mater. Lett. 161 (2015) 53–56.
[76] B. Hiebl, E. Nennig, S. Schiestel, A. Kovacs, F. Jung, H. Fischer, Biocompatibility of a novel zinc stent with a closed-cell-design, Clin. Hemorheol. Microcirc. 61 (2015) 205–211.
[77] A.G. Demir, L. Monguzzi, B. Previtali, Selective laser melting of pure Zn with high density for biodegradable implant manufacturing, Additive Manufacturing 15 (2017) 20–28.
[78] Y. Yang, F. Yuan, C. Gao, P. Feng, L. Xue, S. He, C. Shuai, A combined strategy to enhance the properties of Zn by laser rapid solidification and laser alloying, J. Mech. Behav. Biomed. Mater. 82 (2018) 51–60.
[79] P. Wen, L. Jauer, M. Voshage, Y. Chen, R. Poprawe, J.H. Schleifenbaum, Densification behavior of pure Zn metal parts produced by selective laser melting for manufacturing biodegradable implants, J. Mater. Process. Technol. 258 (2018) 128–137.
[80] P. Wen, M. Voshage, L. Jauer, Y. Chen, Y. Qin, R. Poprawe, J.H. Schleifenbaum, Laser additive manufacturing of Zn metal parts for biodegradable applications: processing, formation quality and mechanical properties, Mater. Des. 155 (2018) 36–45.
[81] K. Törne, M. Larsson, A. Norlin, J. Weissenrieder, Degradation of zinc in saline solutions, plasma, and whole blood, J. Biomed. Mater. Res. B Appl. Biomater. 104 (2016) 1141–1151.
[82] K. Törne, A. Örnberg, J. Weissenrieder, Influence of strain on the corrosion of magnesium alloys and zinc in physiological environments, Acta Biomater. 48 (2017) 541–550.
[83] J. Ma, N. Zhao, D. Zhu, Bioabsorbable zinc ion induced biphasic cellular responses in vascular smooth muscle cells, Sci. Rep. 6 (2016) 26661.
[84] E.R. Shearier, P.K. Bowen, W. He, A. Drelich, J. Drelich, J. Goldman, F. Zhao, In vitro cytotoxicity, adhesion, and proliferation of human vascular cells exposed to zinc, ACS Biomater. Sci. Eng. 2 (2016) 634–642.
[85] M.M. Alves, L.M. Marques, I. Nogueira, C.F. Santos, S.B. Salazar, S. Eugénio, N.P. Mira, M.F. Montemor, In silico, in vitro and antifungal activity of the surface layers formed on zinc during this biomaterial degradation, Appl. Surf. Sci. 447 (2018) 401–407.
[86] H. Yang, C. Wang, C. Liu, H. Chen, Y. Wu, J. Han, Z. Jia, W. Lin, D. Zhang, W. Li, W. Yuan, G. Guo, H. Li, G. Yang, D. Kong, D. Zhu, K. Takashima, L. Ruan, J. Nie, X. Li, Y. Zheng, Evolution of the degradation mechanism of pure zinc stent in the one-year study of rabbit abdominal aorta model, Biomaterials 145 (2017) 92–105.
[87] H.F. Li, X.H. Xie, Y.F. Zheng, Y. Cong, F.Y. Zhou, K.J. Qiu, X. Wang, S.H. Chen, L. Huang, L. Tian, L. Qin, Development of biodegradable Zn-1X binary alloys with nutrient alloying elements Mg, Ca and Sr, Sci. Rep. 5 (2015) 10719.
[88] H. Li, H. Yang, Y. Zheng, F. Zhou, G. Qiu, X. Wang, Design and characterizations of novel biodegradable ternary Zn-based alloys with IIA nutrient alloying elements Mg, Ca and Sr, Mater. Des. 83 (2015) 95–102.
[89] J. Kubásek, D. Vojtěch, Zn-based alloys as an alternative biodegradable materials, in: Metals, Czech Republic, EU, 2012.
[90] J. Kubásek, I. Pospílova, D. Vojtech, E. Jablonská, T. Ruml, Structural, mechanical and cytotoxicity characterization of as-cast biodegradable Zn-xMg (x = 0.8–8.3%) alloys, Mater. Technol. 48 (2014) 623–629.
[91] C. Yao, Z. Wang, S.L. Tay, T. Zhu, W. Gao, Effects of Mg on microstructure and corrosion properties of Zn–Mg alloy, J. Alloys Compd. 602 (2014) 101–107.
[92] H. Gong, K. Wang, R. Strich, J.G. Zhou, In vitro biodegradation behavior, mechanical properties, and cytotoxicity of biodegradable Zn-Mg alloy, J. Biomed. Mater. Res. B. Appl. Biomater. 103 (2015) 1632–1640.
[93] N.S. Murni, M.S. Dambatta, S.K. Yeap, G.R.A. Froemming, H. Hermawan, Cytotoxicity evaluation of biodegradable Zn–3Mg alloy toward normal human osteoblast cells, Mater. Sci. Eng. C 49 (2015) 560–566.
[94] C. Shen, X. Liu, B. Fan, P. Lan, F. Zhou, X. Li, H. Wang, X. Xiao, L. Li, S. Zhao, Z. Guo, Z. Pu, Y. Zheng, Mechanical properties, in vitro degradation behavior, hemocompatibility and cytotoxicity evaluation of Zn-1.2Mg alloy for biodegradable implants, RSC Adv. 6 (2016) 86410–86419.
[95] R.H. Galib, A. Sharif, Development of Zn-Mg alloys as a degradable biomaterial, Adv. Alloys Compd. 1 (2016) 1–7.
[96] E. Mostaed, M. Sikora-Jasinska, A. Mostaed, G. Loffredo, A.G. Demir, B. Previtali, D. Mantovani, R. Beanland, M. Vedani, Novel Zn-based alloys for biodegradable stent applications: design, development and in vitro degradation, J. Mech. Behav. Biomed. Mater. 60 (2016) 581–602.
[97] E. Jablonská, D. Vojtěch, M. Fousová, J. Kubásek, J. Lipov, J. Fojt, T. Ruml, Influence of surface pre-treatment on the cytocompatibility of a novel biodegradable ZnMg alloy, Mater. Sci. Eng. C 68 (2016) 198–204.
[98] M. Dambatta, S. Izman, D. Kurniawan, H. Hermawan, Processing of Zn-3Mg alloy by equal channel angular pressing for biodegradable metal implants, JKSUS, (2017).
[99] M.S. Dambatta, S. Izman, D. Kurniawan, S. Farahany, B. Yahaya, H. Hermawan, Influence of thermal treatment on microstructure, mechanical and degradation properties of Zn–3Mg alloy as potential biodegradable implant material, Mater. Des. 85 (2015) 431–437.
[100] T.A. Vida, A. Conde, E.S. Freitas, M.A. Arenas, N. Cheung, C. Brito, J. de Damborenea, A. Garcia, Directionally solidified dilute Zn-Mg alloys: correlation between microstructure and corrosion properties, J. Alloys Compd. 723 (2017) 536–547.
[101] A. Jarzębska, M. Bieda, J. Kawałko, L. Rogal, P. Koprowski, K. Sztwiertnia, W. Pachla, M. Kulczyk, A new approach to plastic deformation of biodegradable zinc alloy with magnesium and its effect on microstructure and mechanical properties, Mater. Lett. 211 (2018) 58–61.
[102] H. Jin, S. Zhao, R. Guillory, P.K. Bowen, Z. Yin, A. Griebel, J. Schaffer, E.J. Earley, J. Goldman, J.W. Drelich, Novel high-strength, low-alloys Zn-Mg (<0.1wt% Mg) and their arterial biodegradation, Mater. Sci. Eng. C 84 (2018) 67–79.
[103] C.L. Xiao, Y. Wang, S. Ren, E. Sun, C. Zhang, Indirectly extruded biodegradable Zn-0.05wt%Mg alloy with improved strength and ductility: in vitro and in vivo studies, J. Mater. Sci. Technol. (2018).
[104] M.M. Alves, T. Prosek, C.F. Santos, M.F. Montemor, Evolution of the in vitro degradation of Zn-Mg alloys under simulated physiological conditions, RSC Adv. 7 (2017) 28224–28233.
[105] L. Wang, Y. He, H. Zhao, H. Xie, S. Li, Y. Ren, G. Qin, Effect of cumulative strain on the microstructural and mechanical properties of Zn-0.02 wt%Mg alloy wires during room-temperature drawing process, J. Alloys Compd. 740 (2018) 949–957.
[106] Z. Tang, J. Niu, H. Huang, H. Zhang, J. Pei, J. Ou, G. Yuan, Potential biodegradable Zn-Cu binary alloys developed for cardiovascular implant applications, J. Mech. Behav. Biomed. Mater. 72 (2017) 182–191.
[107] S. Zhao, J.M. Seitz, R. Eifler, H.J. Maier, R.J. Guillory, E.J. Earley, A. Drelich, J. Goldman, J.W. Drelich, Zn-Li alloy after extrusion and drawing: Structural, mechanical characterization, and biodegradation in abdominal aorta of rat, Mater. Sci. Eng. C 76 (2017) 301–312.
[108] S. Zhao, C.T. McNamara, P. Bowen, N. Verhun, J.P. Braykovich, J. Goldman, J.W. Drelich, Structural characteristics and in vitro biodegradation of a novel Zn-Li alloy prepared by induction melting and hot rolling, Metall. Mater. Trans. A 48 (2017) 1204–1215.
[109] P.K. Bowen, J.M. Seitz, R.J. Guillory, J.P. Braykovich, S. Zhao, J. Goldman, J.W. Drelich, Evaluation of wrought Zn–Al alloys (1, 3, and 5 wt % Al) through mechanical and in vivo testing for stent applications, J. Biomed. Mater. Res. B Appl. Biomater. (2017) n/a-n/a.
[110] M. Sikora-Jasinska, E. Mostaed, A. Mostaed, R. Beanland, D. Mantovani, M. Vedani, Fabrication, mechanical properties and in vitro degradation behavior of newly developed ZnAg alloys for degradable implant applications, Mater. Sci. Eng. C 77 (2017) 1170–1181.
[111] P. Li, C. Schille, E. Schweizer, F. Rupp, A. Heiss, C. Legner, U.E. Klotz, J. Geis-Gerstorfer, L. Scheideler, Mechanical characteristics, in vitro degradation, cytotoxicity, and antibacterial evaluation of Zn-4.0Ag alloy as a biodegradable material, Int. J. Mol. Sci. 19 (2018) 755.
[112] S. Sun, Y. Ren, L. Wang, B. Yang, H. Li, G. Qin, Abnormal effect of Mn addition on the mechanical properties of as-extruded Zn alloys, Mater. Sci. Eng. A 701 (2017) 129–133.
[113] P. Sotoudeh Bagha, S. Khaleghpanah, S. Sheibani, M. Khakbiz, A. Zakeri, Characterization of nanostructured biodegradable Zn-Mn alloy synthesized by mechanical alloying, J. Alloys Compd. 735 (2018) 1319–1327.
[114] C. Wang, Z. Yu, Y. Cui, Y. Zhang, S. Yu, G. Qu, H. Gong, Processing of a novel Zn alloy micro-tube for biodegradable vascular stent application, J. Mater. Sci. Technol. 32 (2016) 925–929.
[115] X. Liu, J. Sun, Y. Yang, F. Zhou, Z. Pu, L. Li, Y.F. Zheng, Microstructure, mechanical properties, in vitro degradation behavior and hemocompatibility of novel Zn–Mg–Sr alloys as biodegradable metals, Mater. Lett. 162 (2016) 242–245.
[116] X. Liu, J. Sun, F. Zhou, Y. Yang, R. Chang, K. Qiu, Z. Pu, L. Li, Y. Zheng, Micro-alloying with Mn in Zn–Mg alloy for future biodegradable metals application, Mater. Des. 94 (2016) 95–104.
[117] Z. Tang, H. Huang, J. Niu, L. Zhang, H. Zhang, J. Pei, J. Tan, G. Yuan, Design and characterizations of novel biodegradable Zn-Cu-Mg alloys for potential biodegradable implants, Mater. Des. 117 (2017) 84–94.
[118] H.R. Bakhsheshi-Rad, E. Hamzah, H.T. Low, M. Kasiri-Asgarani, S. Farahany, E. Akbari, M.H. Cho, Fabrication of biodegradable Zn-Al-Mg alloy: Mechanical properties, corrosion behavior, cytotoxicity and antibacterial activities, Mater. Sci. Eng. C 73 (2017) 215–219.
[119] Z.Z. Shi, J. Yu, X.F. Liu, L.N. Wang, Fabrication and characterization of novel biodegradable Zn-Mn-Cu alloys, J. Mater. Sci. Technol. (2017).
[120] R. Yue, H. Huang, G. Ke, H. Zhang, J. Pei, G. Xue, G. Yuan, Microstructure, mechanical properties and in vitro degradation behavior of novel Zn-Cu-Fe alloys, Mater. Charact. 134 (2017) 114–122.
[121] Y. Liu, Z. Yin, Y. Liu, C. Geng, X. Chen, J. Xu, J. Peng, Study on the in vitro degradation behavior of commercial Zn-4%Al-Sr alloy for biomedical application, Int. J. Electrochem. Sci. 13 (2018) 1640–1655.

Please cite this article as: J. Venezuela and M. S. Dargusch, The influence of alloying and fabrication techniques on the mechanical properties, biodegradability and biocompatibility of zinc: A comprehensive review, Acta Biomaterialia, https://doi.org/10.1016/j.actbio.2019.01.035

[122] H.R. Bakhsheshi-Rad, E. Hamzah, H.T. Low, M.H. Cho, M. Kasiri-Asgarani, S. Farahany, A. Mostafa, M. Medraj, Thermal characteristics, mechanical properties, in vitro degradation and cytotoxicity of novel biodegradable Zn-Al-Mg and Zn-Al-Mg-Bi alloys, Acta Metall. Sin. 30 (2017) 201–211.
[123] C. Wang, H.T. Yang, X. Li, Y.F. Zheng, In vitro evaluation of the feasibility of commercial Zn alloys as biodegradable metals, J. Mater. Sci. Technol. 32 (2016) 909–918.
[124] M.B. Kannan, C. Moore, S. Saptarshi, S. Somasundaram, M. Rahuma, A.L. Lopata, Biocompatibility and biodegradation studies of a commercial zinc alloy for temporary mini-implant applications, Sci. Rep. 7 (2017) 15605.
[125] S. Kalpakjian, S.R. Schmid, Manufacturing Engineering and Technology, 7th ed., Prentice Hall, Upper Saddle River, NJ, USA, 2014.
[126] J. Čapek, E. Jablonská, J. Lipov, T.F. Kubatík, D. Vojtěch, Preparation and characterization of porous zinc prepared by spark plasma sintering as a material for biodegradable scaffolds, Mater. Chem. Phys. 203 (2018) 249–258.
[127] Y. Hou, G. Jia, R. Yue, C. Chen, J. Pei, H. Zhang, H. Huang, M. Xiong, G. Yuan, Synthesis of biodegradable Zn-based scaffolds using NaCl templates: relationship between porosity, compressive properties and degradation behavior, Mater. Charact. 137 (2018) 162–169.
[128] H. Yang, X. Qu, W. Lin, C. Wang, D. Zhu, K. Dai, Y. Zheng, In vitro and in vivo studies on zinc-hydroxyapatite composites as novel biodegradable metal matrix composite for orthopedic applications, Acta Biomater. 71 (2018) 200–214.
[129] A.A. Shomali, R.J. Guillory, D. Seguin, J. Goldman, J.W. Drelich, Effect of PLLA coating on corrosion and biocompatibility of zinc in vascular environment, Surf. Innov. 5 (2017) 211–220.
[130] S. Bose, D. Ke, H. Sahasrabudhe, A. Bandyopadhyay, Additive manufacturing of biomaterials, Prog. Mater. Sci. 93 (2018) 45–111.
[131] W.S.W. Harun, M.S.I.N. Kamariah, N. Muhamad, S.A.C. Ghani, F. Ahmad, Z. Mohamed, A review of powder additive manufacturing processes for metallic biomaterials, Powder Technol. 327 (2018) 128–151.
[132] T.D. Ngo, A. Kashani, G. Imbalzano, K.T.Q. Nguyen, D. Hui, Additive manufacturing (3D printing): a review of materials, methods, applications and challenges, Compos. Part B Eng. 143 (2018) 172–196.
[133] M. Montani, A.G. Demir, E. Mostaed, M. Vedani, B. Previtali, Processability of pure Zn and pure Fe by SLM for biodegradable metallic implant manufacturing, Rapid Prototyping J. 23 (2017) 514–523.
[134] M. Grasso, A.G. Demir, B. Previtali, B.M. Colosimo, In situ monitoring of selective laser melting of zinc powder via infrared imaging of the process plume, Robot. Comput. Integr. Manuf. 49 (2018) 229–239.
[135] J.R. Freeman Jr., F. Sillers Jr., P.F. Brandt, Pure Zinc at normal and elevated temperatures, Scientific Papers of the Bureau of Standards 20 (1926) 661–695.
[136] E.A. Brandes, G.B. Brook (Eds.), Smithells Metals Reference Book, 7th ed., Butterworth-Heinemann, MA, USA, 1999.
[137] W.D. Callister, D.G. Rethwisch, Materials Science and Engineering: An Introduction, eight ed., John Wiley and Sons, Inc, Hoboken, NJ, 2014.
[138] A. Colombo, G. Stankovic, J.W. Moses, Selection of coronary stents, J. Am. Coll. Cardiol. 40 (2002) 1021–1033.
[139] H.Y. Ang, H. Bulluck, P. Wong, S.S. Venkatraman, Y. Huang, N. Foin, Bioresorbable stents: current and upcoming bioresorbable technologies, Int. J. Cardiol. 228 (2017) 931–939.
[140] ASTM, ASTM /E8M-16a Standard Test Methods for Tension Testing of Metallic Materials, in, ASTM International, West Conshohocken, PA, 2016.
[141] ASTM, ASTM E384-17 Standard Test Method for Microindentation Hardness of Materials, in, ASTM International, West Conshohocken, PA, 2017.
[142] ASTM, ASTM E9-09(2018) Standard Test Methods of Compression Testing of Metallic Materials at Room Temperature, in, ASTM International, West Conshohocken, PA, 2018.
[143] Philippe Poncin, J. Proft, Stent tubing: understanding the desired attributes, in: S. Shrivastava (Ed.), Materials & Processes for Medical Devices Conference, ASM International, Anaheim, California, 2003, pp. 253–259.
[144] G. Song, Control of biodegradation of biocompatable magnesium alloys, Corros. Sci. 49 (2007) 1696–1701.
[145] Michael F. Ashby, Materials Selection in Mechanical Design, 3rd ed., Elsevier Science, Burlington, Burlington, 2004.
[146] L. Liu, Y. Meng, C. Dong, U. Yan, A.A. Volinsky, L. Wang, Initial formation of corrosion products on pure zinc in simulated body fluid, J. Mater. Sci. Technol. (2018).
[147] G.E. Dieter, Mechanical Metallurgy, 3rd ed., McGraw-Hill, NY, USA, 1988.
[148] C.E. Misch, Z. Qu, M.W. Bidez, Mechanical properties of trabecular bone in the human mandible: implications for dental implant treatment planning and surgical placement, J. Oral Maxillofac. Surg. 57 (1999) 700–706.
[149] C. Ohtsuki, M. Kamitakahara, T. Miyazaki, Bioactive ceramic-based materials with designed reactivity for bone tissue regeneration, J. R. Soc. Interface 6 (2009) S349–S360.
[150] D.F. Williams, On the mechanisms of biocompatibility, Biomaterials 29 (2008) 2941–2953.
[151] N.T. Kirkland, N. Birbilis, M.P. Staiger, Assessing the corrosion of biodegradable magnesium implants: a critical review of current methodologies and their limitations, Acta Biomater. 8 (2012) 925–936.
[152] ASTM, ASTM G59-97 Standard Test Method for Conducting Potentiodynamic Polarization Resistance Measurements, in, ASTM International, West Conshohocken, PA, 2014.
[153] J.R. Macdonald, Impedance spectroscopy: models, data fitting, and analysis, Solid State Ionics 176 (2005) 1961–1969.
[154] ASTM, ASTM G31-72 Standard Practice for Laboratory Immersion Corrosion Testing of Metals, in, ASTM International, West Conshohocken, PA, 2004.
[155] ASTM, ASTM G1-03 Standard Practice for Preparing, Cleaning, and Evaluating Corrosion Test Specimens, in, ASTM International, West Conshohocken, PA, 2017.
[156] A. Bruinink, R. Luginbuehl, Evaluation of biocompatibility using in vitro methods: interpretation and limitations, Adv. Biochem. Eng. Biotechnol. 126 (2012) 117–152.
[157] J. Ma, N. Zhao, D. Zhu, Endothelial cellular responses to biodegradable metal zinc, ACS Biomater. Sci. Eng. 1 (2015) 1174–1182.
[158] ISO, ISO 10993-5:2009 Biological evaluation of medical devices. Part 5: Tests for in vitro cytotoxicity, in, International Organisation for Standardization, Geneva, Switzerland 2009.
[159] ISO, ISO 10993-11:2006 Biological evaluation of medical devices. Part 5: Tests for systemic toxicity, in, International Organisation for Standardization, Geneva, Switzerland 2006.
[160] ASTM, ASTM F756-17 Standard Practice for Assessment of Hemolytic Properties of Materials, in, ASTM International, West Conshohocken, PA, 2017.
[161] P.K. Bowen, A. Drelich, J. Drelich, J. Goldman, Rates of in vivo (arterial) and in vitro biocorrosion for pure magnesium, J. Biomed. Mater. Res. A 103 (2015) 341–349.
[162] D.C. Hansen, Metal corrosion in the human body: the ultimate bio-corrosion scenario, Electrochem. Soc. Interface 17 (2008) 31–34.
[163] Y. Chen, W. Zhang, M. Maitz, M. Chen, H. Zhang, J. Mao, Y. Zhao, N. Huang, G. Wan, Comparative corrosion behavior of Zn with Fe and Mg in the course of immersion degradation in phosphate buffered saline, Corros. Sci. 111 (2016) 541–555.
[164] P. Volovitch, C. Allely, K. Ogle, Understanding corrosion via corrosion product characterization: I. Case study of the role of Mg alloying in Zn–Mg coating on steel, Corros. Sci. 51 (2009) 1251–1262.
[165] A. Nazarov, E. Diler, D. Persson, D. Thierry, Electrochemical and corrosion properties of ZnO/Zn electrode in atmospheric environments, J. Electroanal. Chem. 737 (2015) 129–140.
[166] R. LeGeros, C. Bleiwas, M. Retino, R. Rohanizadeh, J. LeGeros, Zinc effect on the in vitro formation of calcium phosphates: relevance to clinical inhibition of calculus formation, Am. J. Dent. 12 (1999) 65–71.
[167] Z. Zhen, T. Xi, Y. Zheng, A review on in vitro corrosion performance test of biodegradable metallic materials, Trans. Nonferrous Met. Soc. China 23 (2013) 2283–2293.
[168] M. Dreher, S. Anderson, ASTM-FDA workshop on absorbable medical devices: Lessons learned from correlations of bench testing and clinical performance, Department of Health and Human Services, Food and Drug Administration, Silver Spring, MD, 2012.
[169] D.A. Jones, Principles and Prevention of Corrosion, 2nd ed., Prentice Hall, NJ, 1996.
[170] S. Jafari, S.E. Harandi, R.K. Singh Raman, A review of stress-corrosion cracking and corrosion fatigue of magnesium alloys for biodegradable implant applications, JOM 67 (2015) 1143–1153.
[171] G.S. Frankel, N. Sridhar, Understanding localized corrosion, Mater. Today 11 (2008) 38–44.
[172] H. Kaesche, Corrosion of Metals: Physicochemical Principles and Current Problems, Springer Science & Business Media, Berlin Heidelberg, 2012.
[173] M. Esmaily, J.E. Svensson, S. Fajardo, N. Birbilis, G.S. Frankel, S. Virtanen, R. Arrabal, S. Thomas, L.G. Johansson, Fundamentals and advances in magnesium alloy corrosion, Prog. Mater. Sci. 89 (2017) 92–193.
[174] R. Hausbrand, M. Stratmann, M. Rohwerder, Corrosion of zinc–magnesium coatings: mechanism of paint delamination, Corros. Sci. 51 (2009) 2107–2114.
[175] S. Wu, X. Liu, K.W.K. Yeung, C. Liu, X. Yang, Biomimetic porous scaffolds for bone tissue engineering, Mater. Sci. Eng. R 80 (2014) 1–36.
[176] J.M. Anderson, Future challenges in the in vitro and in vivo evaluation of biomaterial biocompatibility, Regen Biomater. 3 (2016) 73–77.
[177] W. Li, J. Zhou, Y. Xu, Study of the in vitro cytotoxicity testing of medical devices, Biomed. Rep. 3 (2015) 617–620.
[178] J. Wang, F. Witte, T. Xi, Y. Zheng, K. Yang, Y. Yang, D. Zhao, J. Meng, Y. Li, W. Li, K. Chan, L. Qin, Recommendation for modifying current cytotoxicity testing standards for biodegradable magnesium-based materials, Acta Biomater. 21 (2015) 237–249.
[179] C. Ning, X. Wang, L. Li, Y. Zhu, M. Li, P. Yu, L. Zhou, Z. Zhou, J. Chen, G. Tan, Y. Zhang, Y. Wang, C. Mao, Concentration ranges of antibacterial cations for showing the highest antibacterial efficacy but the least cytotoxicity against mammalian cells: implications for a new antibacterial mechanism, Chem. Res. Toxicol. 28 (2015) 1815–1822.
[180] T.N. Phan, T. Buckner, J. Sheng, J.D. Baldeck, R.E. Marquis, Physiologic actions of zinc related to inhibition of acid and alkali production by oral streptococci in suspensions and biofilms, Oral Microbiol. Immunol. 19 (2003) 31–38.
[181] H. Zreiqat, C.R. Howlett, A. Zannettino, P. Evans, G. Schulze-Tanzil, C. Knabe, M. Shakibaei, Mechanisms of magnesium-stimulated adhesion of osteoblastic cells to commonly used orthopaedic implants, J. Biomed. Mater. Res. A 62 (2002) 175–184.
[182] Little Pro, Mutagenicity and Genotoxicity, in, ChemSafetyPro, 2016.
[183] U. Thormann, V. Alt, L. Heimann, C. Gasquere, C. Heiss, G. Szalay, J. Franke, R. Schnettler, K.S. Lips, The biocompatibility of degradable magnesium

Please cite this article as: J. Venezuela and M. S. Dargusch, The influence of alloying and fabrication techniques on the mechanical properties, biodegradability and biocompatibility of zinc: A comprehensive review, Acta Biomaterialia, https://doi.org/10.1016/j.actbio.2019.01.035

interference screws: an experimental study with sheep, BioMed Res. Int. 2015 (2015) 943603.
[184] C. Ma, L. Chen, J. Xu, A. Fehrenbacher, Y. Li, F.E. Pfefferkorn, N.A. Duffie, J. Zheng, X. Li, Effect of fabrication and processing technology on the biodegradability of magnesium nanocomposites, J. Biomed. Mater. Res. B 101 (2013) 870–877.
[185] C. Lorenz, J.G. Brunner, P. Kollmannsberger, L. Jaafar, B. Fabry, S. Virtanen, Effect of surface pre-treatments on biocompatibility of magnesium, Acta Biomater. 5 (2009) 2783–2789.
[186] M. Lotfi, M. Naceur, M. Nejib, Cell Adhesion to Biomaterials: Concept of Biocompatibility, INTECH Open Access Publisher, 2013.
[187] B. Swetha, S. Mathew, B.V. Sreenivasa Murthy, N. Shruthi, S.H. Bhandi, Determination of biocompatibility: a review, Int. Dent. Med. J Adv. Res. 1 (2015).
[188] A. Kafri, S. Ovadia, G. Yosafovich-Doitch, E. Aghion, In vivo performances of pure Zn and Zn–Fe alloy as biodegradable implants, J. Mater. Sci. Mater. Med. 29 (2018) 94.
[189] A.W. Martinez, E.L. Chaikof, Microfabrication and nanotechnology in stent design, Wiley Interdiscip. Rev. Nanomed. Nanobiotechnol. 3 (2011) 256–268.
[190] G. Catalano, A.G. Demir, V. Furlan, B. Previtali, Prototyping of biodegradable flat stents in pure zinc by laser microcutting and chemical etching, J. Micromech. Microeng. 28 (2018). 095016 (095012 pp).
[191] R. Van Lith, E. Baker, H. Ware, J. Yang, A.C. Farsheed, C. Sun, A. Guillermo, 3D-printing strong high-resolution antioxidant bioresorbable vascular stents, Adv. Mater. Technol. 1 (2016) 1600138, https://doi.org/10.1002/admt.201600138.
[192] ISO, ISO 10993-1:2018 Biological Evaluation of Medical Devices—Part 1: Evaluation and Testing within a Risk Management Process, in, International Organisation for Standardization, Geneva, Switzerland 2018.
[193] R. Packard, ISO 10993-1-2018 Biocompatibility – What's new?, in, Medical Device Academy, Oct 7, 2018.
[194] ASTM, ASTM F1983-14 Standard Practice for Assessment of Selected Tissue Effects of Absorbable Biomaterials for Implant Applications, in, ASTM International, West Conshohocken, PA, 2014.
[195] ISO, ISO/TR 37137 Cardiovascular biological evaluation of medical devices – Guidance for absorbable implants, in, International Organisation for Standardization, Geneva, Switzerland 2014.
[196] ISO, ISO/DTR 37137-2 Cardiovascular biological evaluation of medical devices – Guidance for absorbable implants – Part 2: Standard guide for absorbable metals, in, International Organisation for Standardization, Geneva, Switzerland.
[197] B.K. Hayes, Standardized guidance for the preclinical evaluation of absorbable metal implants, in: A. Singh, K. Solanki, M.V. Manuel, N.R. Neelameggham (Eds.) Magnesium Technology 2016, Springer International Publishing, Cham, 2016, pp. 357–359.
[198] A. Ghallab, In vitro test systems and their limitations, EXCLI J. 12 (2013) 1024–2026.
[199] A.H.M. Sanchez, B.J.C. Luthringer, F. Feyerabend, R. Willumeit, Mg and Mg alloys: how comparable are in vitro and in vivo corrosion rates? A review, Acta Biomater. 13 (2015) 16–31.
[200] A.N. Rowan, The benefits and ethics of animal research, in: Scientific American, Scientific American, Inc, 1997, pp. 79–93.
[201] N.D. Barnard, S.R. Kaufman, Animal research is wasteful and misleading, Sci Am. 276 (1997) 80–82.
[202] J.H. Botting, A.R. Morrison, Animal research is vital to medicine, Sci Am. 276 (1997) 83–85.
[203] M. Mukerjee, Trends in animal research, Sci Am. 276 (1997) 86–93.
[204] N. Kranzlin, M. Niederberger, Controlled fabrication of porous metals from the nanometer to the macroscopic scale, Mater. Horiz. 2 (2015) 359–377.
[205] K. Brannigan, M. Griffin, An update into the application of nanotechnology in bone healing, Open Orthop. J. 10 (2016) 808–823.
[206] M.S. Uddin, C. Hal, P. Murphy, Surface treatments for controlling corrosion rate of biodegradable Mg and Mg-based alloy implants, Sci. Technol. Adv. Mater. 16 (2015) 053501.
[207] T. DebRoy, H.L. Wei, J.S. Zuback, T. Mukherjee, J.W. Elmer, J.O. Milewski, A.M. Beese, A. Wilson-Heid, A. De, W. Zhang, Additive manufacturing of metallic components – process, structure and properties, Prog. Mater. Sci. 92 (2018) 112–224.
[208] M. Moravej, F. Prima, M. Fiset, D. Mantovani, Electroformed iron as new biomaterial for degradable stents: development process and structure–properties relationship, Acta Biomater. 6 (2010) 1726–1735.
[209] P.K. Chu, Plasma surface engineering of biomaterials, in: 2014 IEEE 41st International Conference on Plasma Sciences (ICOPS) held with 2014 IEEE International Conference on High-Power Particle Beams (BEAMS), IEEE, Washington DC, USA, 2014, pp. 1-1.
[210] J. Levesque, H. Hermawan, D. Dube, D. Mantovani, Design of a pseudo-physiological test bench specific to the development of biodegradable metallic biomaterials, Acta Biomater. 4 (2008) 284–295.
[211] E.E. Antoine, F.P. Cornat, A.I. Barakat, The stentable in vitro artery: an instrumented platform for endovascular device development and optimization, J. R. Soc. Interface 13 (2016) 20160834.
[212] J. Wang, C.E. Smith, J. Sankar, Y. Yun, N. Huang, Absorbable magnesium-based stent: physiological factors to consider for in vitro degradation assessments, Regen. Biomater. 2 (2015) 59–69.
[213] W. Lilienblum, W. Dekant, H. Foth, T. Gebel, J.G. Hengstler, R. Kahl, Alternative methods to safety studies in experimental animals: role in the risk assessment of chemicals under the new European Chemicals Legislation (REACH), Arch. Toxicol. 82 (2008) 211–236.

Please cite this article as: J. Venezuela and M. S. Dargusch, The influence of alloying and fabrication techniques on the mechanical properties, biodegradability and biocompatibility of zinc: A comprehensive review, Acta Biomaterialia, https://doi.org/10.1016/j.actbio.2019.01.035